

GEOPHYSICAL CONSTRAINTS ON THE HUECO AND MESILLA BOLSONS:  
STRUCTURE AND GEOMETRY

VICTOR MANUEL AVILA

Doctoral Program in Geological Sciences

APPROVED:

---

Diane I. Doser, Ph.D., Chair

---

Laura Serpa, Ph.D.

---

Aaron Velasco, Ph.D.

---

Terry Pavlis, Ph.D.

---

Oscar S. Dena, Ph.D.

---

Charles H. Ambler, Ph.D.  
Dean of the Graduate School

Copyright ©

By

Victor Manuel Avila

2016

Dedication

To

The Church in Ciudad Juárez

To

My parents and brothers,

Manuel, Irma Rosa, Iram and Julio

For their love and support in every aspect in my life.

To

My family

Iralva, Danica and Manuel

To you that are the blessings from God to me.

“It is not the critic who counts; not the man who points out how the strong man stumbles, or where the doer of deeds could have done them better. The credit belongs to the man who is actually in the arena, whose face is marred by dust and sweat and blood; who strives valiantly; who errs, who comes short again and again, because there is no effort without error and shortcoming; but who does actually strive to do the deeds; who knows great enthusiasms, the great devotions; who spends himself in a worthy cause; who at the best knows in the end the triumph of high achievement, and who at the worst, if he fails, at least fails while daring greatly, so that his place shall never be with those cold and timid souls who neither know victory nor defeat. “

“The man in the arena”

Theodore Roosevelt

**GEOPHYSICAL CONSTRAINTS ON THE HUECO AND MESILLA BOLSONS:  
STRUCTURE AND GEOMETRY**

by

Victor Manuel Avila M.S., B.S.

**DISSERTATION**

Presented to the Faculty of the Graduate School of  
The University of Texas at El Paso  
in Partial Fulfillment  
of the Requirements  
for the Degree of

**DOCTOR OF PHILOSOPHY**

Department of Geological Sciences  
THE UNIVERSITY OF TEXAS AT EL PASO  
May 2016

ProQuest Number: 10133864

All rights reserved

INFORMATION TO ALL USERS

The quality of this reproduction is dependent upon the quality of the copy submitted.

In the unlikely event that the author did not send a complete manuscript and there are missing pages, these will be noted. Also, if material had to be removed, a note will indicate the deletion.



ProQuest 10133864

Published by ProQuest LLC (2016). Copyright of the Dissertation is held by the Author.

All rights reserved.

This work is protected against unauthorized copying under Title 17, United States Code  
Microform Edition © ProQuest LLC.

ProQuest LLC.  
789 East Eisenhower Parkway  
P.O. Box 1346  
Ann Arbor, MI 48106 - 1346

## ACKNOWLEDGEMENTS

First and foremost, I would like to express my gratitude to the members of my doctoral committee, Dr. D. Doser, Dr. L. Serpa, Dr. A. Velasco, Dr. T. Pavlis, Dr. O. Dena, who have shaped my professional career to very high standards, and I still continue to learn from them, thank you for your unconditional support and guidance.

In particular, I must extend my sincere gratitude to Dr. Doser for her encouragement to conclude my masters and continued with a Ph.D. The success of this study is due to her guidance and patience throughout these years, my family and I will always be grateful for your support thanks.

I will like to acknowledge Dr. Goodell for his support and friendship; He always has a door open to talk and help out when need it. Gracias Felipe.

Dr. Carrick and Dr. Velasco thank you for opening the doors to the Geology department, and giving me a second chance; I will always wear the UTEP Geology shirt because of you. Thank You. Dr. Harder and mi amigo Galen Kaip, my field Jefes in the seismic projects, I learned a lot working with you guys, thank you for taking care me while working around the holes, and the equipment and the explosives.

Special Thanks to the UTEP, staff Carlos Montana, Carlos muchas gracias, and to Pam Hart, as I consider part of my UTEP family, This could not be done with your help.

To all my UACJ friends, Jesus Leyva, Manuel Moncada, Mitchell Luna, Miguel Galdean, Azael Avalos, Griselda Obeso Gracias for your help.

The field crew geology friends: Felix Ziwu, Manuel Moncada, Martin Sandoval, Richard Alfaro, Arturo Ramirez, Yousef, Robert, Raquel, Jonathan, Luke Baker, Thank you guys.

Special thanks to Felix Ziwu and Meny Moncada and Oscar Romero, and Luis Martin Sandoval, for their unconditional friendship, thank you for being my brothers.

Thanks to Dr. Ben Drenth from USGS for your support and friendship and helping out with the analysis for the Horizontal Gradient Magnitude. Thanks Ben.

This dissertation was accomplished with the help of the Consejo Nacional y Tecnología (CONACYT) scholarship. Thanks for their support towards this degree.

## ABSTRACT

The Hueco and Mesilla Bolsons are part of the intramountain basins of the Rio Grande Rift system. These bolsons are the primary source of groundwater for the El Paso-Ciudad Juarez metropolitan area and contain faults that show evidence of repeated earthquakes during the Quaternary. The region is also associated with has low-level ( $M<4$ ) seismicity. The collection and analysis of precision gravity data, coupled with information from water wells, multichannel analysis of surface waves (MASW) studies and previously published seismic reflection lines, have been used to examine the structure and faulting within these bolson. This study reveals that the Hueco and Mesilla Bolsons are very different structurally. The southern Mesilla Bolson contains about 500 m of sediment. Faults are difficult to trace and have less than 50-100 m of displacement across them. The southernmost bolson contains numerous Tertiary intrusions and the thickness of Cretaceous bedrock appears to decrease from south to north, possibly delineating the edge of Laramide age deformation within the bolson. The northern Hueco Bolson contains 1800 to 2500 m of basin fill. Displacement along the East Franklin Mountains fault (EFMF), a fault with evidence for repeated earthquakes within the past 64,000 years, is about 1500 m, and displacement on intrabasin faults is 200-300 m. Several intrabasin faults appear to control the saline to freshwater contact within the bolson. The EFMF may extend over 30 km south of the end of its mapped trace at the end of the Franklin Mountains and a number of intrabasin faults also extend south into the urbanized regions of the study area. The EFMF and other basin structures appear to be offset or disrupted at the speculated edge of Laramide deformation that lies beneath the bolson. Horizontal Gradient Methods (HGM) were applied to the gravity data and were successful for tracing faults and older Laramide features within the Hueco Bolson beneath the urbanized regions of the cities. HGM were not as successful at tracing faults within

the Mesilla Bolson, however they were helpful for tracing the subsurface extent of igneous intrusions including the Mt. Cristo Rey, River, Three Sisters, and the Westerner outcrops. Some of these features appear linked at depth by a series of dikes and faults. MASW data were used to determine the average shear wave velocity in the upper 30m ( $V_s$  30) at ~70 sites within the Hueco Bolson. These observations were combined with similar data collected previously in Juarez to produce regional velocity and site classification maps. The results show low velocities are found close to the river within fluvial deposits with higher velocities close to the Franklin Mountains where bedrock is close to the surface and higher velocities in upland regions of northeast El Paso where soils appear to be more highly cemented. These data will be used in conjunction with information on bolson geometries to model the expected effects of strong ground motion from earthquakes in the El Paso-Ciudad Juarez region.

## TABLE OF CONTENTS

ACKNOWLEDGEMENTS .....	vi
ABSTRACT.....	viii
LIST OF TABLES.....	xii
LIST OF FIGURES .....	xiii
CHAPTER 1 .....	1
1.1. Introduction .....	1
CHAPTER 2 .....	3
2.1 Previous Geophysical Studies .....	3
2.2 Hueco Bolson Studies .....	3
2.3 Mesilla Bolson.....	5
2.4 Previous Seismic Studies .....	7
2.5 References .....	15
CHAPTER 3 .....	17
3.1 Location of the Study Area.....	17
CHAPTER 4 .....	18
4.1 Regional Tectonic Setting .....	18
4.2 References .....	21
CHAPTER 5 .....	23
5.1 Gravity Methodology .....	23
5.2 Gravity Field Survey .....	23
5.3 Final gravity database.....	24
5.4 Gravity Data Processing.....	24
5.5 Residual Anomaly .....	25
5.6 Boundary Analysis .....	25
5.7 References .....	29
CHAPTER 6 .....	30
6.1 Hueco Bolson Gravity Maps .....	30
6.2 Forward Modeling.....	32
6.3 Discussion .....	34
6.4 References .....	46

<b>CHAPTER 7 .....</b>	<b>47</b>
7.1    Mesilla Gravity Maps.....	47
7.2    Forward Modeling.....	48
7.3    2D Density Profiles .....	49
7.4    Discussion .....	51
7.5    References .....	63
<b>CHAPTER 8 .....</b>	<b>64</b>
Shear Wave Velocity of Soils and NEHRP Site Classification Map in El Paso West Texas.....	64
8.1    Abstract .....	64
8.2    Introduction .....	64
8.4    Methodology .....	65
8.4.1.  Survey.....	66
8.5    Processing.....	67
8.5.1  Pickwin Module. ....	68
8.5.2  Wave Equation .....	68
8.6    Results .....	69
8.7    Discussion .....	69
8.8    References .....	86
<b>CHAPTER 9 .....</b>	<b>88</b>
9.1    Future Directions.....	88
9.2    Data Collection.....	88
9.3    Data Compilation and Modeling .....	89
9.4    Communication of Results .....	89
<b>CURRICULUM VITA .....</b>	<b>92</b>

## **LIST OF TABLES**

Table 6.1 Densities used in forward modeling. Modified from Avila et al (2016). .....	33
Table 7.1. Densities used in the 2D gravity models for the Mesilla Bolson.....	49
Table 8.1 Definition of NEHRP site classes by velocity V100 (average shear velocity in the top 100 feet) VS30 and blow count N100. Modify from Building Seismic Safety Council (1997)...	72
Table 8.2 Acquisition parameters for the MASW Surveys .....	79

## LIST OF FIGURES

Figure 2.1 Isopach map of Cenozoic lower basin fill. Constructed from seismic interpretations (Modified from Collins and Raney, 1994).....	10
Figure 2.2. Isopach map of Cenozoic upper basin fill. Interpretations of seismic data were used to construct map. (Modified from Collins and Raney, 1994). ....	10
Figure 2.3. Cross sections interpreted from seismic data throughout the Hueco bolson. Sections A through F correspond to seismic locations A through F on index map. Modified from Collins and Raney (1994).....	11
Figure 2.4. Geological map of Averill's study area with location of seismic survey. Surface geology labeling modified for consistency across state and national borders for New Mexico (after Green and Jones, 1997), Texas (after Hartmann and Scranton (1992), and the state of Chihuahua, Mexico (after INEGI, 1981). Gray box in regional inset map shows boundary of study area. The seismic survey crosses series of late Cenozoic basins and ranges. Modified from Averill (2013).....	12
Figure 2.5 Tomographic velocity model, shows interpretation of late Tertiary geologic features. Velocity model was calculated with a 0.5 km grid interval.....	13
Figure 2.6. Tomographic velocity model showing interpretation of Mesozoic to early Tertiary tectonic features. (A) Diagram showing interpreted geometry of a Laramide arch in Wyoming from Erslev (1993). ....	14
Figure 3.1. Shows the location of the study area for the Hueco and Mesilla Bolson .....	17
Figure 4.2. Major Paleozoic to Cenozoic tectonic features in the study area. Shaded areas show outline of the Paleozoic Pedregosa and Orogrande Basins (after Greenwood et al., 1977).....	20
Figure 5.1 New gravity stations (red triangles) collected in the urbanized area of El Paso, TX..	27
Figure 5.2 Gravity stations added to existing UTEP gravity database (purple symbols). ....	28
Figure 6.1 Complete Bouguer Anomaly for the regional area of Hueco Bolson. White lines are Quaternary faults from Collins and Raney (1994).....	36
Figure 6.2. Residual Bouguer Anomaly for the regional area of the Hueco Bolson. See Figure 6.1 for explanation of symbols and lines. ....	37

Figure 6.3 Horizontal Gradient Magnitude regional map for the Hueco Bolson. See Figure 6.1 for explanation of symbols and lines. EFMF is East Franklins Mountain fault. M1 is concealed fault from Marrufo (2011) .....	38
Figure 6.4 Complete Bouguer Anomaly map for the urbanized El Paso-Ciudad Juárez area. Red squares denote location of airports, diamond is deep geothermal well (~1675m) that did not reach basement, star is M2.5 earthquake occurring in 2012.....	39
Figure 6.5 Residual Bouguer Anomaly map for the urbanized part of El Paso-Ciudad Juárez area. See explanation of symbols in Figure 6.4.....	40
Figure 6.6 Horizontal Gradient Magnitude Map for the urbanized El Paso-Ciudad Juárez area. See explanation of symbols in Figure 6.4.....	41
Figure 6.7 Complete Bouguer Anomaly map showing the 2D-Gravity profiles along Hueco Bolson study area. (Modified from Avila et al., 2016) . Faults F1 to F7 are from work of Collins and Raney (1994).....	42
Figure 6.8 Two-dimensional gravity models for cross-section A-A' and B-B'. Black lines indicate faults. (Modified from Avila et al 2016). Seismic section on A-A' is from Figuers (1987).....	43
Figure 6.9 Two-dimensional gravity models for cross-section C-C' and D-D'. Black solid lines indicate faults with surface expression, dashed line indicates concealed fault.....	44
Figure 6.10 HGM of the Hueco Bolson, with black dashed lines showing possible extension of the quaternary faulting into the urban part of El Paso-Ciudad Juárez. ....	45
Figure 7.1 Complete Bouguer Anomaly Map. High gravity values correspond to high density rocks. Solid lines are faults from Witcher (1998) or Hawley and Kennedy (2004), dashed lines are faults from this study or from Hiebing (2016). Gray regions indicate outcrops of Tertiary igneous intrusions from Hawley and Kennedy (2004). Symbols indicate gravity observations.....	53
Figure 7.2. Residual Bouguer Anomaly Map.....	54
Figure 7.3 Horizontal Gradient Magnitude Map. HGM helps to delineates features with steep vertical density contrasts such as faults and igneous bodies.....	55

Figure 7.4 Complete Bouguer Anomaly map showing locations of gravity cross-sections.....	56
Figure 7.5 Velocity model modified from Averill 2007. A. Ray traced 1 km gridded velocity model.. B. 2-D tomography velocity model with 500 m cell size. Dashed lines show interpretation of faults.....	57
Figure 7.6. A) Geologic cross section K-K' from hydrostratigraphic framework of Hawley and Kennedy (2004), that was used as the base for the two-dimensional gravity model (shown in B. ....)	58
Figure 7.7 HGM map with gravity profiles .....	59
Figure 7.8 Two-dimensional gravity profile for section Q-Q' from Figure 7.4, densities constrained with profile K-K'. WF= Witcher Fault. MVFZ= Mesilla Valley Fault Zone. UV1= Upper Valley Fault 1. UV2= Upper Valley Fault 2.....	60
Figure 7.9. Figure A shows J-J' geologic cross-section from hydrostratigraphic framework of Hawley and Kennedy (2004). A portion of this cross section indicated by red dashed lines was used as a constraint for the two-dimensional density profile J-J' .....	61
Figure 7.10 Figure A displays NW-SE geologic cross-section from hydrostratigraphic framework from Hawley 2004. Figure a two-dimensional gravity profile build from Complete Bouguer Anomaly data. Densities obtained from velocities model study.....	62
Figure 8.1. Seismicity in West Texas- Southern New Mexico, Northern Chihuahua from 2009-2016 from U.S. Geological Survey (2016) .....	71
Figure 8.2 Location of 370 Seismic stations in Ciudad Juarez where Vs30 was determined using the MASW technique. Modified from Dena (2011).....	73
Figure 8.3 Average Vs30 determined for the Hueco Bolson in Ciudad Juarez using the MASW technique. Modified from Dena (2011) .....	74
Figure 8.4 Site classification determined by relating Vs30 to soil type in Ciudad Juarez. Modified from Dena (2011).....	75
Figure 8.5 Expected resonant frequency amplification in Hz for Ciudad Juarez estimated from MASW and site classification. Modified from Dena (2011).....	76

Figure 8.6. Vs30 locations (triangles) in the urban area of El Paso TX.....	77
Figure 8.6 A) Example of shot gathers from site location. B) Dispersion curve (Pink dots) for the phase velocity (horizontal axis)-frequency (vertical axis) transformation. C) Dispersion curve but with phase velocity on vertical axis D) Vs30curve (black line?) is obtained by inverting the initial model. Table 8.2 Acquisition parameters for the MASW.....	78
Figure 8.8 Process flow for processing 1D MSAW .....	80
Figure 8.9 Left figure shows high quality data with high signal to noise ratio. Right figure shows low quality data with a lot of contamination with lower frequency signals. ....	81
Figure 8.10 Initial shear velocity model from dispersion curve (left). Vs30model with optional parameters (right).....	82
Figure 8.11 Vs30 map of the urbanized part of El Paso .....	83
Figure 8.12 NEHRP site Classification for the Vs30 in the urbanized part of El Paso. ....	84
Figure 8.13 Combined Vs30 results for El Paso and Ciudad Juarez .....	85
Figure 9.1 Hueco Bolson gravity data needs to be collected to continue studding the faults .....	90
Figure 9.2 Gravity database for Mesilla Bolson .....	91

## **CHAPTER 1**

### **1.1. Introduction**

Basin structure is an important factor that controls the quantity and quality of groundwater and influence groundwater flow. Fault locations are important to earthquake hazards studies, and they also serve as barriers or conduits to groundwater. Basin geometry affects strong ground motion and wave amplification during earthquakes. In addition, basin structure and basin geometry will help to explain the development of the southern Rio Grande Rift and its relation to older features such as Laramide structures and the Jurassic age Chihuahua trough. The extent of andesitic intrusions related to Cristo Rey and the Campus andesite in the southern Mesilla Bolson and in the Sierra de Juarez will help us to understand the extent of regional late Cretaceous volcanism and its effects on present day groundwater flow. The first part of this dissertation,, will focus on gravity studies of the northern part of the Hueco Bolson I collected additional gravity data in the downtown El Paso and combined that with gravity data from Ciudad Juarez area to better constrain the locations of faults and the basin shape. These data will be used in 2-D and 3-D modeling techniques. The final models obtained from this investigation will be compared to existing groundwater information (e.g. chemistry, groundwater flow directions, water well logs).

The second part of the Investigation is the Mesilla Bolson where is a much different structure than the Hueco Bolson, as it is a lot shallower basin, the investigation will show the depth to basement using 2D gravity models based on well logs information. For this we also need it to take additional Gravity within the Mesilla Bolson that later was added it to the UTEP Gravity database for the analysis. in this part of the dissertation contains the analysis of the

extent of cretaceous volcanism with in the basin using gravity data analysis to look for the lateral density variations.

The third part of the dissertation will consist of an earthquake strong motion site response study for the El Paso area. Shallow Hueco Bolson basin sediments contain both lacustrine and fluvial deposits that may serve to amplify strong ground motions during earthquakes. Studies throughout the world have shown that the determination of  $V_s^{30}$  (shear velocity structure of the upper 30 meters) is an important measure of soil response that can be used to predict strong ground motions. Basin shape and depth to bedrock also play an important role in amplifying strong ground motion. Thus, many aspects of this dissertation will help in estimating earthquake hazards in the El Paso-Juarez region.

These investigations detail a more comprehensive model of the geometry Hueco and Mesilla Bolsons and how this structure influences groundwater flow. Although the region does not experience frequent earthquakes, the recent (March 2012) El Paso (M~2.5) earthquake and ongoing seismic activity in southern Chihuahua are reminders that the region is tectonically active.

## CHAPTER 2

### 2.1 Previous Geophysical Studies

Numerous geophysical studies have focused on the Mesilla and Hueco Bolsons. The main geophysical techniques applied or combined in these studies include gravity, magnetics, well logs and seismic. Each study has served a different purpose but all of them are building blocks for this study. In the following section I will review the most relevant surveys for the purpose of my research.

### 2.2 Hueco Bolson Studies

The first gravity studies conducted in south-central New Mexico and West Texas were able to delineate the basic basin structures as shown on Bouguer gravity maps. These studies found a good correlation between the gravity highs and exposed bedrock or shallow subsurface structures of pre-Cenozoic strata, while gravity lows correlated with the Cenozoic basins (e.g., Barrie 1975). Ramberg et al (1978) were some of the first to use gravity anomaly maps to characterize the extent of the Hueco and Mesilla bolsons.

Hadi (1993) conducted a regional gravity study and found that the Hueco Bolson was composed of two deep elongated basins separated by a relatively shallow hinge zone. Both sub-basins are asymmetrical graben structures controlled by the extensional tectonics of the Rio Grande Rift.

Burgos (1993) merged gravity collected in the El Paso area with added gravity stations from Ciudad Juarez to determine the thickness of the basin fill deposits as well as their geometry and extent. He also identified 3 sub-basins within the Hueco Bolson, and confirmed the NW-SE trend of the basin.

Hawley et al., (2009) provided a hydrogeological framework for the Hueco Bolson based on well log and water well information. This study summarized the complexities of the evolution of groundwater flow and hydro-geochemical regimes throughout the Cenozoic extension of the Rio Grande rift. A similar study by Hawley et al. (2004) was conducted for the Mesilla Bolson. Both studies produced extensive cross sections showing the thickness and structural controls within the three main stratigraphic units of the basins, the Lower, Middle and Upper Santa Fe group. The Upper Santa Fe Group correlates with Camp Rice Formation and consists of sand and gravel deposited from ancestral Rio Grande channel. The Middle Santa Fe Group consists of fine-grained, intertonguing of alluvial and basin-floor deposits. The Lower Santa Fe Group is the oldest stratigraphic unit and consists of fine grained partly consolidated playa deposits and eolian sands, with coarser material deposited at the edges of the basin.

Avila (2011) demonstrated that it was possible to trace the East Franklin Mountains Boundary fault into the highly urbanized regions of El Paso and Ciudad Juarez based on the gravity technique. Since this fault crosses downtown El Paso and Ciudad Juarez, it poses a seismic risk to both cities. Marrufo (2011) correlated well logs and well cuttings to determine different depositional environments and facies in the Hueco Bolson. She was able to use these correlations to identify a number of new faults within the basin as well as confirm the subsurface location of faults mapped by Collins and Raney (2000). Marrufo used gravity as an additional tool to confirm the location of these faults. The study also revealed the limits of brackish and fresh water and the role that the faults play in separating these regions of differing salinity.

Moncada (2011) presented results of a detailed gravity study done at the southern end of the northern Hueco Bolson within the city limits of Ciudad Juarez. The objective of this work was to identify an underground recharge area for the Hueco Bolson aquifer, where faults play a

major role in the recharge process. His gravity models were constrained with logs from municipal water wells and with time domain electromagnetics where he was able to construct 2D profiles of the possible recharge area. This study also attempted to follow the extent of the East Franklin Mountains Fault into Ciudad Juarez where the strike of the fault changes orientation from N-S to SE-NW orientation.

Gravity studies by Budhathoki (2013) and groundwater geochemical studies by Thapalia (2014) revealed additional faults within the northwestern portion of the northern Hueco Bolson and the role these faults play in controlling groundwater salinity. Avila et al. (2016) used existing gravity data and the horizontal gradient method to map concealed faults within the Hueco Bolson.

### 2.3 Mesilla Bolson

Figuers (1987) conducted a detailed gravity study in the northern part of the Mesilla Bolson along the Pipeline Road that parallels the Texas-New Mexico border. This study was also accompanied by the recording of a 33km long seismic reflection line. The study determined the location and orientation of the Eastern and Western Boundary Faults of the Franklin Mountains.

Imana (1993) compared the differences and similarities of the East African and Rio Grande Rift. His work was based on gravity data he collected and combined with previously available data for the Mesilla Bolson. This study not only provided a greater understanding of continental rifting, but also helped to determine more about the petroleum and groundwater resources of the area.

Gillespie (2002) integrated gravity data, seismic reflection lines, well control and remote sensing information to study the Mesilla Bolson and Jornada del Muerto basin (located north of

the Mesilla Bolson). For the Mesilla Bolson she used seismic reflection data to interpret that the Love Ranch formation formed a piggyback basin on top of thrust sheets of Laramide age. Her results showed two possible two stages of regional extension, one at 30 Ma with low-angle rift faulting and one at 10 Ma where high-angle faults cut the older normal faults. Furthermore, the study confirmed the presence Rio Grande uplift and showed the filling of the Potrillo basin by the Love Ranch formation.

Imana (2003) continued studying the shallow structures within the Mesilla Bolson, such as faults and river channels, using gravity, resistivity and well log data. He was able to identify N-S and NW-SE trending faults but not in great detail. The study estimated a depth to bedrock of no more than 3 km in the deepest part of the basin, indicating a shallower basin than the Hueco Bolson.

Khatun (2003) and Khatun et al. (2007) continued studying faults in the Mesilla Bolson. Khatun's objectives were to look for faults in the southern part of the Mesilla bolson and augment the resolution of the faults mapped by Imana in 2003. Her gravity study consisted of three N-S oriented gravity transects that were perpendicular to Imana's transects. Khatun suggested different orientations for the three faults previously named by Imana, in addition to evidence for a fault located north of Mt Cristo Rey that truncates the north-south trending faults

Sellepack (2003) studied the Cenozoic evolution of the Mesilla Bolson, using field and laboratory research. She conducted grain size and lithological analysis at outcrops and in wells using well cuttings and well log correlation. She proposed that faulting in the Mesilla Bolson may have taken place intermittently during the deposition of the upper Santa Fe sediments.

Facies analysis results indicate that the sediments were deposited in fluvial channels, fluvial overbanks, playas and alluvial fans

Hawley et al. (2004) created a hydrogeologic-framework model for the Mesilla Bolson and parts of the southern Jornada del Muerto Basin. These models took into account modifications and updates of the existing groundwater flow model for the Lower Rio Grande-Mesilla Bolson area. The study was built from 160 “key wells” that include 60 geophysical logs, drill cutting logs and ground water chemical data. The study standardized other studies that had a variety maps and sections with inconsistent scales and spatial coverage.

## 2.4 Previous Seismic Studies

One of the significant seismic studies in the Mesilla and Hueco Bolson was made by Figuers (1987). He conducted a seismic refraction/reflection survey at the northern end of the Franklin Mountains at Anthony Gap. He also used other seismic data collected previously in the Mesilla Bolson. His purpose was to analyze important geologic structures such as Western Boundary Fault and the East Boundary Fault at the edges of the Franklin Mountains Figuers (1987) relied on velocity information from other seismic studies (Mattick, 1967) to constrain his model as well as sonic logs to estimate the velocities of different stratigraphic units in the Hueco Bolson.

Collins and Raney (1994) described the Tertiary and Quaternary tectonics of the Hueco Bolson, based on seismic reflection and well log studies, air-photos, surface geological mapping and measurements on fault scraps. The study produced isopach maps (Figures 2.1and 2.2) of the lower and upper basin fill sequences. They suggested that the southeastern portion of the Hueco Bolson subsided more during the early phase of basin evolution (deposition of lower fill sequence), while the northwestern portion of the bolson subsided more during deposition of the

upper fill sequence. They estimated 150-200 m of Cenozoic basin fill on the east and northeast bolson margins and ~ 2850 m in the central bolson.

Collins and Raney (1994) concluded that the most active faults since the Pleistocene have been the East Franklin Mountains fault and the Amargosa fault. They also indicated that the Hueco bolson is composed of two distinct subbasins. The northwest basin developed along north-striking normal faults, and the southeast basin was developed along northwest striking normal faults. The southeast basin appears to have extended more rapidly during early Cenozoic development of the Rio Grande rift (see Figures 2.1 and 2.2).

Another notable seismic study was the regional scale wide angle reflection/refraction study of Averill et al (2013). This study was conducted in the southernmost part of New Mexico and westernmost Texas and was able to model the upper part of the crust of the Rio Grande rift. The 205 km east-west seismic transect also crossed a portion of the southern Basin and Range province. (Figure 2.4). The study revealed two velocity models based on P-wave arrival times. One model shows low to high velocity zones that correlate with Tertiary to Holocene Basin and Range structure. In this model, topographic basins are 10-20 km wide 1-3 km deep and correlate with 1.5-4 km/sec velocities, and topographic ranges correspond to velocities greater than 4-5.5 km/sec as shown in Figure 2.5. The second structural model is based on first arrival tomographic modeling that produced the crustal image shown in Figure 2.6. This tomographic model was derived using the method of Hole (1992). This model helps to interpret Mesozoic to early Tertiary features.

The tomographically derived velocity model for the Rio Grande segment shows the Mesilla Bolson and the Hueco Bolson as the broadest and deepest basins along the seismic

profile. The Mesilla Bolson is a ~35-km wide, asymmetric basin. Velocities identified in the western portion of the Mesilla Bolson range from 2.4 to 4.0 km/sec to depths of 1.5 km.

Material velocities in the eastern part of the Mesilla Bolson are no less than 3 km/sec, suggesting very little upper Cenozoic fill in this portion of the basin. The Hueco Bolson was identified as an asymmetric graben with a maximum thickness of ~3 km. This tomographic section shows a velocity deflection that was identified as the East Franklin Mountain fault that bounds the western Hueco Bolson.

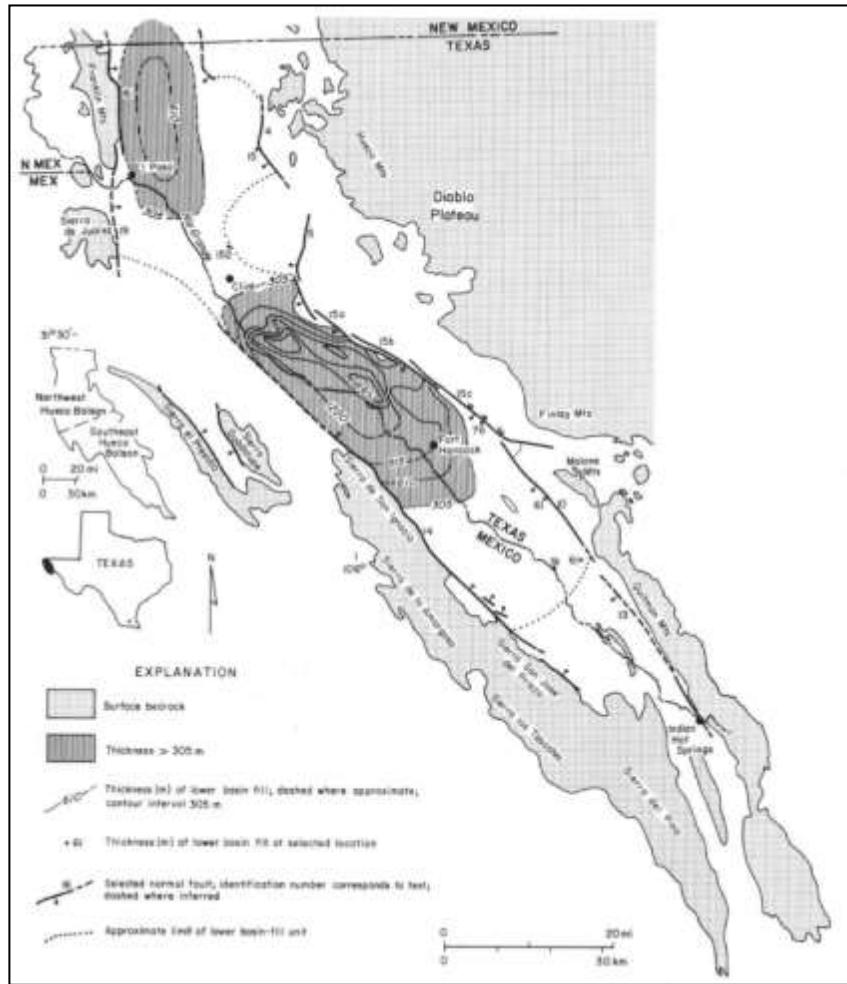


Figure 2.1 Isopach map of Cenozoic lower basin fill. Constructed from seismic interpretations (Modified from Collins and Raney, 1994)

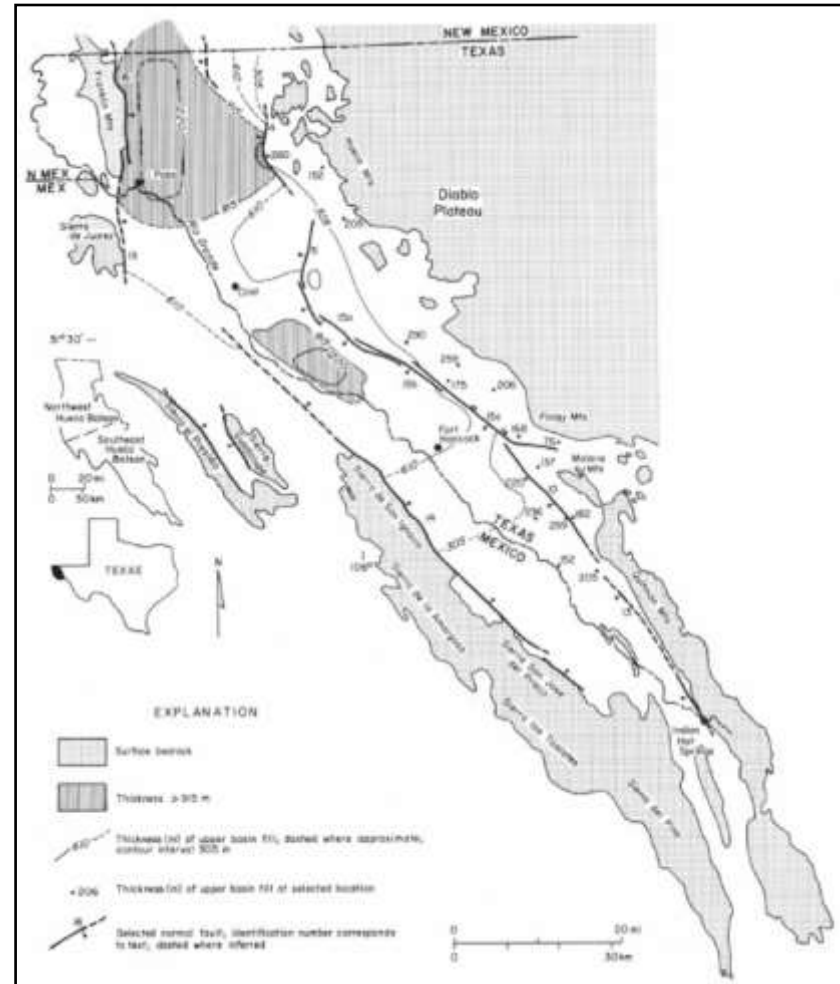


Figure 2.2. Isopach map of Cenozoic upper basin fill. Interpretations of seismic data were used to construct map. (Modified from Collins and Raney, 1994).

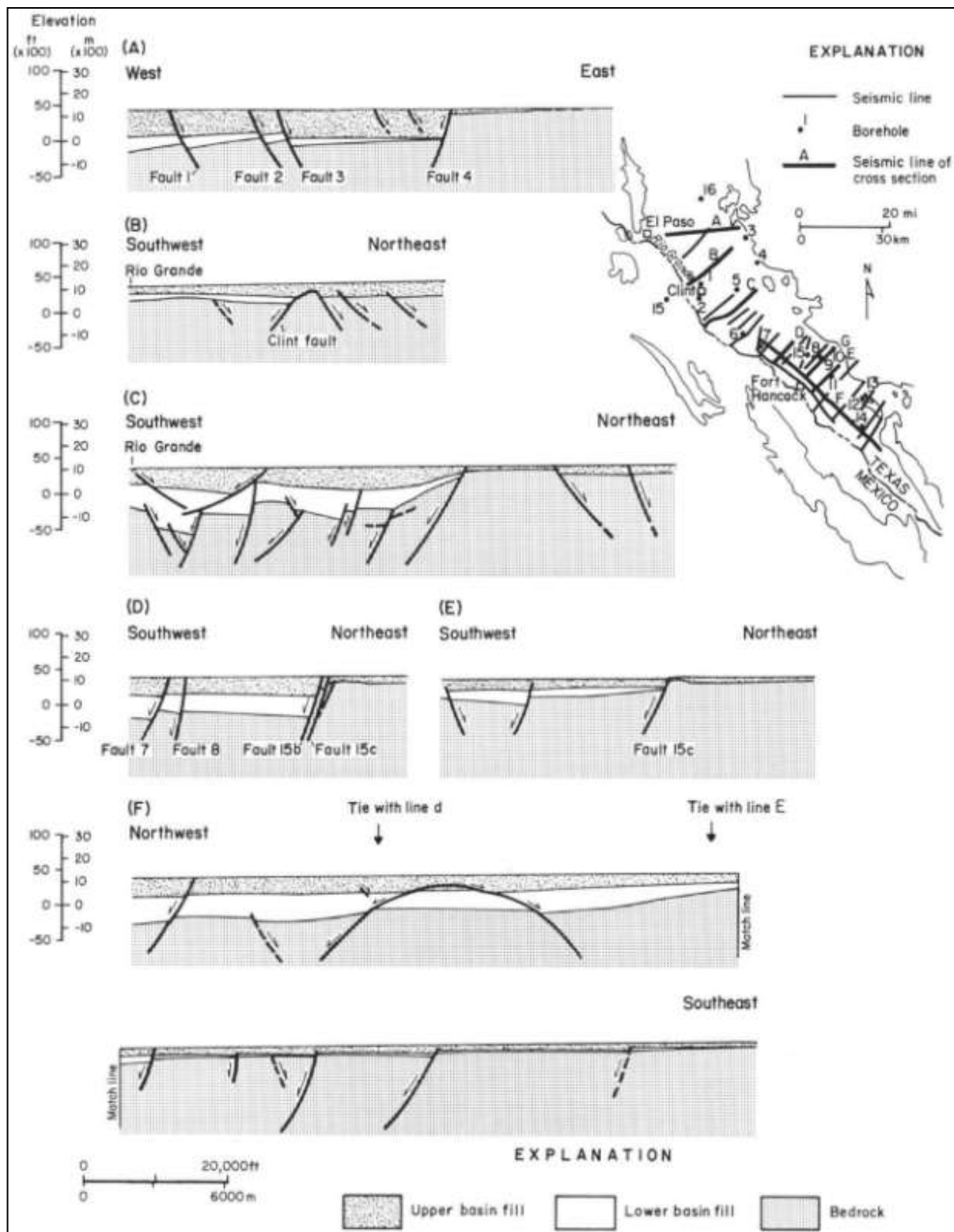


Figure 2.3. Cross sections interpreted from seismic data throughout the Hueco bolson. Sections A through F correspond to seismic locations A through F on index map. Modified from Collins and Raney (1994).

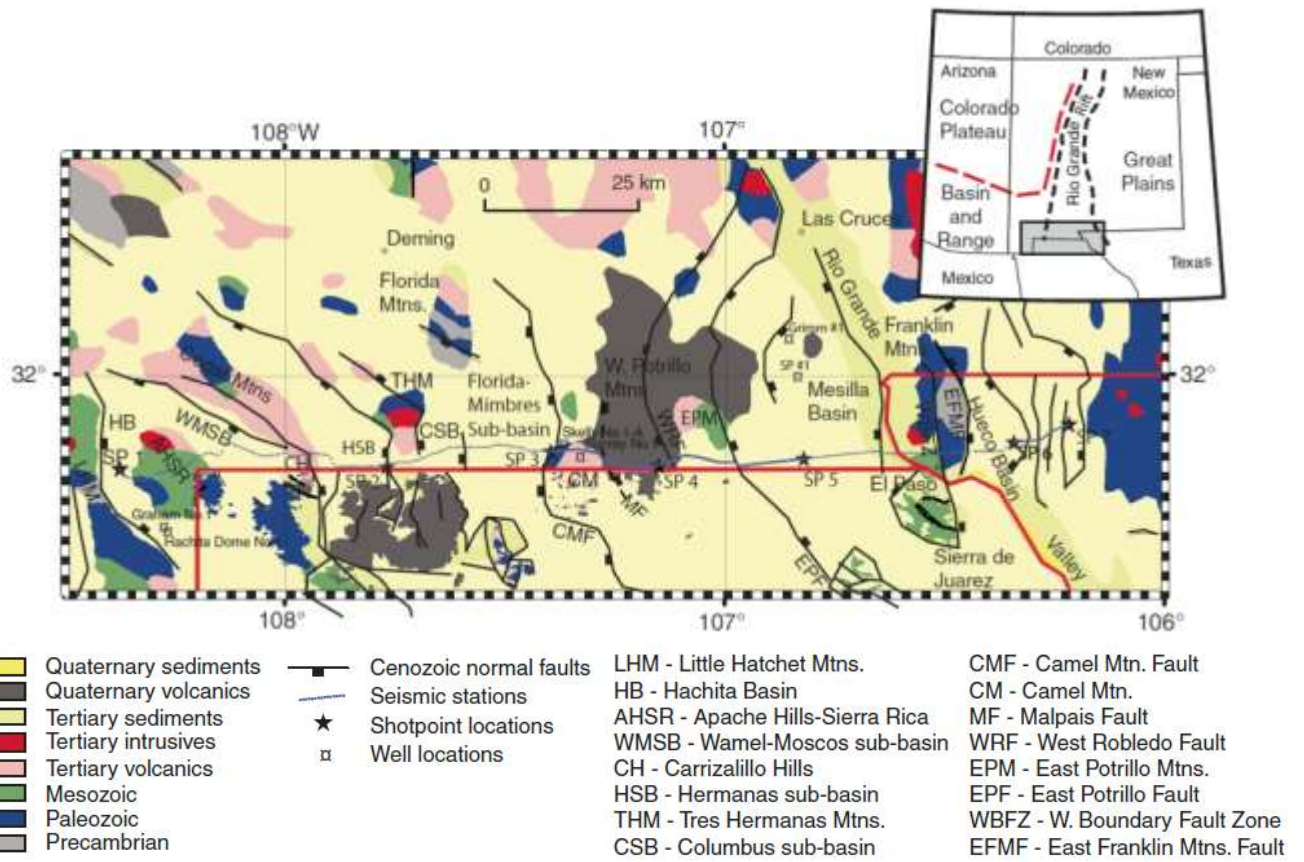


Figure 2.4. Geological map of Averill's study area with location of seismic survey. Surface geology labeling modified for consistency across state and national borders for New Mexico (after Green and Jones, 1997), Texas (after Hartmann and Scranton (1992), and the state of Chihuahua, Mexico (after INEGI, 1981). Gray box in regional inset map shows boundary of study area. The seismic survey crosses series of late Cenozoic basins and ranges. Modified from Averill (2013).

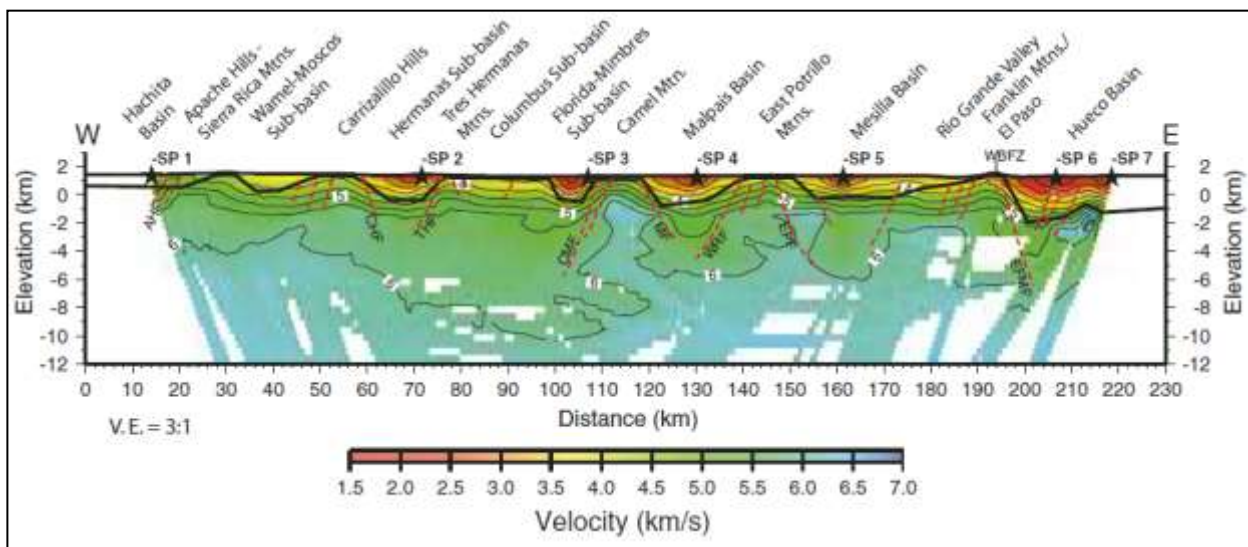


Figure 2.5 Tomographic velocity model, shows interpretation of late Tertiary geological features. Velocity model was calculated with a 0.5 km grid interval.

Abbreviations: AHF—Apache Hills fault; CHF—Carrizalillo Hills fault; THF—Tres Hermanas Fault; CMF— Camel Mountain Fault; MF— Malpais fault; WRF—West Robledo fault; EPF—East Potrillo fault; EFMF—East Franklin Mountain fault. V.E.—vertical exaggeration. Modified from Averill (2013)

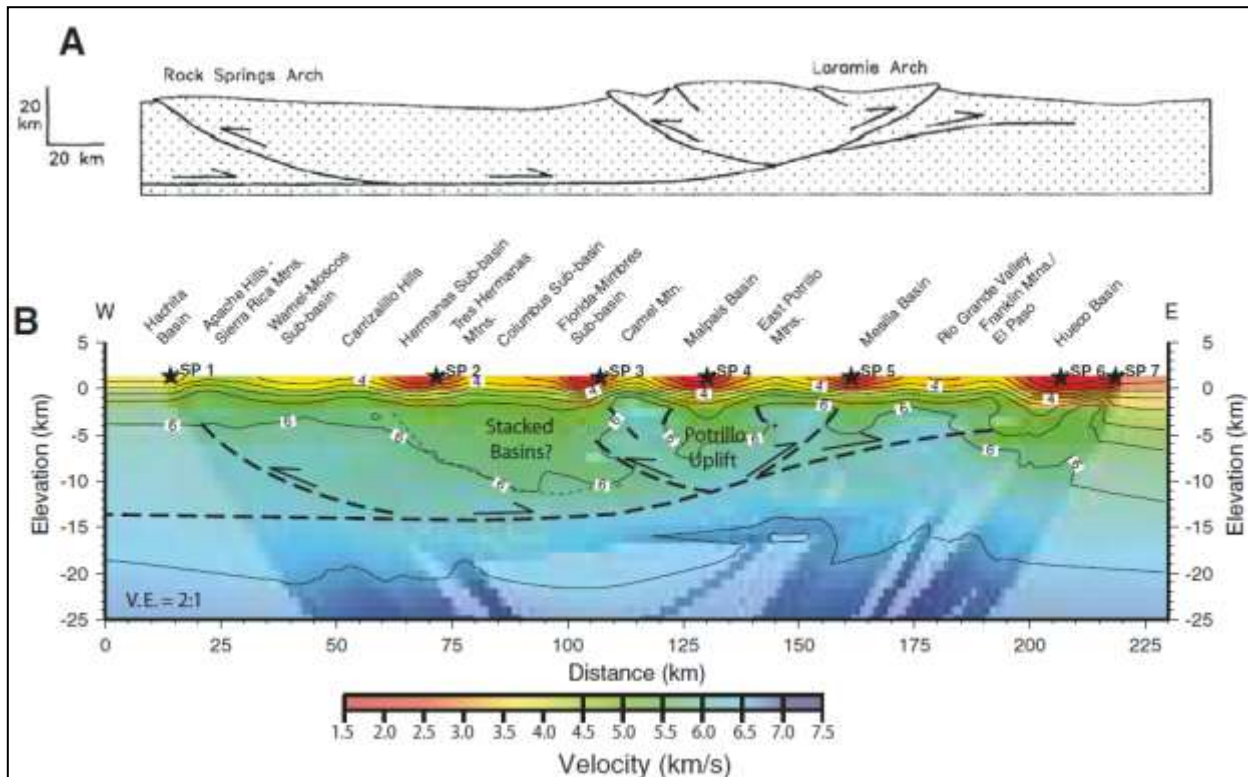


Figure 2.6. Tomographic velocity model showing interpretation of Mesozoic to early Tertiary tectonic features. (A) Diagram showing interpreted geometry of a Laramide arch in Wyoming from Erslev (1993).

These geometries are interpreted to be analogous to those observed in southern New Mexico. (B) Tomographic velocity model calculated at a 1 km grid interval. Areas of subdued color in the model have no ray coverage for constraining velocity values. Stars indicate shotpoint (SP) locations. Locations of basins and mountain ranges at the surface are annotated. V.E.—vertical exaggeration. Modified from Averill (2013).

## 2.5 References

- Averill, M.G., Miller, K.C., 2013. Upper crustal structure of the southern Rio Grande rift: A composite record of rift and pre-rift tectonics. Geological Society of America Special Papers 494, 463–474.
- Avila, V.M., 2011. An investigation of the seismic hazards of the El Paso-Juarez region: The nature and extent of the southern east Franklin Mountains fault zone (M.S.). The University of Texas at El Paso, United States -- Texas.
- Avila, V. M., D. I. Doser, O. S. Dena-Ornelas, M. M. Moncada, and S. S. Marrufo-Cannon, 2016, Using geophysical techniques to trace active faults in the urbanized northern Hueco Bolson, West Texas, USA, and northern Chihuahua, Mexico: Geosphere, v. 12, no. 1, p. 264–280, doi:10.1130/GES01228.1.
- Barrie, F.J., 1975. A gravimetric survey of south-central New Mexico and West Texas (M.S.). The University of Texas at El Paso, United States -- Texas.
- Budhathoki, P., 2013, Integrated geological and geophysical studies of the Indio Mountains and Hueco bolson, west Texas, Ph.D.: United States -- Texas, The University of Texas at El Paso, 124 p.
- Collins, E.W., Raney, J.A. 2000. Geologic map of West Hueco Bolson, El Paso Region, Texas. Bureau of Economic Geology. The University of Texas at Austin, Texas 78713-8924
- Collins, E. W., and J. A. Raney, 1994, Tertiary and Quaternary tectonics of the Hueco bolson, Trans-Pecos Texas and Chihuahua, Mexico, *in* Geological Society of America Special Papers: Geological Society of America, p. 265–282.
- Barrie, F.J., 1975. A gravimetric survey of south-central New Mexico and West Texas (M.S.). The University of Texas at El Paso, United States -- Texas.
- Burgos, A., 1993. A gravimetric study of the thickness of the unconsolidated materials in the Hueco Bolson Aquifer, Juárez Area, Chihuahua, Mexico, Master's thesis / University of Texas at El Paso.
- Figuers, S.H., 1987. Structural Geology and Geophysics of the Pipeline Complex, Northern Franklin Mountains, El Paso, Texas (D.G.S.). The University of Texas at El Paso, United States -- Texas.
- Gillespie, C.L., 2002. Integrated geophysical, geological and remote sensing study of selected basins in the Rio Grande rift (Ph.D.). The University of Texas at El Paso, United States -- Texas.

- Hadi, J., 1991. A study of the structure and subsurface geometry of the Hueco Bolson, Master's thesis / University of Texas at El Paso.
- Imana, E.M.C., 1994. A comparative study of Lokichar, Kerio, and Mesilla Basins. MS thesis / University of Texas at El Paso.
- Imana, E.M.C., 2002. The Mesilla Bolson: an integrated geophysical, hydrological, and structural analysis utilizing free air anomalies. PhD thesis / University of Texas at El Paso.
- Khatun, S., 2003. A precision gravity study of the Southern Mesilla bolson, West Texas (M.S.). The University of Texas at El Paso, United States -- Texas.
- Marrufo, S.S., 2011. An integrated geological and geophysical study of the fresh and brackish water boundary in the Hueco Bolson, West Texas (M.S.). The University of Texas at El Paso, United States -- Texas.
- Mattick, R. E., 1967, A seismic and gravity profile across the Hueco bolson, Texas: US Geological Survey Professional Paper, p. 85–91.
- Moncada, M.M., 2011, Estudios geofísicos para la recarga de acuíferos en la zona norte del Estadode Chihuahua, [B.S. thesis]: Ciudad Juárez, Universidad Autónoma de Ciudad Juárez, 87 p.
- Hawley, J. W., and J. F. Kennedy, 2004, Creation of a digital hydrogeologic framework model of the Mesilla Basin and southern Jornada del Muerto Basin: New Mexico Water Resources Research Institute, New Mexico State University.
- Hole, J. A., 1992, Nonlinear high-resolution three-dimensional seismic travel time tomography: Journal of Geophysical Research: Solid Earth, v. 97, no. B5, p. 6553–6562, doi:10.1029/92JB00235.
- Ramberg, I.B., Cook, F.A., Smithson, S.B., 1978. Structure of the Rio Grande rift in southern New Mexico and West Texas based on gravity interpretation. Geological Society of America Bulletin 89, 107. doi:10.1130/0016-7606(1978)89<107:SOTRGR>2.0.CO;2
- Sellepack, B.P., 2003. The stratigraphy of the Pliocene-Pleistocene Santa Fe Group in the southern Mesilla Basin. MS Thesis
- Thapalia, A., 2014, Geochemical studies of backfill aggregates, lake sediment cores and the Hueco Bolson Aquifer, Ph.D.: United States -- Texas, The University of Texas at El Paso, 144 p.

## CHAPTER 3

### 3.1 Location of the Study Area.

The study focuses on the Mesilla and Hueco basin which are the main aquifers for the city of El Paso, Texas. The study area is located in the southernmost part of New Mexico, the western part of Texas, and the northern part of Chihuahua, Mexico (Figure 4.1). The Mesilla basin is a broad ~35 km wide, asymmetric basin that is bounded by the Potrillo Mountains on the West and extends to the western flank of the Franklin Mountains to the East. The Hueco basin is also an asymmetric graben that is confined by the Hueco Mountains to the East. The Hueco basin floor dips westward into the Franklin Mountains, and is bounded by the East Franklin Mountain fault. Hueco basin extends south into Ciudad Juarez and reaches south to the Presidio and Sierra de Guadalupe in Northern Chihuahua. These basins contain thin upper Quaternary fluvial deposits of the inner Rio Grande Valley over thick intermontane basin sedimentary fill.

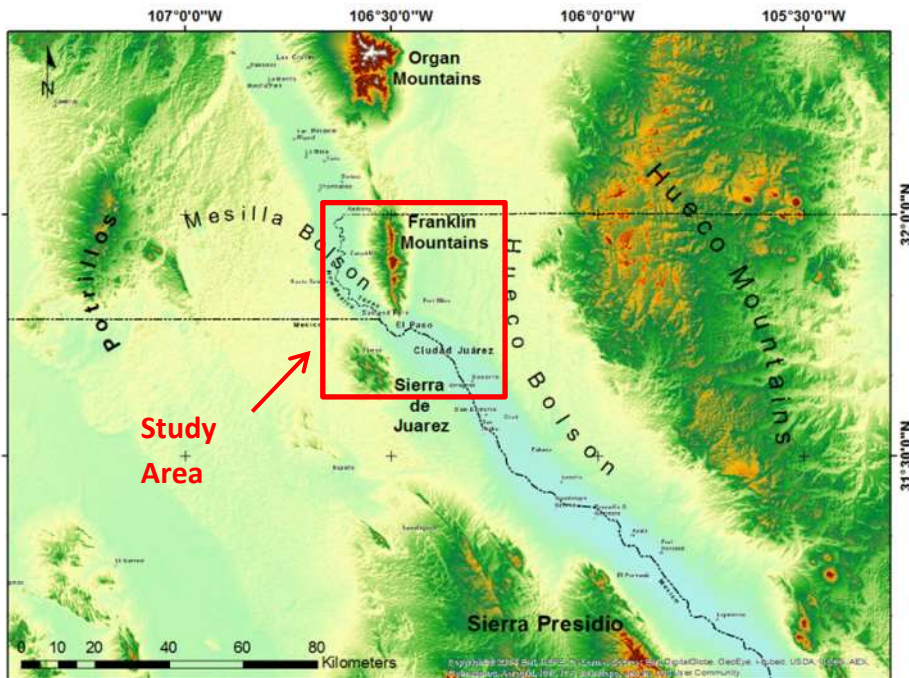


Figure 3.1. Shows the location of the study area for the Hueco and Mesilla Bolson

## CHAPTER 4

### 4.1 Regional Tectonic Setting

The outcrops around the study area range from Precambrian to Holocene in age. The region is located in the southern part of the Rio Grande Rift tectonic province, and the modern geologic structures are predominantly the result of Tertiary and Quaternary extension (Keller 1990; Haller 2002). Rio Grande Rift tectonic features are characterized by north-south trending deep structural basins between tilted fault block ranges and Tertiary volcanic highlands. This major continental rift zone extends through central New Mexico from southern Colorado to west Texas and northern Chihuahua (Chapin and Seager 1975, Hawley 1978). The Rio Grande Rift is characterized by young volcanic activity, high heat flow anomalies, large intermontane basins, and young episodes of normal faulting (Seager and Morgan, 1979; Keller et al., 1990; Chapin and Cather, 1994)

The pre-Tertiary history of the region includes formation of the Precambrian basement made of rocks that range in age from 1.8 to 1.6 Ga and episodes of pervasive intracratonic tectonism at about 1.45-1.35 Ga (Karlstrom et al., 2004), and deposition of dominantly marine sedimentary sequences during Paleozoic and Mesozoic time in both platformal and basinal settings (Greenwood et al., 1977; Dickinson 1981; Fig 2). The Paleozoic Pedregosa and Orogrande Basins are characterized by the thickest sedimentary rocks. (Greenwood et al., 1977). The Chihuahua trough was a NW-SE trending basin that formed by the deposition of sediments during Jurassic and Cretaceous periods (Figure 4.1). This basin was located in westernmost Texas, southern New Mexico and northern Chihuahua (Henry et al., 1985) and was bounded by the Aldama Platform to the southwest and by the Diablo Platform to the northeast. The stratigraphy in general is composed of siliciclastic rocks built on a base of Jurassic evaporates

(Gries, 1970). This period of sedimentation was followed by the Laramide orogeny, which began in late Cretaceous time and lasted into the early Eocene. (Chapin and Cather, 1981; Seager 2004). The Chihuahua trough basin was strongly deformed, with contractional structures associated with the Laramide orogeny and the extensional structures within the basin related to Rio Grande Rift. The transition period from the Laramide orogeny to Rio Grande rift extension showed very little tectonic activity (Chapin 1974; Aldrich et al., 1986). The present extensional environment began 30-32 Ma (Aldrich et al., 1986; Newcomer and Giordano, 1986) and has been identified to have occurred in two separate phases (Aldrich et al., 1986; Keller et al., 1990). The first “early rift” phase formed northwest striking faults and basins and produced volcanism. The ‘late rift’ phase, which began at 10 Ma and continues to operate today (Keller et al., 1990), comprises approximately east-west extension and the development of narrow fault-bound ranges and associated basins that trend north-south. This second phase of rifting is also characterized by a large reduction of volcanic activity (Mack, 2004). The Rio Grande Rift is currently active today producing Quaternary normal faulting, such as faults concealed in the urbanized areas of El Paso. One purpose of this thesis is to assess how these faults control the basin geometry and their role in seismic hazards and groundwater flow.

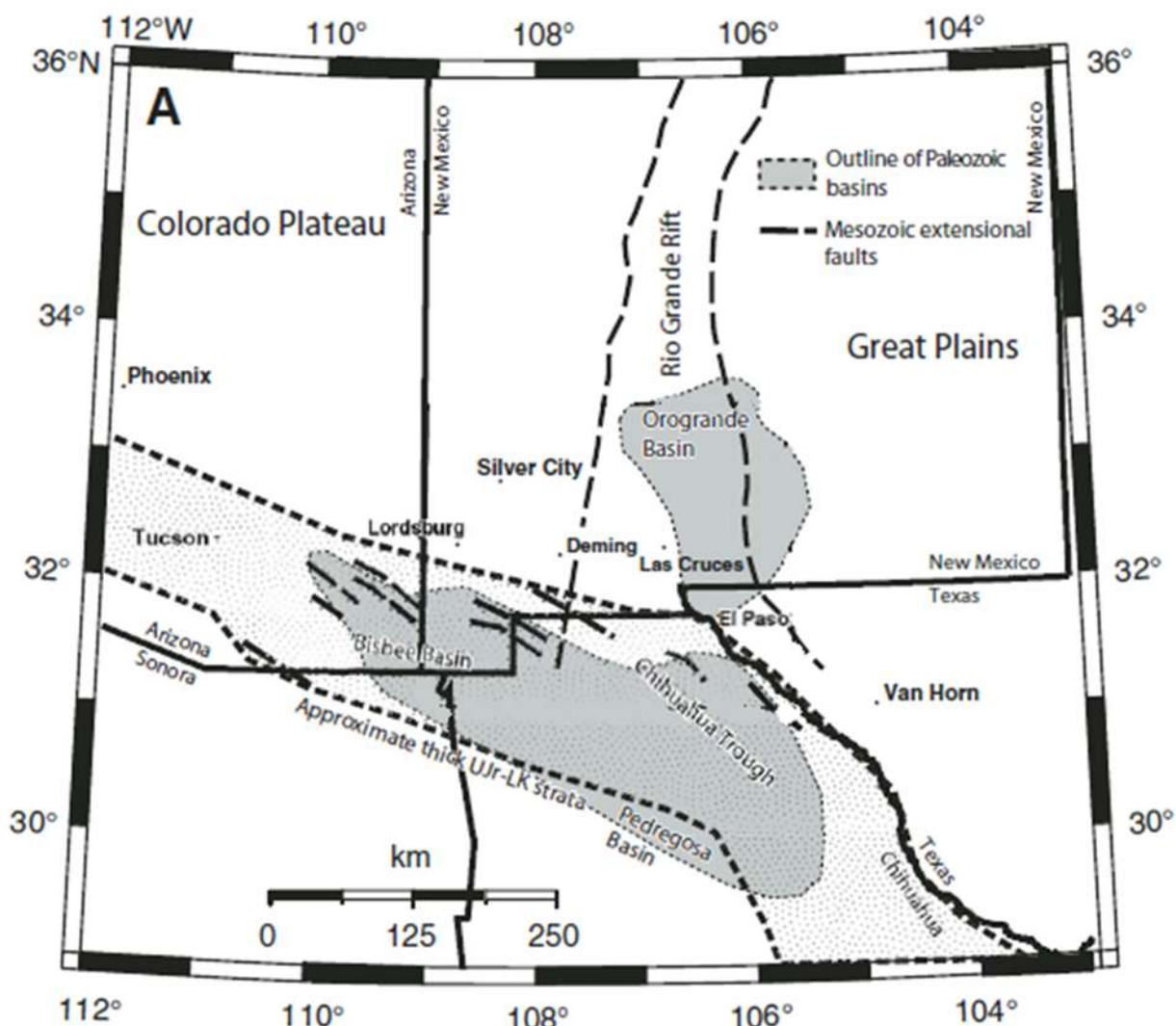


Figure 4.1. Major Paleozoic to Cenozoic tectonic features in the study area. Shaded areas show outline of the Paleozoic Pedregosa and Orogrande Basins (after Greenwood et al., 1977).

Stippled region shows areal extent of Upper Jurassic to Lower Cretaceous (UJr-LK) deposits in the Bisbee Basin and Chihuahua Trough (after Seager, 2004). Modified from Averill et al.(2013).

## 4.2 References

- Aldrich, M.J., Chapin, C.E., Laughlin, A.W., 1986. Stress history and tectonic development of the Rio Grande Rift, New Mexico. *J. Geophys. Res.* 91, 6199–6211. doi:10.1029/JB091iB06p06199
- Averill, M.G., Miller, K.C., 2013. Upper crustal structure of the southern Rio Grande rift: A composite record of rift and pre-rift tectonics. *Geological Society of America Special Papers* 494, 463–474.
- Chapin, C.E., 1974, Three-fold tectonic subdivision of the Cenozoic in the Cordilleran foreland of Colorado, New Mexico and Arizona, Geological Society of America, Abstracts with Programs, v. 6, no. 5, p. 433
- Chapin, C. E. and Cather, S. M., 1994, Tectonic setting of the axial basins of the northern and central Rio Grande rift, in Keller, G. R. and Cather, S. M., eds., *Basins of the Rio Grande Rift: Structure, Stratigraphy, and Tectonic Setting*, Geological Society of America, Special Paper 291, p. 5-25.
- Dickinson, W. R., 1981. Plate Tectonic Evolution of the Southern Cordilleran. In: Dickinson, W. R., Payne, W. D., (Eds.). *Relation of Tectonics to Ore Deposits in the Southern Cordilleran*. Arizona Geological Society Digest 14, 113-136.
- Greenwood, E., Kottolowski, F.E., and Thompson, S., III, 1977, Petroleum potential and stratigraphy of Pedrogosa Basin: Comparison with Permian and Orogrande Basins: American Association of Petroleum Geologists Bulletin, v. 61, p. 1448–1469.
- Gries, J. C., Haenggi, W. T., 1970. Structural evolution of the eastern Chihuahua tectonic belt. In: Seewald, K., Sundein, D., (Eds.). *The Geologic Framework of the Chihuahua Tectonic Belt*. WestTexas Geological Society Publication, 71-59, 119-137.
- Haller, K.M. Wheeler, R.L. and Ruckstales, KS. (2002). Documentation of changes in fault parameters for the 2002 National Seismic Hazard maps –Conterminous United States except California. U.S Geological Survey Open-file report 02-467, v. 1 on  
<http://pubs.usgs.gov/of/2002/ofr-02-467/>
- Hawley, J. W., 1978, Guidebook to the Rio Grande rift in New Mexico and Colorado: New Mexico Bureau of Mines and Mineral Resources Circular 163, 239 p.
- Henry, C. D., and Price, J. G., 1985, Summary of the tectonic development of Trans Pecos Texas: The University of Texas at Austin, Bureau of Economic Geology Miscellaneous Map No. 36, 8 p.

Keller, G.R., Morgan, P., Seager, W.R., 1990. Crustal structure, gravity anomalies and heat flow in the southern Rio Grande rift and their relationship to extensional tectonics. *Tectonophysics, Heat and Detachment in Continental Extension* 174, 21–37. doi:10.1016/0040-1951(90)90382-I

Karlstrom, K.E., Amato, J.M., Williams, M.L., Heizler, M., Shaw, C.A., Read, A.S., and Bauer, P., 2004, Proterozoic tectonic evolution of the New Mexico region: A synthesis, in Mack, G.H., and Giles, K.A., eds., *The Geology of New Mexico, A Geologic History: New Mexico Geological Society Special Publication 11*, p. 1–34.

Mack, G.H., 2004, Middle and late Cenozoic crustal extension, sedimentation, and volcanism in the southern Rio Grande rift, Basin and Range, and southern transition zone of southwestern New Mexico, in Mack, G.H., and Giles, K.A., eds., *The Geology of New Mexico, A Geologic History: New Mexico Geological Society Special Publication 11*, p. 389–406.

Newcomer, R.W., Jr., and Giordano, T.H., 1986, Porphyry-type mineralization and alteration in the Organ mining district, south-central New Mexico: *New Mexico Geology*, v. 8, p. 83–86.

Ramberg, I.B., Cook, F.A., Smithson, S.B., 1978. Structure of the Rio Grande rift in southern New Mexico and West Texas based on gravity interpretation. *Geological Society of America Bulletin* 89, 107. doi:10.1130/0016-7606(1978)89<107:SOTRGR>2.0.CO;2

Seager, W.R., 2004, Laramide (Late Cretaceous–Eocene) tectonics of southwestern, New Mexico, in Mack, G.H., and Giles, K.A., eds., *The Geology of New Mexico, A Geologic History: New Mexico Geological Society Special Publication 11*, p. 183–202.

Seager, W.R. and Morgan, P. (1979) Rio Grande Rift in southern New Mexico, west Texas , and northern Chihuahua: in Riecker, R.E., [editor], *Rio Grande rift : Tectonics and Magmatism*; American Geophysical Union, Washington. D.C., p. 87-106

Seager, W. R., 1975, Charles E. Chapin, in Guidebook of the Las Cruces Country: twenty-sixth field conference, November 13, 14 and 15, 1975: New Mexico Geological Society, p. 297.

## CHAPTER 5

### 5.1 Gravity Methodology

The gravity method involves measuring the earth's gravitational field at specific points to determine the location of subsurface density variations. These density variations can then be related to changes in geologic structures such as faults and basin geometry.

### 5.2 Gravity Field Survey

There are a large number of gravity stations around the Mesilla and Hueco Bolsons that form a starting gravity data base that is used for this study. Although the data base is extensive there are a few regions where more stations were required to help constrain changes in bedrock geology especially in the urbanized portion of Hueco and Mesilla Basin.

The gravity survey completed for this dissertation consisted in measuring approximately 500 new gravity stations as seen in figure 5.1. The instrumentation employed for the survey consisted of a Lacoste and Romberg Model G gravimeter that has a 0.005 mGal resolution. Elevation control was established using with a differential GPS receiver (*Topcon GB-1000*) capable of 5 mm vertical and 3 mm horizontal precision. I used the absolute gravity station at Kidd Memorial Seismic Observatory, located on campus of The University of Texas at El Paso, as my reference station. All gravity stations I measured are referenced to this station, by taking a reading at the Kidd station at the beginning and at the end of each day that I collected gravity data. This was also done to account for the instrumental drift and Earth tide

### 5.3 Final gravity database

The final gravity database for Mesilla and Hueco bolson consisted in adding the new data I collected with recent gravity studies in El Paso (e.g. Budhathoki, 2013), and additional gravity data from Ciudad Juárez that was collected by Universidad Autonoma de Ciudad Juarez, The final gravity data base was assembled with the help of Carlos Montana with the intention of insuring that the new data collected is consistent with previous data sets and that all data in the data base used the same reference datum, WGS84. Figure 5.2 shows the final database.

### 5.4 Gravity Data Processing

The observed gravity data collected in the field is a sum of the following contributors, according to Blakely (1995):

Observed gravity = attraction of the reference ellipsoid  
+ effect of elevation above sea level (*free-Air*)  
+ effect of “normal” mass above sea level (*Bouguer and Terrain*)  
+ time-dependent variations (*tidal*)  
+ effect of moving platform (*Eötvös*)  
+ effect of masses that support topographic loads (*Isostatic*)  
+ effect of crust and upper mantle density variations (“*geology*”)

Eq. 1

Once we correct for all effects but the last term we have an anomaly that represents crust and upper mantle density variations and can be modeled to determine possible geologic structures. The Complete Bouguer Anomaly is a result of the following equation:

$$\Delta_{gcb} = g_{obs} - g_{fa} - g_{sb} - g_t - g_o \quad \text{Eq. 2}$$

Where:

$\Delta_{gcb}$  = Complete Bouguer Anomaly

$g_{obs}$  = Observed Gravity

$g_{fa}$  = Free Air Correction (0.386 mGal/m)

$g_{sb}$  = Bouguer Correction ( $0.0419\rho$  mGal/m) where  $\rho$  = assumed average rock density  $g/cm^3$

$g_t$  = Terrain Corrections (generally based on a Digital Elevation Model (DEM))

$g_o$  = Theoretical Gravity

Terrain Corrections, which compensate for the measurements made near topographic features, were calculated using a combination of the method described by Nagy (1966) and Kane (1962) which consists of using a Digital Elevation Model (DEM). A UTM Zone 13 WGS84 DEM was gridded using Oasis Montaj software in order attain the topography used for the Complete Bouguer Anomaly.

## 5.5 Residual Anomaly

Although Complete Bouguer Anomaly process removes the gravitational effect of topography to a datum of sea level, the anomalies caused by the compensating masses are generally long in wavelength and approximately negatively correlated with long-wavelength attributes of topography (Blakely, 1995). In order to remove these long-wavelength features from the gravity measurements a 3<sup>rd</sup> order polynomial surface is fitted to the Complete Bouguer Anomaly and then subtracted from it to produce a Residual Bouguer Anomaly.

## 5.6 Boundary Analysis

The final objective of this analysis is to determine the structures within sedimentary basins. Ideally the anomalies due to these structures should be isolated from the surrounding geologic environment. For this purpose the Horizontal Gradient Magnitude (HGM) was applied.

This method has been commonly used to locate the steepest parts of gradients associated with near-vertical physical-property boundaries, such as faults. (Grauch et al., 2002; Blakely and Simpson, 1986; Cordell and Grauch, 1985; Heywood, 1992). The HGM is applied directly to the residual Bouguer anomaly grid in order to delineate the structures within the basin. The FORTRAN codes to run HGM are in the form of Geosoft executables (GX's) that are used in Geosoft's Oasis Montaj<sup>TM</sup> geophysical data processing system and were provided by USGS..

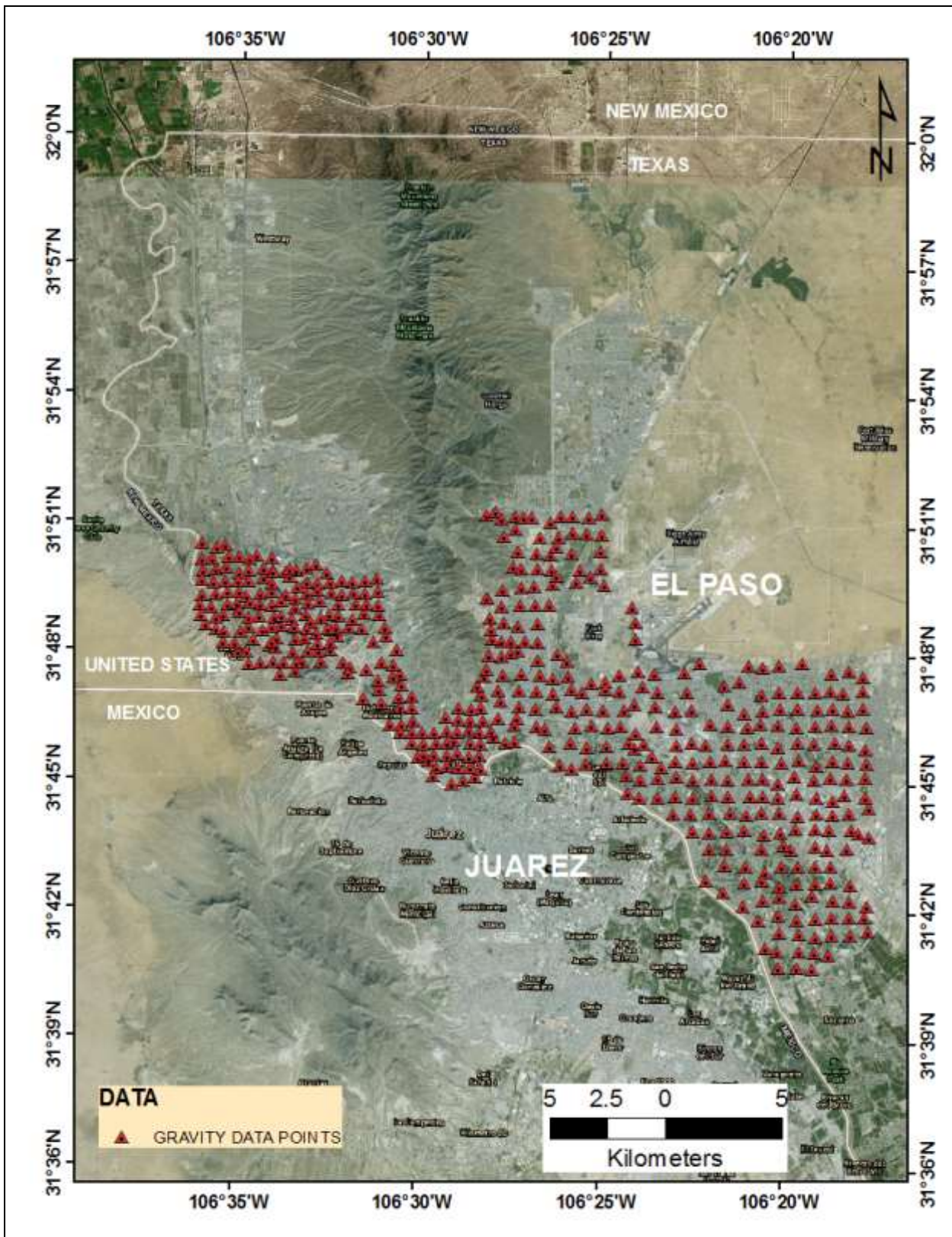


Figure 5.1 New gravity stations (red triangles) collected in the urbanized area of El Paso, TX.

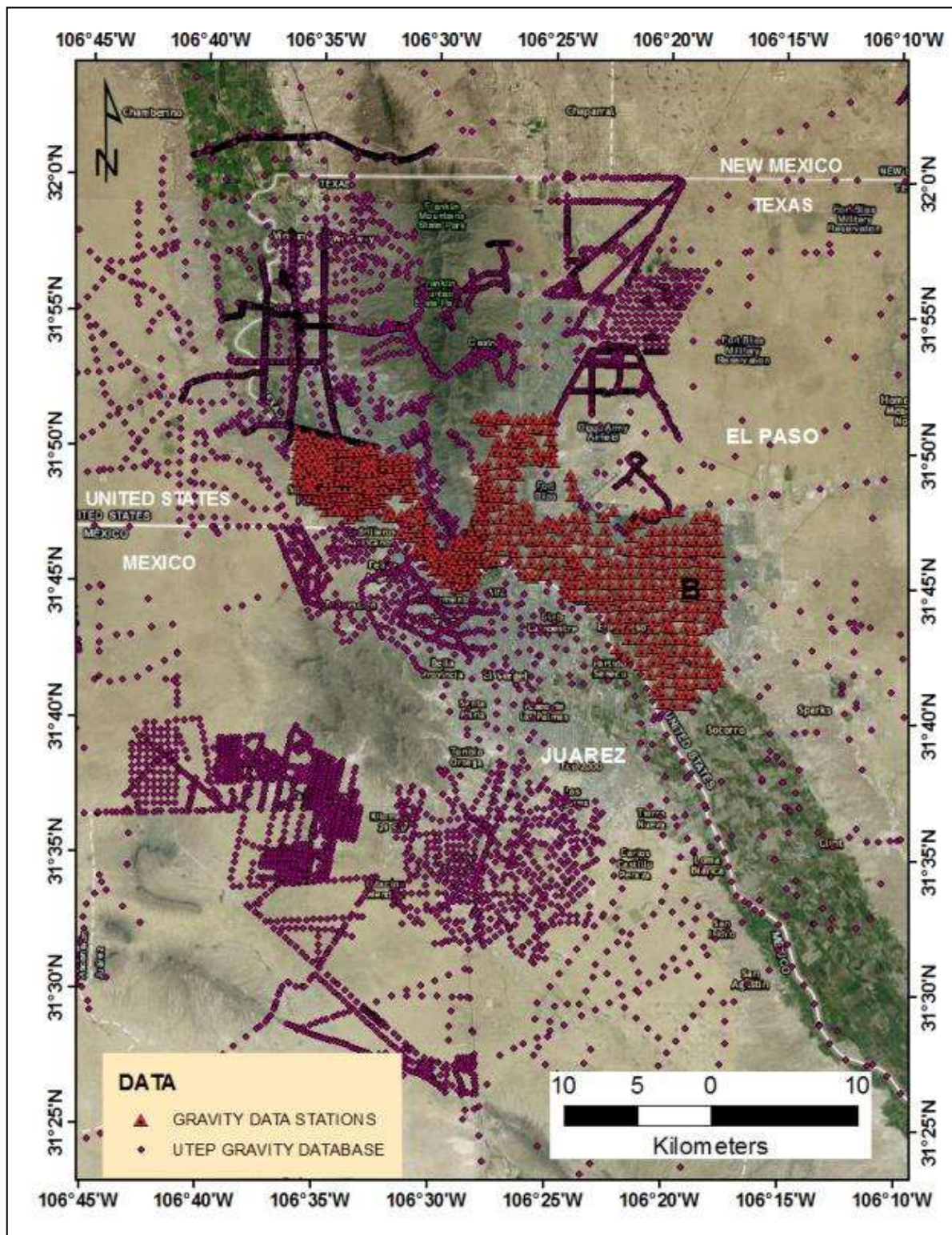


Figure 5.2 Gravity stations added to existing UTEP gravity database (purple symbols).

## 5.7 References

- Baranov, V., 1957, A new method for interpretation of aeromagnetic maps; pseudo-gravimetric anomalies: *Geophysics*, v. 22, no. 2, p. 359–382, doi:10.1190/1.1438369.
- Blakely, R. J., 1995, Potential theory in gravity and magnetic applications: Cambridge [England]; New York, Cambridge University Press, \*\*pp..
- Blakely, R. J., and R. W. Simpson, 1986, Approximating edges of source bodies from magnetic or gravity anomalies: *Geophysics*, v. 51, no. 7, p. 1494–1498, doi:10.1190/1.1442197.
- Budhathoki, P., 2013, Integrated geological and geophysical studies of the Indio Mountains and Hueco Bolson, West Texas: \*\*p.
- Cordell, L., and V. Grauch, 1985, 16. Mapping Basement Magnetization Zones from Aeromagnetic Data in the San Juan Basin, New Mexico, in *The Utility of Regional Gravity and Magnetic Anomaly Maps*: Society of Exploration Geophysicists, General Series, p. 181–197.
- Grauch, V. J. S., C. S. Johnston, and others, 2002, Gradient window method: a simple way to separate regional from local horizontal gradients in gridded potential-field data, in *Society of Exploration Geophysicists Technical Program Expanded Abstracts*: p. 762–765.
- Heywood, C. E., 1992, Isostatic residual gravity anomalies of New Mexico, USGS Numbered Series 91-4065: U.S. Geological Survey ; Books and Open-File Reports [distributor], Water-Resources Investigations Report, \*\* pp..
- Jacoby, W., and P. L. Smilde, 2009, Gravity interpretation fundamentals and application of gravity inversion and geological interpretation: Berlin; Heidelberg, Springer.
- Kane, M., 1962, A comprehensive system of terrain corrections using a digital computer: *Geophysics*, v. 27, no. 4, p. 455–462, doi:10.1190/1.1439044.
- Nagy, D., 1966, The prism method for terrain corrections using digital computers: pure and applied geophysics, v. 63, no. 1, p. 31–39.
- Swain, C. J., 1976, A FORTRAN IV program for interpolating irregularly spaced data using the difference equations for minimum curvature: *Computers & Geosciences*, v. 1, no. 4, p. 231–240, doi:10.1016/0098-3004(76)90071-6.

## CHAPTER 6

### 6.1 Hueco Bolson Gravity Maps

The complete Bouguer anomaly (CBA) map for the large study area (Figure 6.1) shows the lateral variation in density in the Hueco Bolson. It gives a typical response for a rift basin which consist of high density rocks associated with gravity highs, such as the Franklin Mountains, and gravity lows occur where there are large volumes of low-density deposits, such as the ones found in The Hueco Bolson which consist of low unconsolidated sediments. The white lines shown in Figure 6.1 show Quaternary faults mapped at the surface, by Collins and Raney (2000). The red dashed line indicates the edge of Laramide thrusting as mapped by Collins and Raney (2000). The CBA map distinctly shows a change in trend from north-south in the northern bolson to northwest-southeast in the southern bolson occurring between 31°33'N and 31°41'N in a region where the edge of Laramide thrusting is projected to pass through the bolson. The edge of Laramide thrusting may also influence the bend in the East Franklin Mountains fault (EFMF) near the U.S.-Mexican border. Uplifted Cretaceous bedrock mapped by Collins and Raney (2000) (blue lines, Figure 6.1) along the eastern edge of the bolson corresponds with a CBA high. This bedrock high may have served as the structural control that influenced segmentation of the bolson. The deepest low is associated with the southern bolson.

Figure 6.2 shows the residual Bouguer anomaly map for the large study area. The residual Bouguer anomaly is obtained by fitting a third order polynomial surface to the CBA data and then subtracting this surface from the CBA data. This process serves as a high pass filter to accentuate upper crustal features. Dashed white lines represent faults mapped on the basis of gravity and well log information based on the studies of Avila (2011), Avila et al. (2016) and Marrufo (2011) (Figure 6.2). The northern bolson shows up as a distinct low extending from the

Texas-New Mexico border to southern Ciudad Juarez ( $31^{\circ}33'N$ ) with a width of 10-15 km. The western edge of the low is constrained by the EFMF and the eastern side by several intrabasin faults that appear to extend farther into the urbanized region than mapped at the surface, as suggested by Avila et al. (2016). The Cretaceous bedrock uplift remains a conspicuous high, but the southern bolson low has decreased in amplitude. In this case the major change in the trend of the bolson appears to occur near the southern edge of the bedrock high.

Figure 6.3 shows the Horizontal Gradient Magnitude (HGM) map for the larger study area. The HGM applied to the residual Bouguer gravity field, to enhance the steeply dipping edges of geological features, such as faults or edges of igneous intrusions. The map shows that the EFMF follows the western edge of a HGM high and may extend as far south as  $31^{\circ}33'N$ . Fault M1, first mapped by Marrufo (2011) and extended by Avila et al (2016), corresponds well to the eastern edge of this HGM high. Several other intrabasin faults appear to extend to the south into the urbanized region of El Paso, but the patterns in the eastern bolson are complicated by the edge of Laramide thrusting. The HGM high associated with the eastern edge of the northern bolson begins to trend northwest-southeast near the edge of Laramide thrusting at about  $31^{\circ}4'N$ . In the easternmost portion of the bolson (east of  $106^{\circ}10'W$ ) the intrabasin faults and HGM values continue to trend north-south to  $31^{\circ}33'N$ , however data in this region are limited.

A separate set of maps were constructed for the most urbanized regions of El Paso and Ciudad Juarez within the northern bolson where the densest gravity data were located. These are shown in Figures 6.4 to 6.6.

Figure 6.4 shows the CBA for the local urbanized region. Note that the greatest lows are found in the northern region near the Texas-New Mexico border, in a region extending from

south of the El Paso airport to just North of the U.S.-Mexican border, and a region from  $31^{\circ}43'N$  to  $31^{\circ}32'N$  (the deepest low). The central and southern lows appear to be cut by the edge of Laramide thrusting.

Figure 6.5 shows the residual Bouguer anomaly map of the urban study area. This map suggests that the deepest part of the basin lies between the El Paso airport and  $31^{\circ}32'N$ . A complicated change in basin structure is indicated in the vicinity of the edge of the Laramide thrusting. The data suggest that the Cretaceous bedrock high mapped on the U.S. side of the border does not appear to extend into Mexico.

The HGM map for the urban region (Figure 6.6) suggests a westward step over in the EFMF at  $31^{\circ}45'N$  at about the point the edge of Laramide thrusting might be expected to intersect the fault. Faults M1 and F0 (mapped by Avila et al. 2016) also appear related to HGM highs. The edge of Laramide thrusting appears to correlate with a northwest-southeast trending HGM high. It is possible that many intrabasin faults such as F1 and F2 do not extend farther than the edge of the thrusting.

## 6.2 Forward Modeling

Structure of the Hueco Bolson modeled in the gravity profiles correspond to Avila et al. (2016). These models reflect an approximation of the structure of the basin fill and the basement of the Hueco Bolson. Four models, A-A', B-B', C-C' and D-D' were constructed along the Hueco Bolson using the complete Bouguer anomaly values (Figure 6.7). The software used for the gravity profiles was GM-SYS<sup>TM</sup> which is based on the forward modeling techniques of Talwani et al. (1959). Profile A-A' was constructed lengthways to the seismic and gravity profile of Figuers (1987). Profile B-B' was constructed using the structural cross-section of Collins and Raney (2000) as constraints and was also located near another profile modeled by Marrufo

(2011) that used water well logs as constraints. Profile C-C' was constructed using a seismic section of Collins and Raney (1994) and is located into the more urbanized region of south central El Paso. Profile D-D' constructed in Ciudad Juárez was constrained by two water utilities wells and densities from C-C'.

Table 6.1 shows the densities used for the profiles. These densities are based on studies of Figures (1987), Hadi (1991), and Burgos (1993).

Age or formation	Profile	Density (kg/m <sup>3</sup> )
Upper basin fill	A-A', B-B', C-C', D-D'	2100
Lower basin fill	A-A', B-B', C-C', D-D'	2300
Upper Paleozoic	A-A', B-B'	2600
Lower Paleozoic	A-A', B-B'	2700
Precambrian	A-A', B-B'	2800
Bedrock	C-C', D-D'	2670

Table 1 Table 6.1 Densities used in forward modeling. Modified from Avila et al (2016).

Profile A-A' (Figure 6.8) shows the model that is in good agreement with the seismic-reflection interpretation of Figuers (1987). Depth of the basement Precambrian rock is ~1800 m and there is about 1000 m of sediment adjacent to the EFMF.

Profile B-B' (Figure 6.8) Shows approximately same depths to Precambrian rock and thickness of basin fill as profile A-A' but with a more complicated network of intrabasin faults based on those mapped at the surface by Collins and Raney (2000) A concealed fault, M1, proposed by Marrufo (2011) also is required for this profile.

Profile C-C' (Figure 6.9) delineates the structure near downtown El Paso extending from gravity data collected along US highway 65 (Montana St) east to join with seismic line A

interpreted by Collins and Raney (1994). The profile includes faults F1-F7 mapped at the surface by Collins and Raney (2000). M1 is a concealed fault from Marrufo (2011). The profile shows the deepest part of the basin close to the EFMF with approximately 1500 meters of basin fill. Faults F1 and F2 bound the deepest part of the subbasin where the basin fill is about 1800 m.

Profile D-D' (Fig 6.9) is located at Ciudad Juarez Mexico and it was constrained with two water wells spaced 3 km apart. The first well located 2 km west of the inferred EFMF encounters bedrock at 60 m depth. The second well is ~2.5 km east of the EFMF with a depth of 250 meters and does not encounter bedrock. Similar to profile C-C' the deepest part of the basin is bounded by faults F1 and F2. In this profile another concealed fault was required to fit the gravity data (labeled fault F0) that is located between the EFMF and fault M1.

### 6.3 Discussion

The gravity study in the urban part of the Hueco Bolson shows that the Hueco Bolson, in contrast to the Mesilla Bolson, is a much deeper basin, in accordance with other studies such Averill (2007). Most of the water wells located in Hueco Bolson do not encounter bedrock. Quaternary Faulting is much more pervasive in the Hueco Bolson than Mesilla Bolson, with the EFMF having a slip rate of 0.145 mm/year McCalpin (2006). The M2.5 earthquake occurring in the Hueco Bolson in 2012 (USGS, 2012) indicates that intrabasin faults may also move independently of the EFMF within the basin.

The Horizontal Gradient Magnitude (HGM) analysis conducted in the Hueco Bolson show deeper structures that have geophysical signals aligned with known and suspected faults. The EFMF is clearly associated with an HGM anomaly and the HGM maps suggest the EFMF extends ~25 km from the urbanized part of downtown El Paso through Ciudad Juarez to the southern Juarez city limits. The new gravity data also show that faults mapped by Collins and

Raney (2000) extend into the urban part of El Paso. Some appear to extend across the border and continue through downtown Juarez similar to the EFMF (Figure 6.10). The black dashed lines on the HGM map show the possible extension of these faults. The HGM also shows a feature that aligns with the edge of the Laramide deformations mapped by Collins and Raney (2000). More gravity data are required to better trace the edge of this feature and determine if it controls the change in strike of the EFMF

In conclusion, although the central Hueco Bolson is heavily urbanized, gravity analysis was very effective for delineating the major faults and structures within the Hueco Bolson. This is in contrast with Mesilla Bolson that appears to have a complex sequence of faults and igneous intrusions that were not as easily imaged by the gravity data.

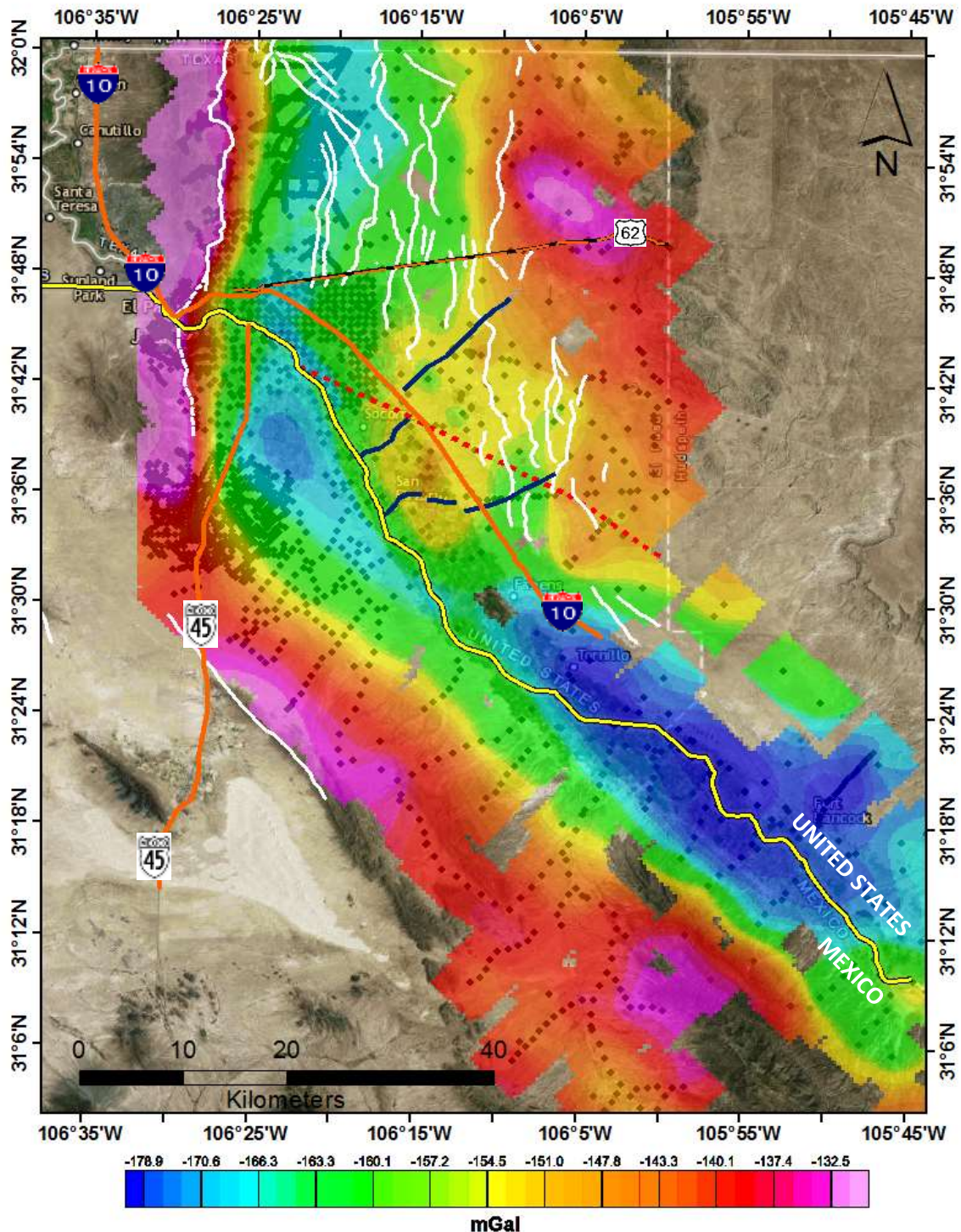


Figure 6.1 Complete Bouguer Anomaly for the regional area of Hueco Bolson. White lines are Quaternary faults from Collins and Raney (1994).

Red dashed line is edge of Laramide deformation (Collins and Raney, 1994), symbols are gravity observation points, and blue lines show edges of Cretaceous uplift from Collins and Raney (2000). Major roads are shown in orange and the border is shown in yellow.

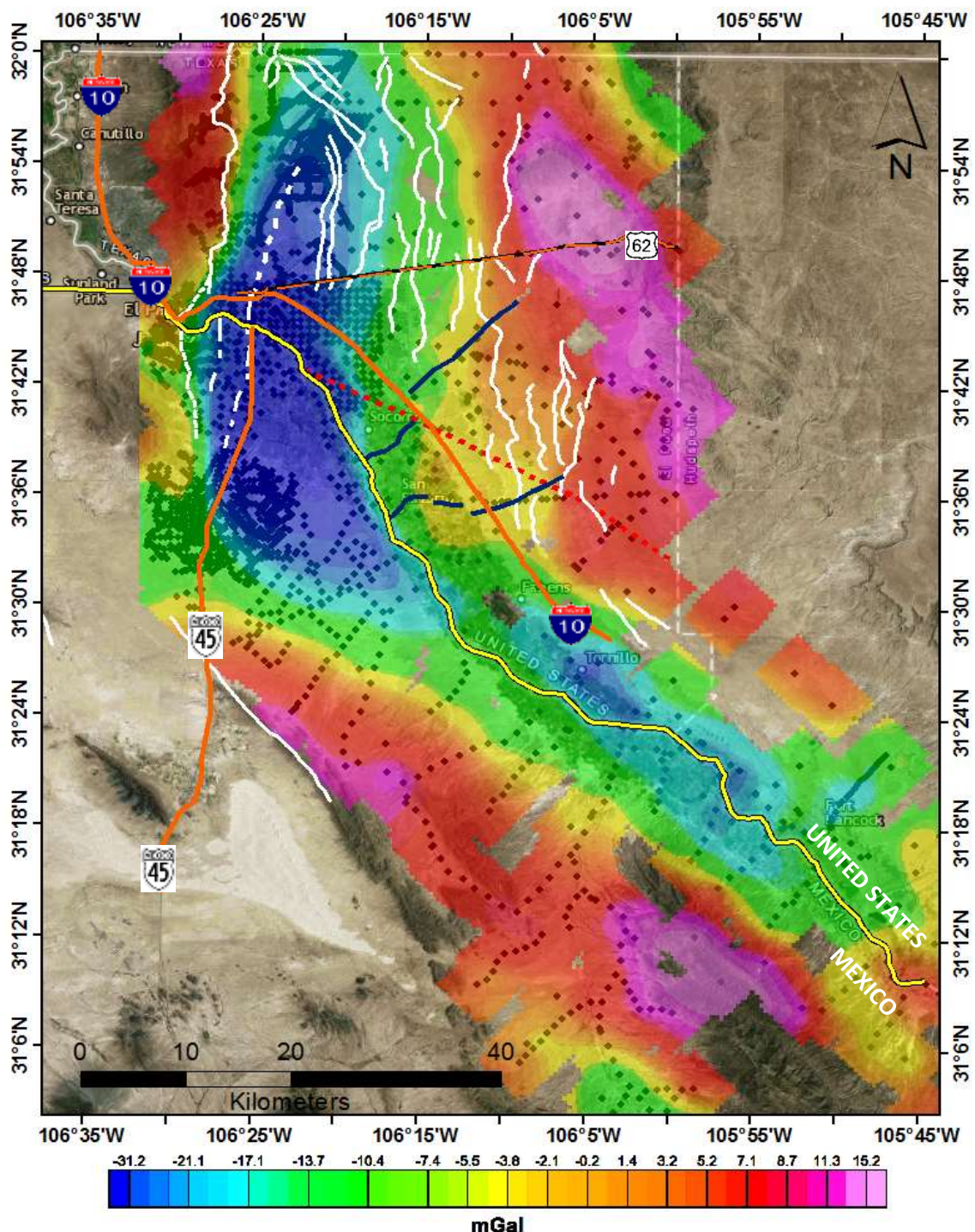


Figure 6.2. Residual Bouguer Anomaly for the regional area of the Hueco Bolson. See Figure 6.1 for explanation of symbols and lines.

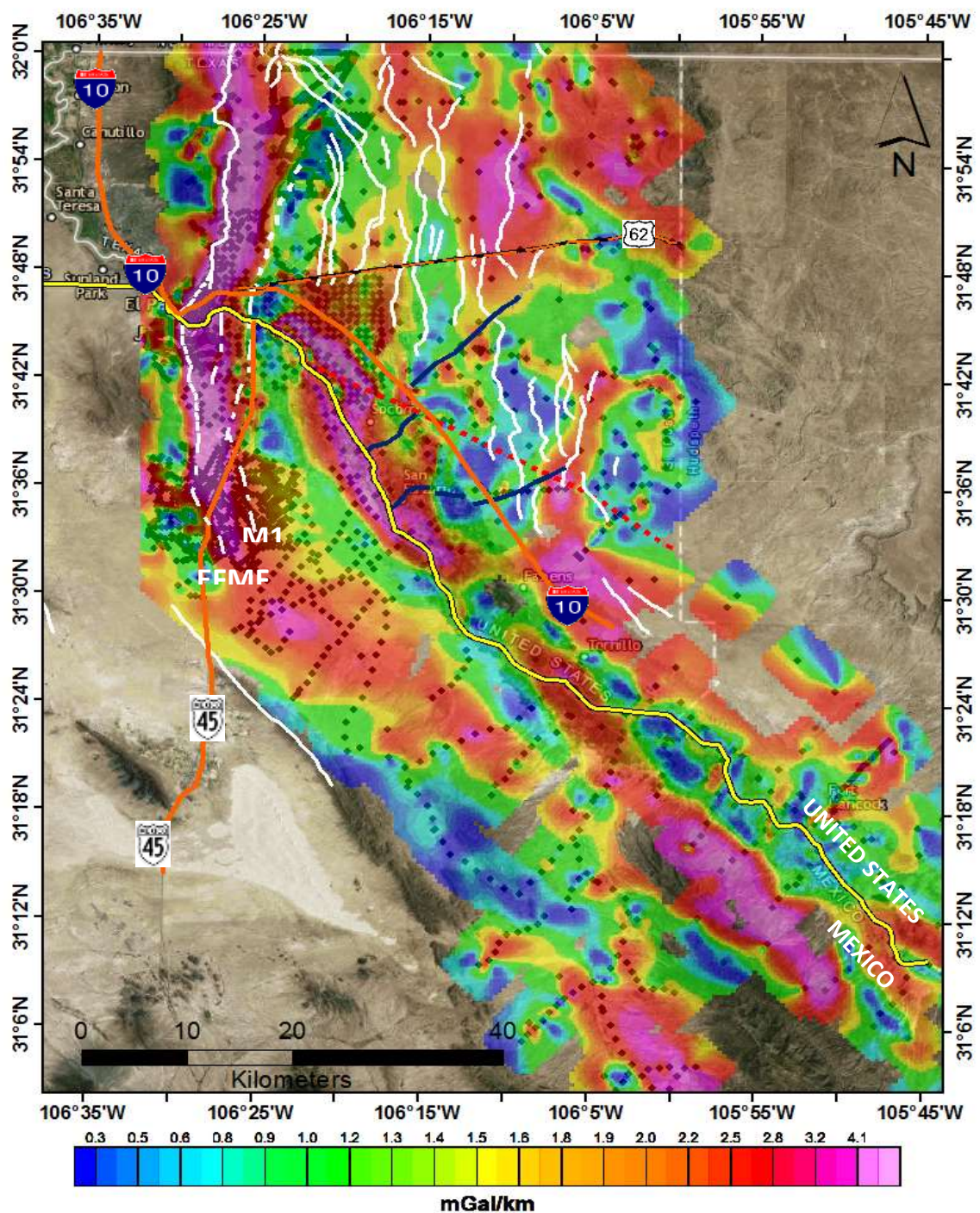


Figure 6.3 Horizontal Gradient Magnitude regional map for the Hueco Bolson. See Figure 6.1 for explanation of symbols and lines. EFMF is East Franklins Mountain fault. M1 is concealed fault from Marrufo (2011).

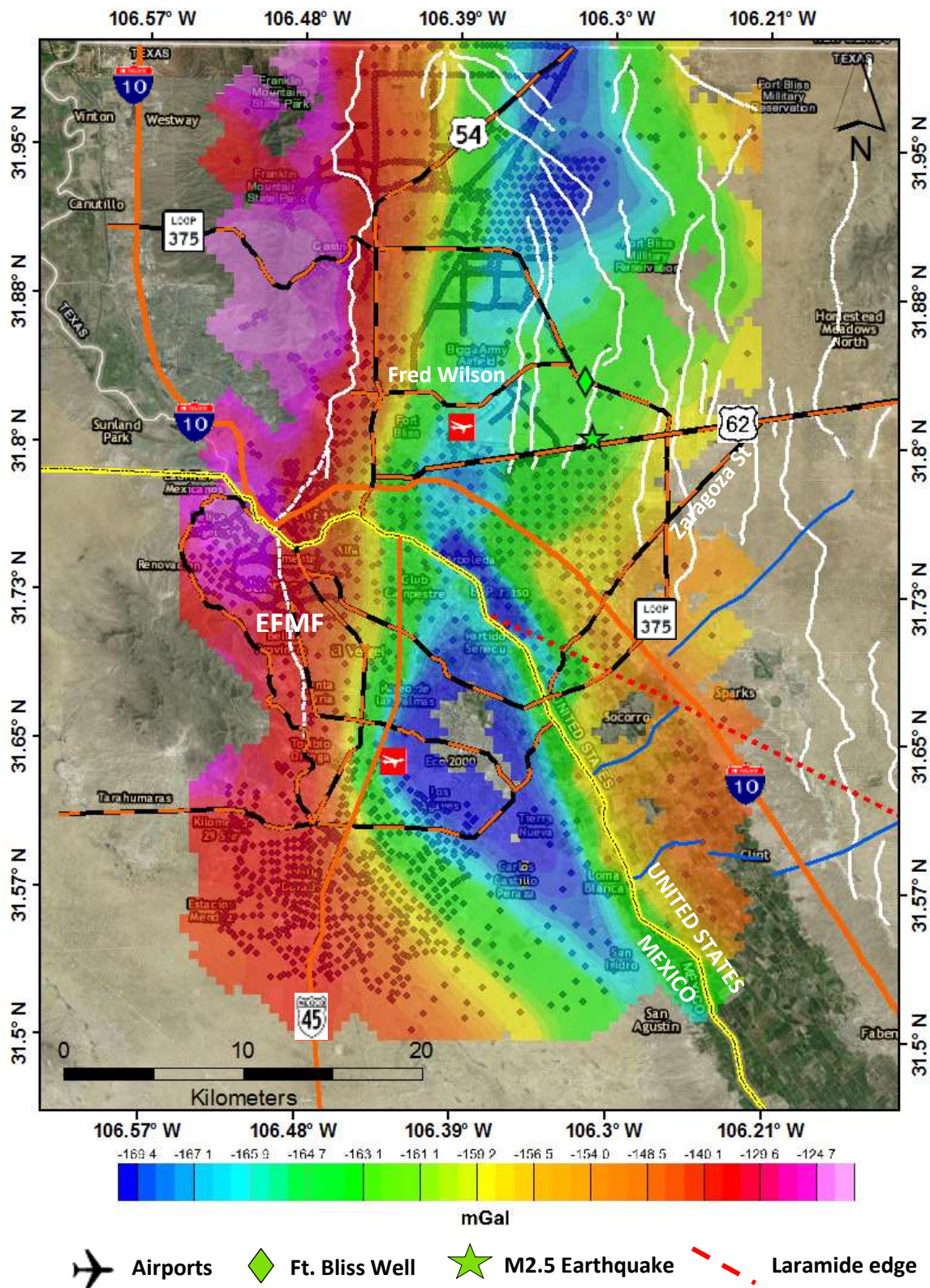


Figure 6.4 Complete Bouguer Anomaly map for the urbanized El Paso-Ciudad Juárez area. Red squares denote location of airports, diamond is deep geothermal well (~1675m) that did not reach basement, star is M2.5 earthquake occurring in 2012.

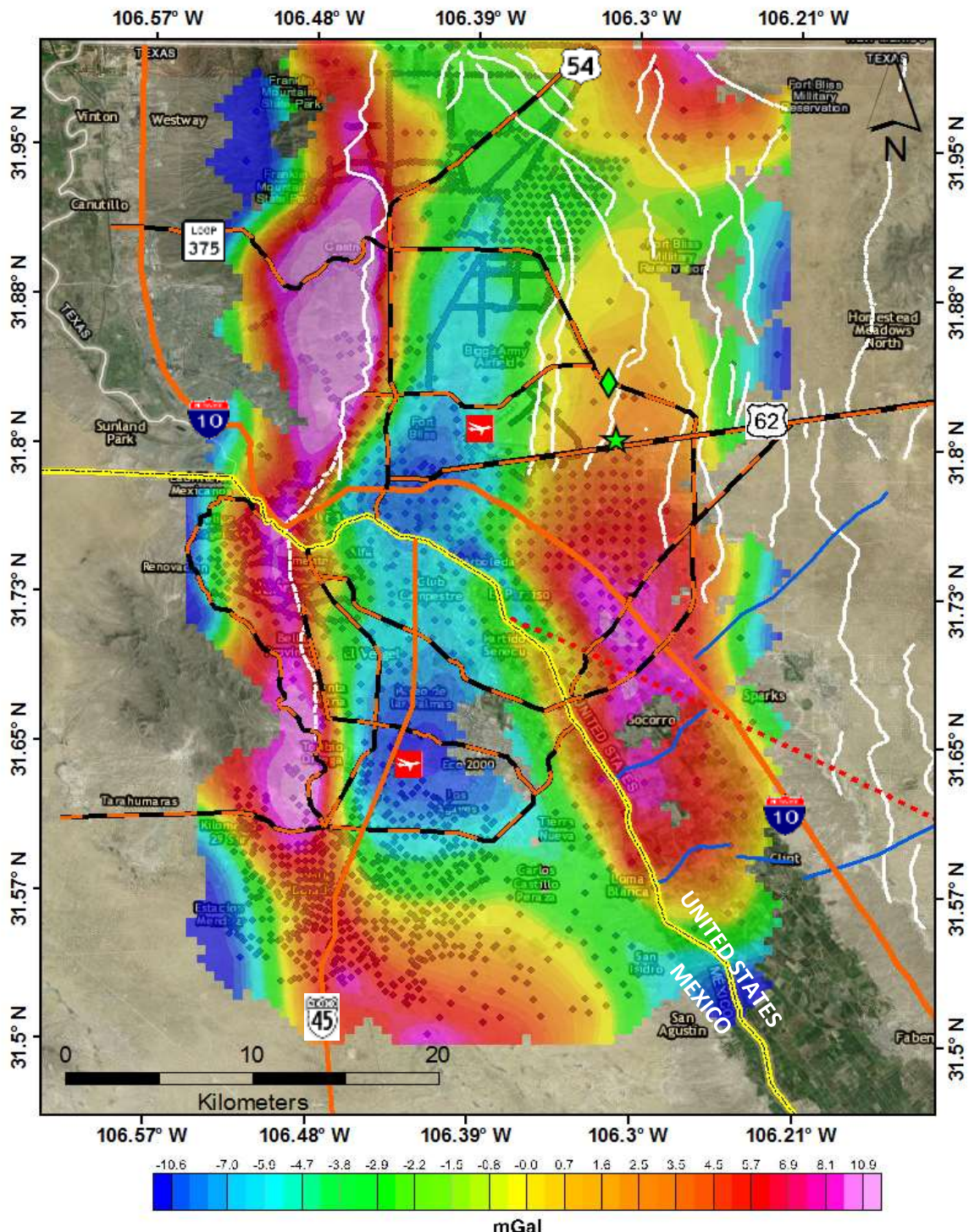


Figure 6.5 Residual Bouguer Anomaly map for the urbanized part of El Paso-Ciudad Juárez area. See explanation of symbols in Figure 6.4.

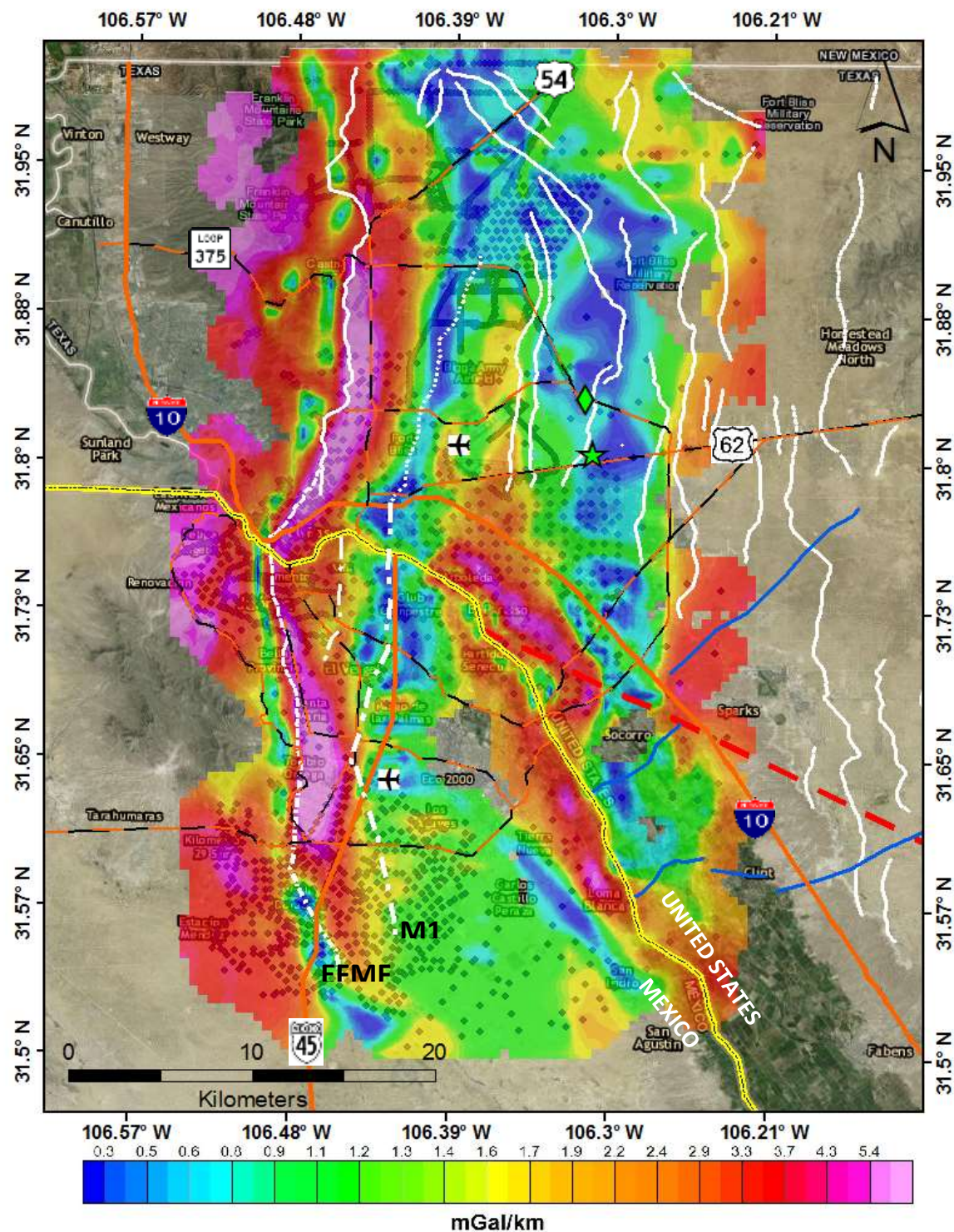


Figure 6.6 Horizontal Gradient Magnitude Map for the urbanized El Paso-Ciudad Juárez area. See explanation of symbols in Figure 6.4.

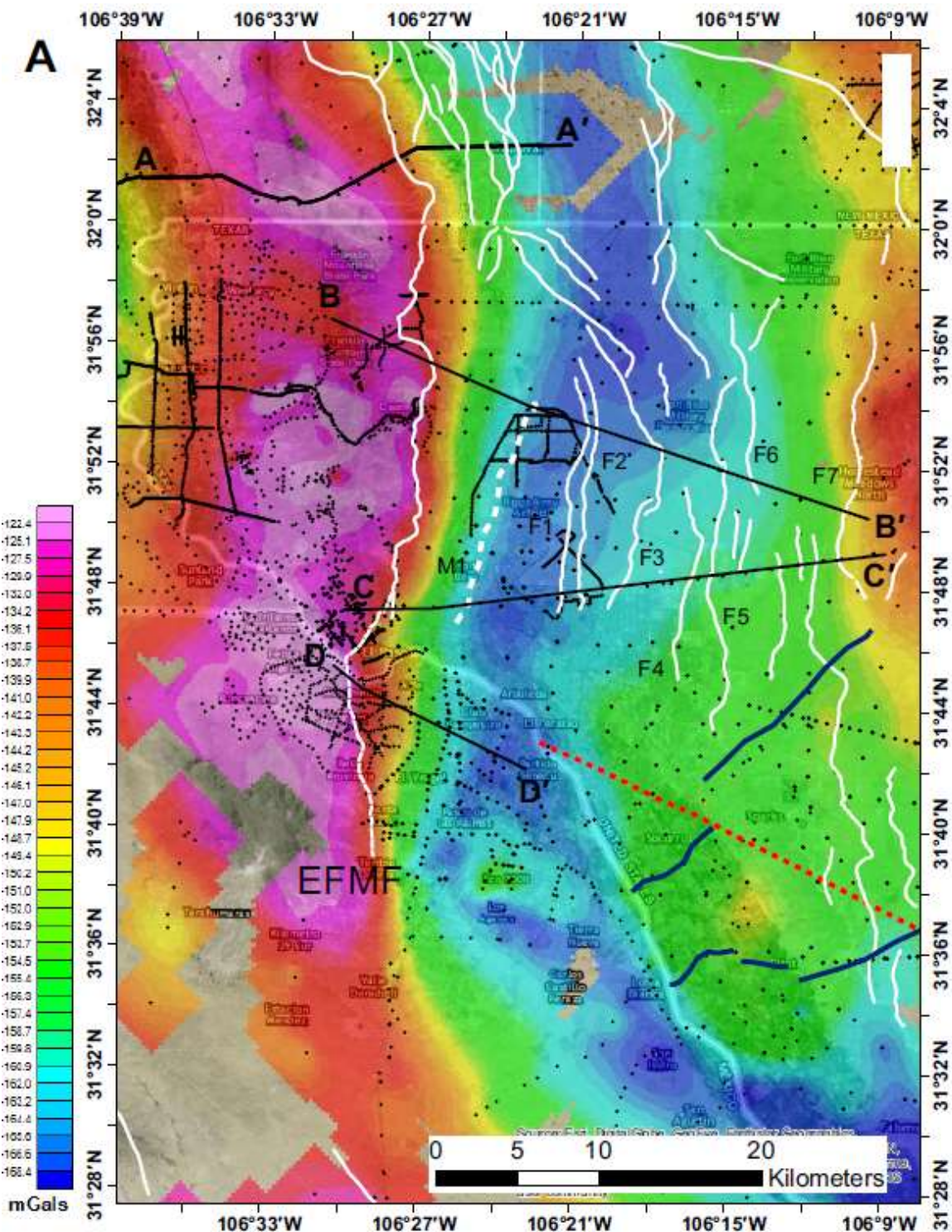


Figure 6.7 Complete Bouguer Anomaly map showing the 2D-Gravity profiles along Hueco Bolson study area. (Modified from Avila et al., 2016). Faults F1 to F7 are from work of Collins and Raney (1994).

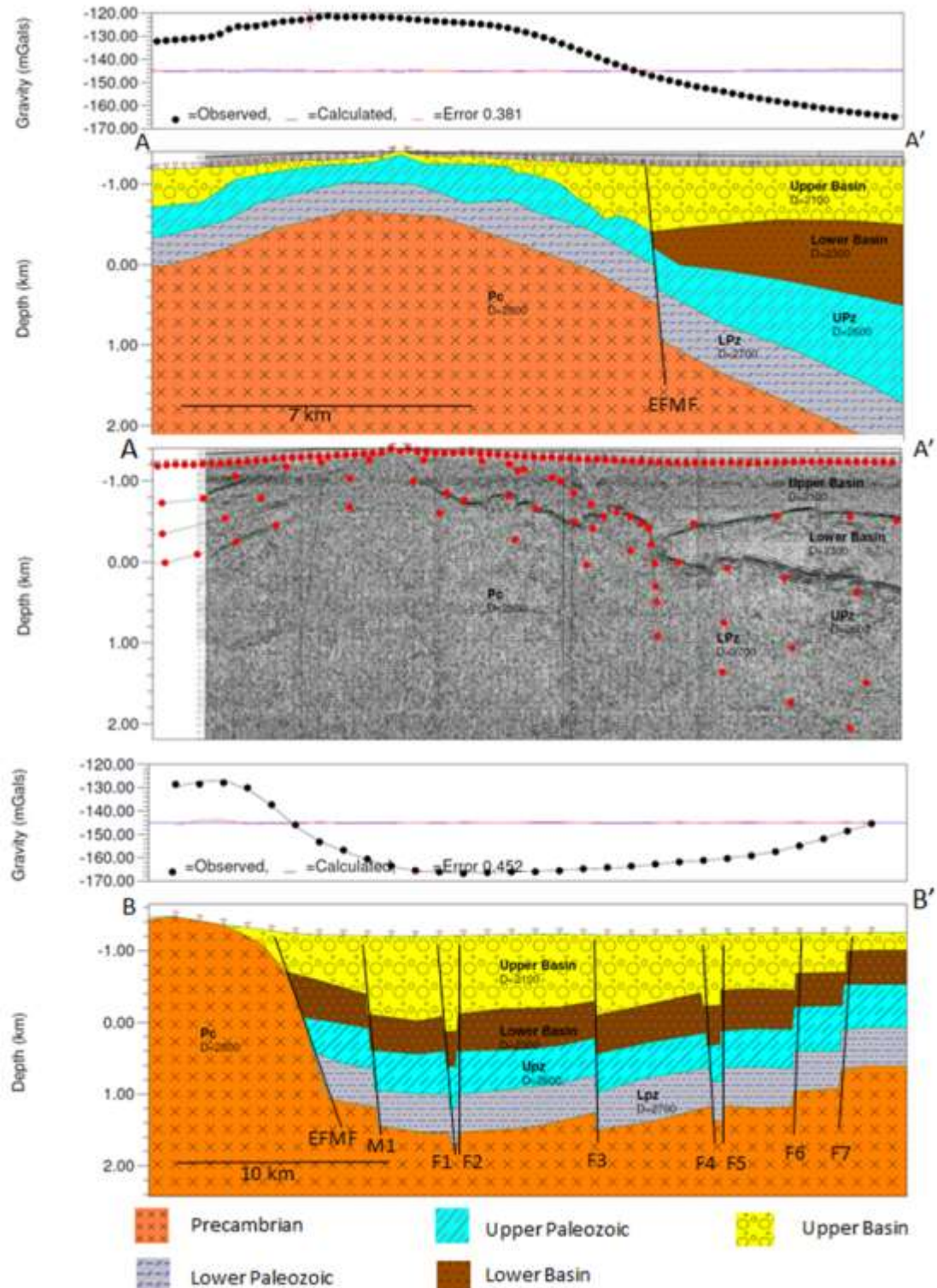


Figure 6.8 Two-dimensional gravity models for cross-section A-A' and B-B'. Black lines indicate faults. (Modified from Avila et al 2016). Seismic section on A-A' is from Figuers (1987).

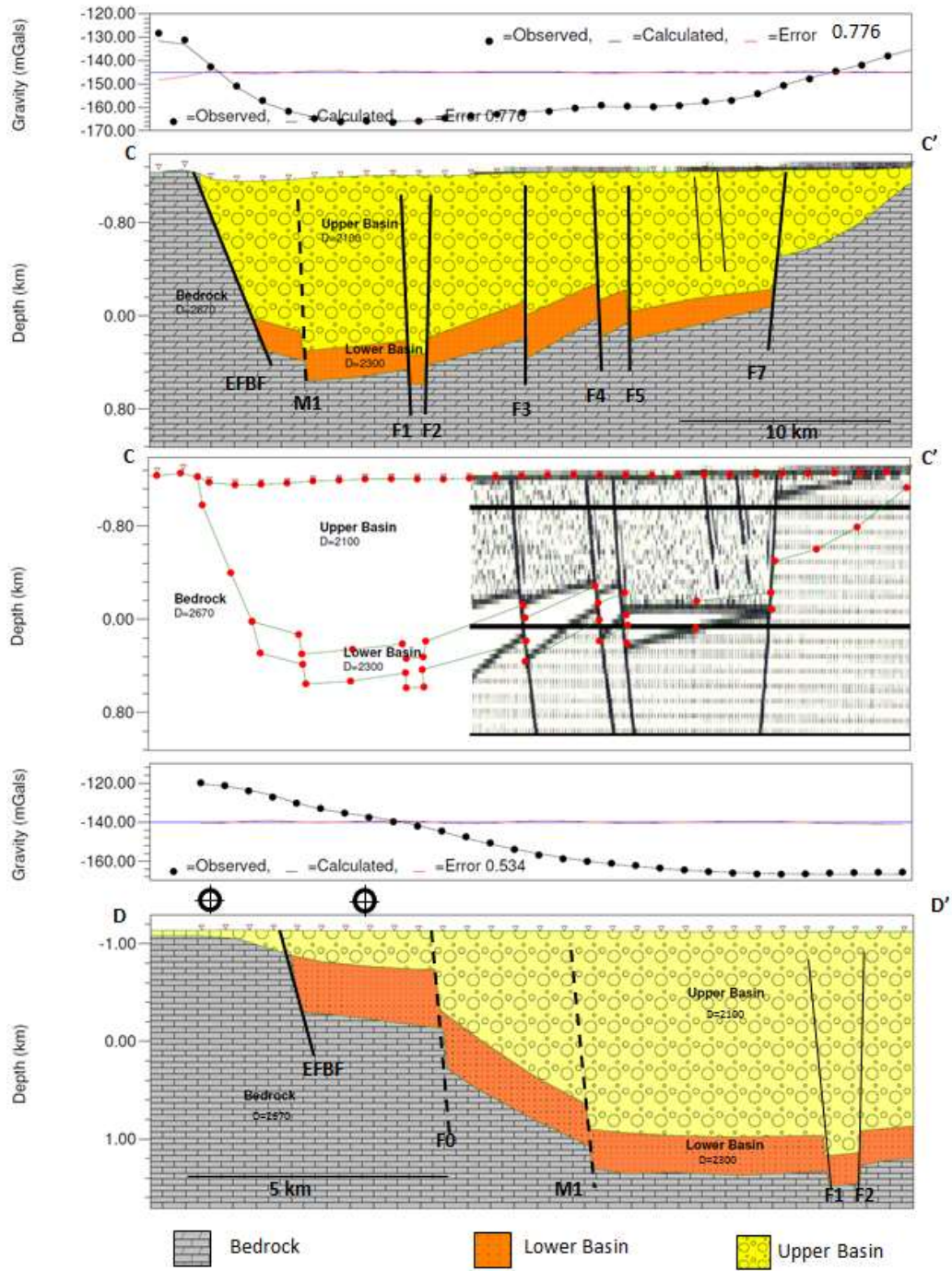
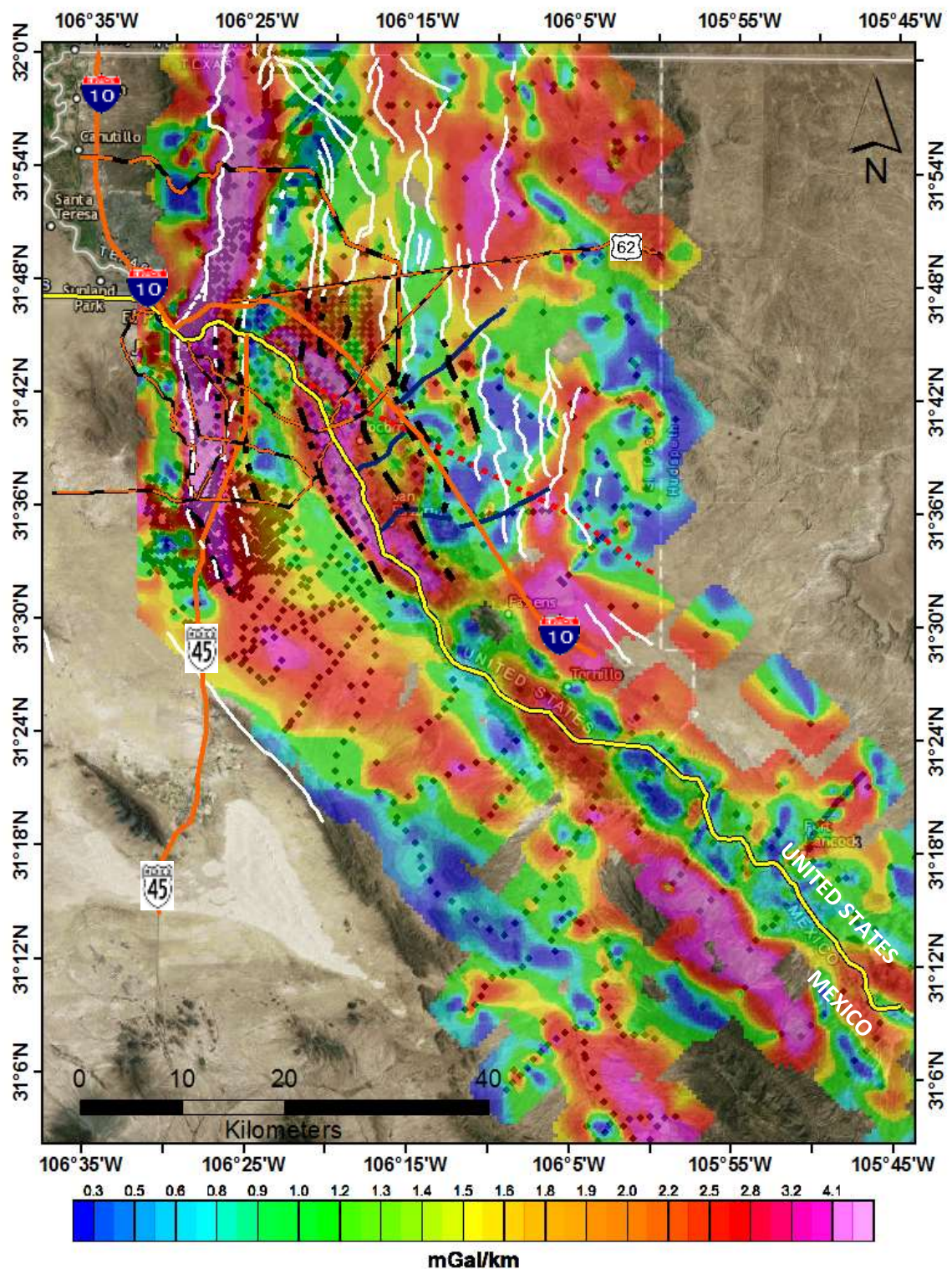


Figure 6.9 Two-dimensional gravity models for cross-section C-C' and D-D'. Black solid lines indicate faults with surface expression, dashed line indicates concealed fault.

(Modified from Avila et al 2016). F0 is concealed fault required by gravity data. Symbols in D-D' denote water wells. Seismic section on C-C' is from Collins and Raney (1994).



#### 6.4 References

- Avila, V.M., 2011. An investigation of the seismic hazards of the El Paso-Juarez region: The nature and extent of the southern east Franklin Mountains fault zone (M.S.). The University of Texas at El Paso, United States -- Texas.
- Avila, V. M., D. I. Doser, O. S. Dena-Ornelas, M. M. Moncada, and S. S. Marrufo-Cannon, 2016, Using geophysical techniques to trace active faults in the urbanized northern Hueco Bolson, West Texas, USA, and northern Chihuahua, Mexico: *Geosphere*, v. 12, no. 1, p. 264–280, doi:10.1130/GES01228.1.
- Collins, E. W., and J. A. Raney, 1994, Tertiary and Quaternary tectonics of the Hueco bolson, Trans-Pecos Texas and Chihuahua, Mexico, in Geological Society of America Special Papers: Geological Society of America, p. 265–282.
- Collins, E. W., and J. A. Raney, 2000, Geologic Map of West Hueco Bolson, El Paso Region, Texas, 1:100,000-scale color map
- Burgos, A., 1993. A gravimetric study of the thickness of the unconsolidated materials in the Hueco Bolson Aquifer, Juárez Area, Chihuahua, Mexico, Master's thesis / University of Texas at El Paso.
- Figuers, S.H., 1987. Structural Geology and Geophysics of the Pipeline Complex, Northern Franklin Mountains, El Paso, Texas (D.G.S.). The University of Texas at El Paso, United States -- Texas.
- Hadi, J., 1991. A study of the structure and subsurface geometry of the Hueco Bolson, Master's thesis / University of Texas at El Paso.
- Marrufo, S. S., 2011, An integrated geological and geophysical study of the fresh and brackish water boundary in the Hueco Bolson, West Texas, M.S.: United States -- Texas, The University of Texas at El Paso, 122 p.
- McCalpin, J., 2006, Quaternary Faulting and Seismic Source Characterization in the El Paso-Juarez Metropolitan Area: Collaborative Research with the University of Texas at El Paso: GEO-HAZ Consulting.
- Talwani, M., J. L. Worzel, and M. Landisman, 1959, Rapid gravity computations for two-dimensional bodies with application to the Mendocino submarine fracture zone: *Journal of Geophysical Research*, v. 64, no. 1, p. 49–59, doi:10.1029/JZ064i001p00049.

## CHAPTER 7

### 7.1 Mesilla Gravity Maps

Analysis of gravity and well information within the southeastern Mesilla Bolson indicates that the basin has considerable structural complexities. The deepest part of the Bolson lies to the northwest (lowest gravity in Figure 7.1) with the basin shallowing toward the east near the west flank of the Franklin Mountains and to the south at the edge of the Cerro de Cristo Rey intrusion. Smaller intrusions that are similar in composition to Cristo Rey (Garcia, 1970) are found throughout the southeastern part of the study area (Figure 7.1). The CBA map (Figure 7.1) indicates the highest densities are found in the southeastern portion of the study area and could also be related to buried intrusions. The Mesilla Valley fault zone (Figure 7.1) as mapped by Hawley and Kennedy (2004) does not appear as a distinct feature in the CBA map, unlike many faults within the Hueco Bolson, although data coverage in this region is sparser than within the river valley.

The residual Bouguer anomaly (Figure 7.2) also does not show a good correspondence between gravity anomalies and the Mesilla Valley fault zone. The map indicates a number of linear features within the main river valley that correspond well with water well geochemical and temperature anomalies (Hiebing, 2016), suggesting these features are faults. Other features that cannot be tied with known geology include an anomaly high in the southwestern portion of the study area and a low on the northwestern flank of the Franklin Mountains located north of Transmountain Drive. Bouguer anomaly highs are clearly associated with known andesite intrusions and the patterns of anomalies suggest buried dikes that may link a number of the outcrops. Figure 7.2 distinctly shows that north-south trending structures in the valley end near  $31^{\circ}48'N$ , with a change to a northwest-southeast strike of many features near  $31^{\circ}51'N$ . Seager

(2004) indicates that the edge of Laramide deformation occurs near  $31^{\circ}51'N$ , suggesting that older Laramide features may be controlling the density variations within the southernmost basin (see discussion of cross sections).

The HGM map for the study area (Figure 7.3) shows many features in the southeastern portion of the study area that are likely related to the edges of igneous intrusions. Some linear features within the river valley appear to be associated with faults (locations based on water well information), they are very difficult to trace from north to south. The HGM even better highlights the change from north-south to northwest-southeast striking structures south of  $31^{\circ}51'N$ . Neither the southwestern Bouguer anomaly high or northeastern anomaly low (Figure 7.2) are associated with distinct changes in the HGM (Figure 7.3).

## 7.2 Forward Modeling.

We constructed four 2-D gravity profiles, from our Complete Bouguer Anomaly (Figure 7.4) to better understand the basements rocks of the Mesilla Bolson. Several previous studies helped to constrain these models including Hawley and Kennedy (2004) and Imana (2003). Density profiles were constructed along portions of the geologic profiles K-K', J-J' and NW-SE (Figure 7.4) (Hawley and Kennedy, 2004) to insure that we could obtain reasonable density models that fit the observed gravity and closely matched the known geology. Note that most profiles of Hawley and Kennedy (2004) only extended to maximum depths of 1000 m beneath the surface. .

The densities for the deeper portions of the 2D gravity models were obtained from the velocity models of Averill (2007) (Figure 7.5) using the velocity to density conversion of Gardner et al. (1974). Density values for basin fill were based on Avila et al. (2016) and Imana (2003). Density values used in this study are summarized in Table 7.1.

<b>Age or Formation</b>	<b>Profile</b>	<b>Density (gr/cc)</b>
<b>Quaternary Fill</b>	Q-Q', NW-SE	2.1
<b>Upper Santa Fe</b>	K-K', J-J',	2.3
<b>Middle Santa Fe</b>	K-K', Q-Q', J-J',NW-SE	2.3
<b>Lower Santa Fe</b>	K-K', Q-Q', J-J',NW-SE	2.3
<b>Cretaceous</b>	K-K' Q-Q', J-J',NW-SE	2.5
<b>Upper Paleozoic</b>	K-K', Q-Q', J-J',NW-SE	2.6
<b>Lower Paleozoic</b>	K-K' J-J',NW-SE	2.7
<b>Tertiary Volcanics</b>	K-K', J-J',NW-SE	2.8

Table 2 Table 7.1. Densities used in the 2D gravity models for the Mesilla Bolson

### 7.3 2D Density Profiles

Profile K-K' (Figure 7.6) was constructed based on Hawley and Kennedy's geologic profile K-K'. The profile crosses 3 faults,: WF= Witcher Fault MVFZ=Mesilla Valley Fault Zone, and FK= Fault from K-Profile. The Witcher and Mesilla Valley faults have been previously mapped by Witcher (1998) and Hawley and Kennedy (2004). The FK fault is required to fit our forward model and is consistent with several linear features seen in the gravity anomaly maps (Figures 7.2 and 7.3) The model also shows an intrusive body from 11 to 15 Km along the profile. This feature is consistent with a intrusion previously mapped by Garcia (1970) called the Westerner intrusion. This intrusion also is seen as anomaly in The Horizontal Gradient Magnitude, (HGM) map for the Mesilla Bolson (Figure 7.7). The density model also suggests that the Lower Santa Fe formation is probably 200 meters thicker than previously estimated by Hawley and Kennedy.

Profile Q-Q' (Figure 7.8) was constrained by the densities used in model K-K'. The profile shows the Witcher Fault, WF, and the MVFZ as observed to the south along profile K-K'. The profile also contains faults UV1 = Upper Valley Fault 1, and UV2= Upper Valley Fault 2. UV1 and UV2 are faults that are based on the HGM gravity data (Figure 7.7) and information on groundwater temperature and geochemistry (Hiebing, 2016). Note that there is no well information to constrain the thickness of the Santa Fe Group along this profile, but the thicknesses are consistent with those shown to the south along K-K' and north along J-J'. Profile J-J' (Figure 7.9) extends along a portion of the geologic profile J-J' of from Hawley and Kennedy (2004). Water wells constrain the thickness of the Santa Fe group at several places along the profile. Note that the deepest part of the Lower Santa Fe group on the western side of the profile is about 500 meters thicker than shown by Hawley and Kennedy (2004), but they had no well that penetrated to bedrock in this region. The Cretaceous layer along this profile is thinner than to the south, suggesting a thinning of this unit as we move north of the limit of Laramide deformation.

Faults WF, MVFZ are from Witcher (1998) and Hawley and Kennedy (2004). Faults UV1 and UV2 are observed on the HGM map (Figure 7.7) and also associated with temperature and geochemical anomalies (Hiebing, 2016). The location of the I-10 fault is based on Khatun (2004) Faults labeled "F" may be faults or near vertical edges of intrusions as observed on the HGM and residual Bouguer maps. The gravity data are best fit by including an intrusion to the east of I-10. This feature is seen as a gravity anomaly high on both the complete Bouguer and residual Bouguer maps. It may represent a continuation of intrusions associated with the Cristo Rey andesite complex or it may be related to the Vado intrusion exposed ~20 km to the north. Profile J-J' also crosses the gravity low (Figures 7.1 and 7.2) observed near the Franklin

Mountains at 31°57'N. The geologic map of Hawley and Kennedy (2004) indicates that there is a notable lack of Paleozoic outcrop in this region compared to the foothills located to the north or south. The gravity data are consistent with a shallow (~200 m) basin containing upper or middle Santa Fe group materials.

The final 2-D gravity profile that was modeled extends from northwest to southeast (Figure 7.4) from 32°N to 31°48'N at the southernmost end of the valley. This profile follows a major portion of the geologic cross-section constructed by Hawley and Kennedy (2004) (see Figure 7.10A). The cross-section shows valley fill thinning from about 750 m at the northwest end to less than 90 m at the southeast end. The most significant decrease in thickness occurs across the MVFZ.

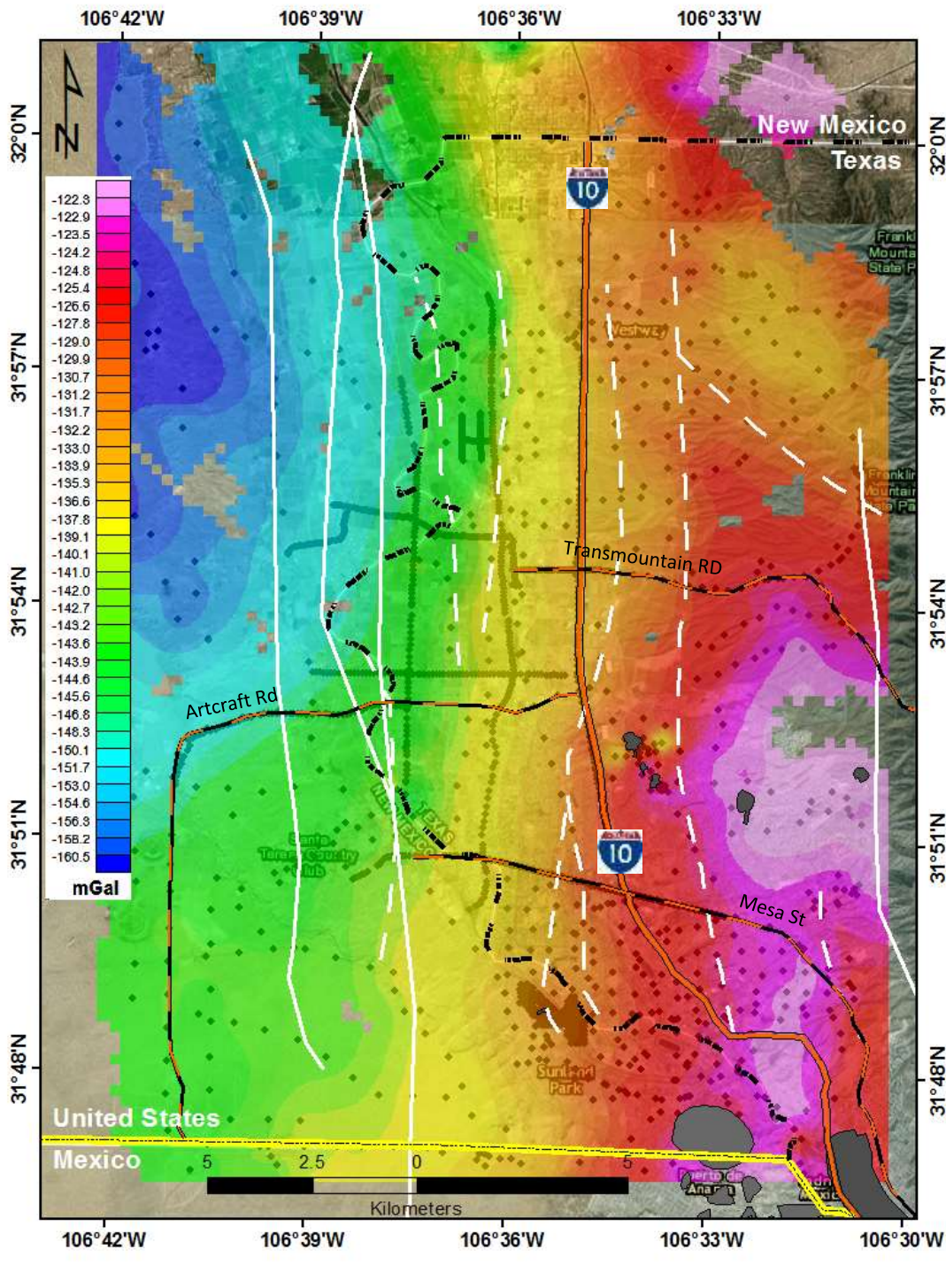
The gravity data (Figure 7.10B) are matched well by the density model constrained by Hawley and Kennedy's structures. The density model includes a slight offset (~100 m) in units along the fault mapped by Witcher and a total offset of 700-800 m along the MVFZ. The gravity data support the bedrock high and shallow "Sunland Paleo Valley" mapped by Hawley and Kennedy.

#### 7.4 Discussion

The Mesilla Bolson gravity maps show very complex structures within the basin. Structure in the southern basin is partly controlled by igneous intrusions of the Cristo Rey andesite complex and the edge of the Laramide deformational front. Several residual anomaly highs observed in the south western and northeastern portions of the study area may also be related to igneous intrusions; however more data are needed to confirm these observations. A residual anomaly low near the Franklin Mountains appears to be related to a small basin.

In contrast to the Hueco Bolson, faults in the Mesilla Bolson were a lot harder to trace with HGM. HGM anomalies in the Mesilla Bolson could be related to either faults or igneous intrusions and if faults are cutting the older intrusions it may be difficult to identify them. The HGM did not clearly define even the better constrained faults such as the Mesilla Valley fault, although gravity profiles clearly required its presence.

HGM and residual maps were available to trace the deeper extent of igneous intrusions within the Mesilla Bolson including the River Outcrop, Three Sisters, and the Westerner Outcrop (Garcia, 1970). Some of these features appear linked at depth by a series of dikes and faults.



Tertiary Volcanics

Figure 7.1 Complete Bouguer Anomaly Map. High gravity values correspond to high density rocks. Solid lines are faults from Witcher (1998) or Hawley and Kennedy (2004), dashed lines are faults from this study or from Hiebing (2016). Gray regions indicate outcrops of Tertiary igneous intrusions from Hawley and Kennedy (2004). Symbols indicate gravity observations

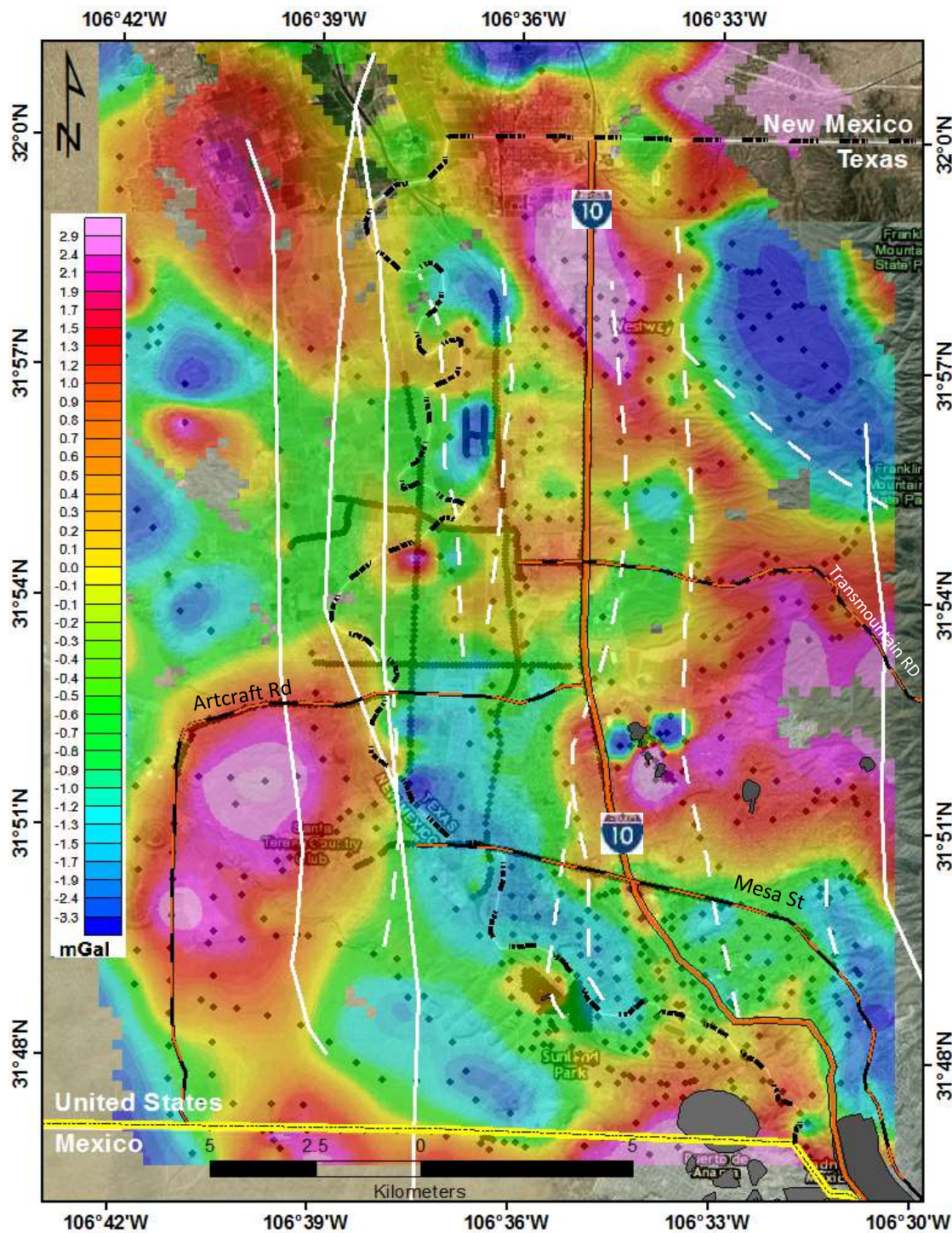


Figure 7.2. Residual Bouguer Anomaly Map.

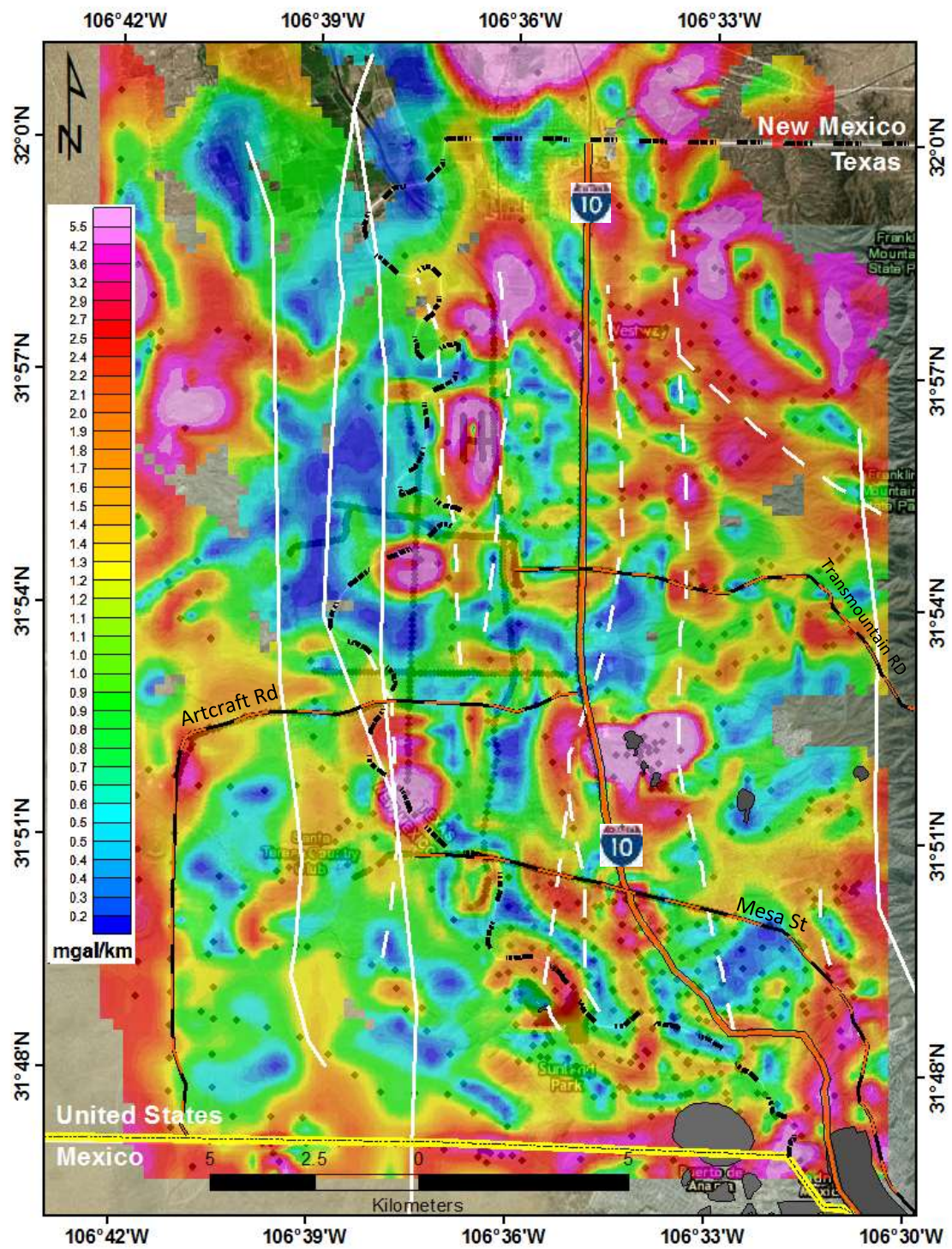


Figure 7.3 Horizontal Gradient Magnitude Map. HGM helps to delineates features with steep vertical density contrasts such as faults and igneous bodies.

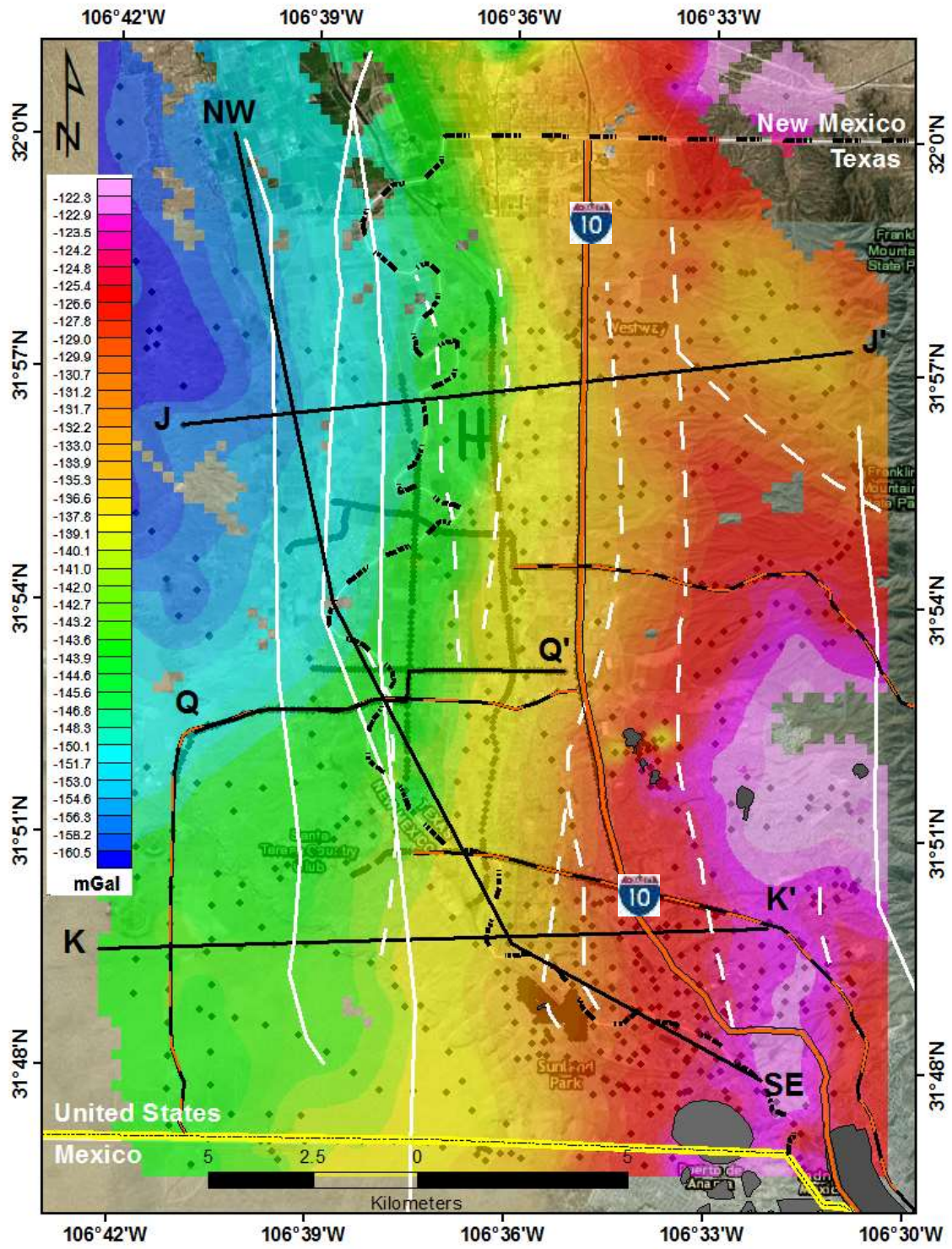


Figure 7.4 Complete Bouguer Anomaly map showing locations of gravity cross-sections

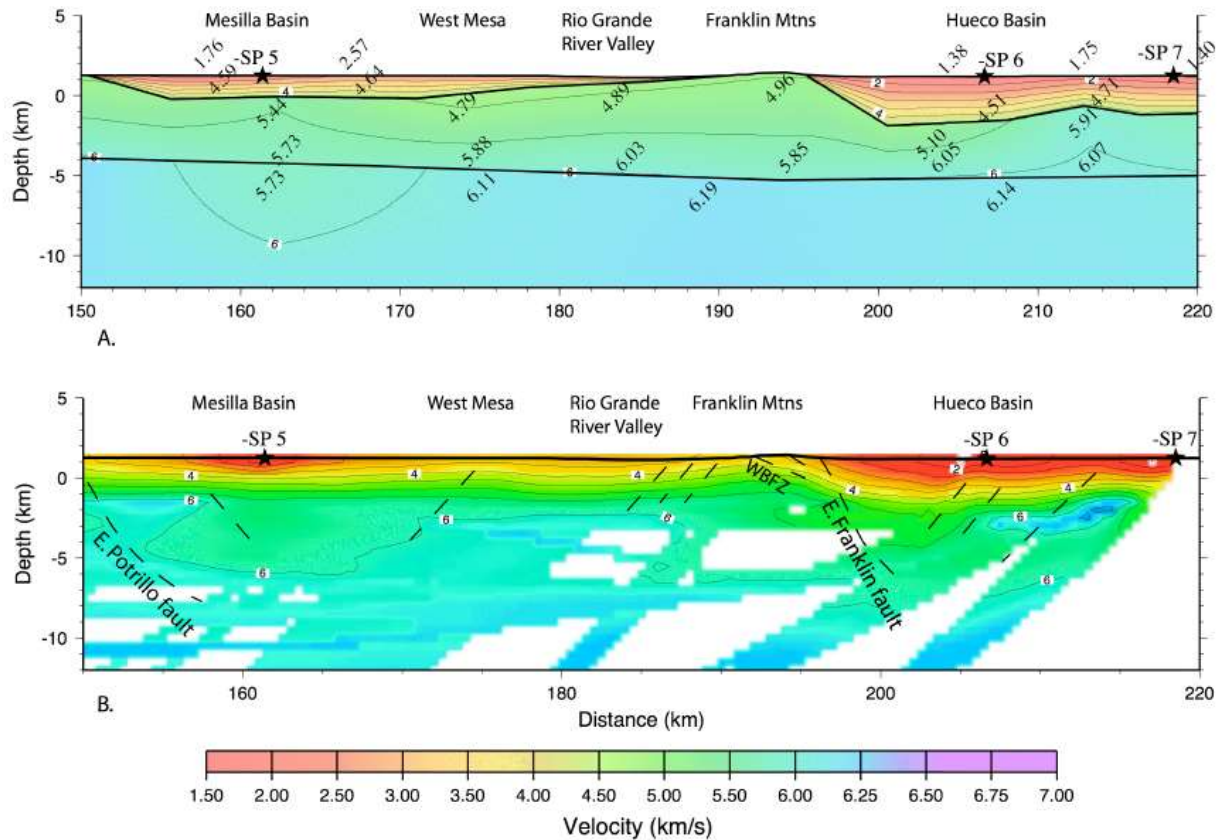


Figure 7.5 Velocity model modified from Averill 2007. A. Ray traced 1 km gridded velocity model.. B. 2-D tomography velocity model with 500 m cell size. Dashed lines show interpretation of faults.

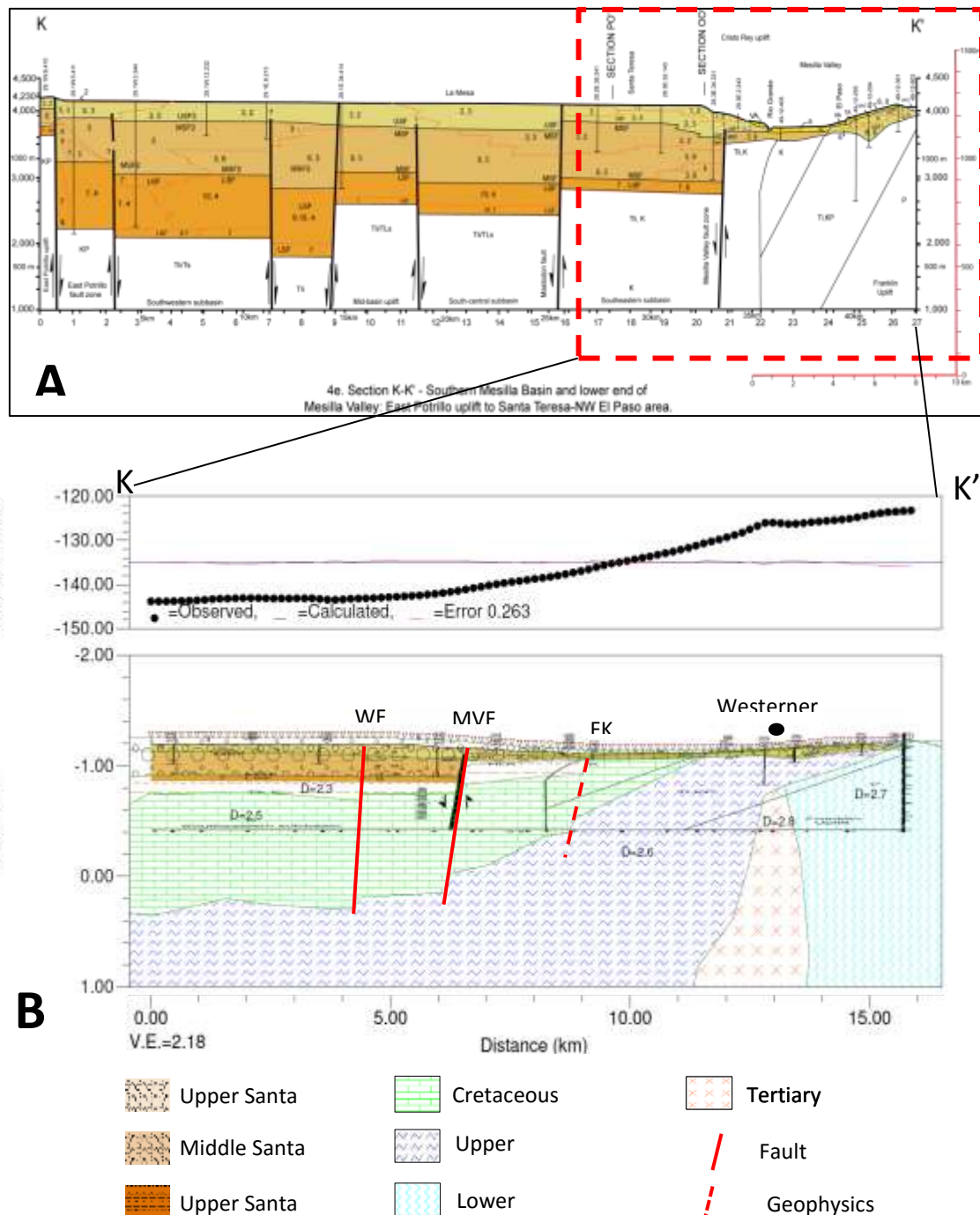


Figure 7.6. A) Geologic cross section K-K' from hydrostratigraphic framework of Hawley and Kennedy (2004), that was used as the base for the two-dimensional gravity model (shown in B).

Dashed red lines show region modeled in B. B) Density model across Mesilla Bolson for profile K-K' (see Figure 7.4) Top shows observed (dots) and calculated (line) gravity data and bottom shows interpreted density-geologic model. Model above -0.4 km based on Hawley and Kenney. . WF is Witcher fault, MVFZ is Mesilla Valley fault zone, FK is fault required by density model. Dot notes position of Western intrusion found just to the north of the profile.

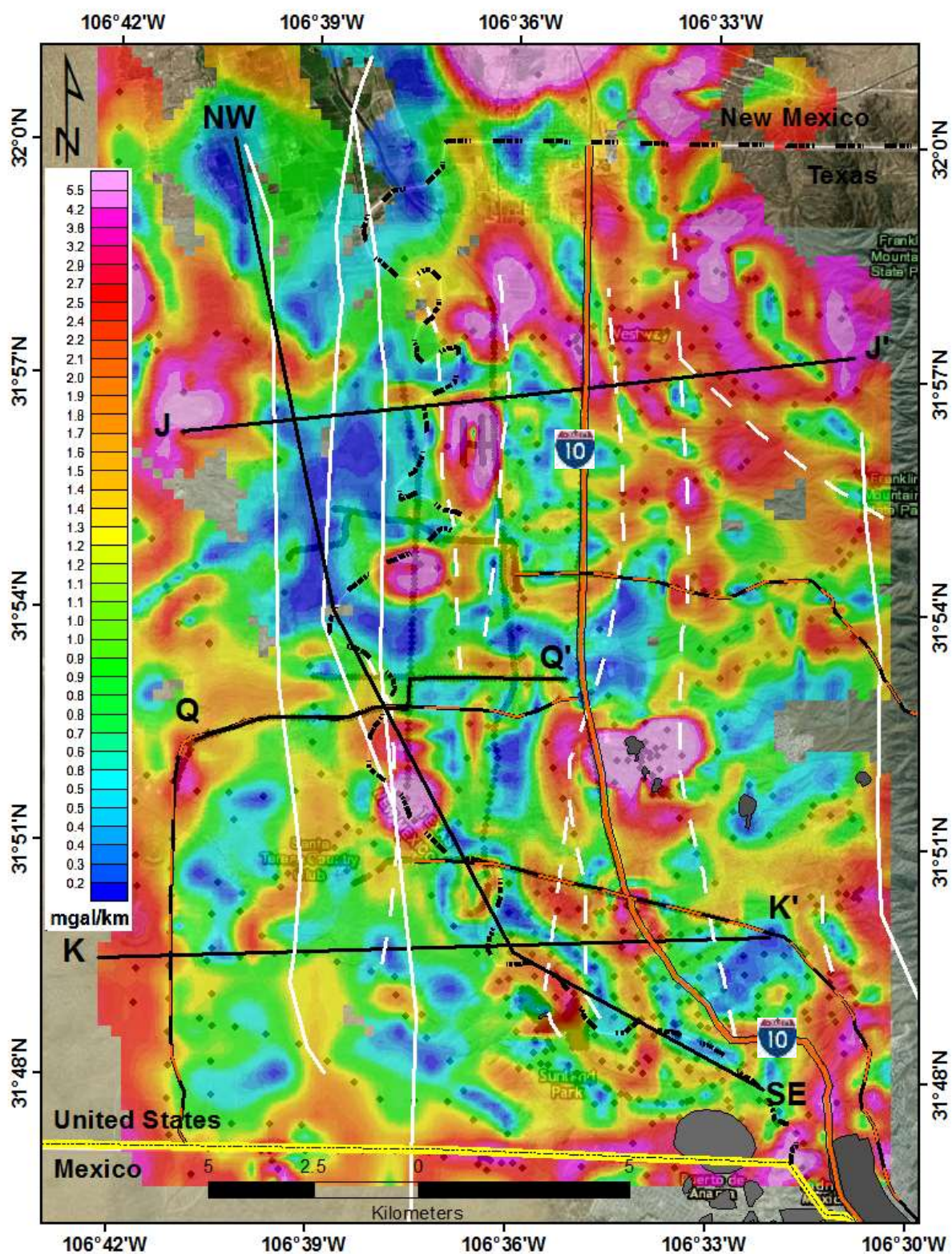


Figure 7.7 HGM map with gravity profiles

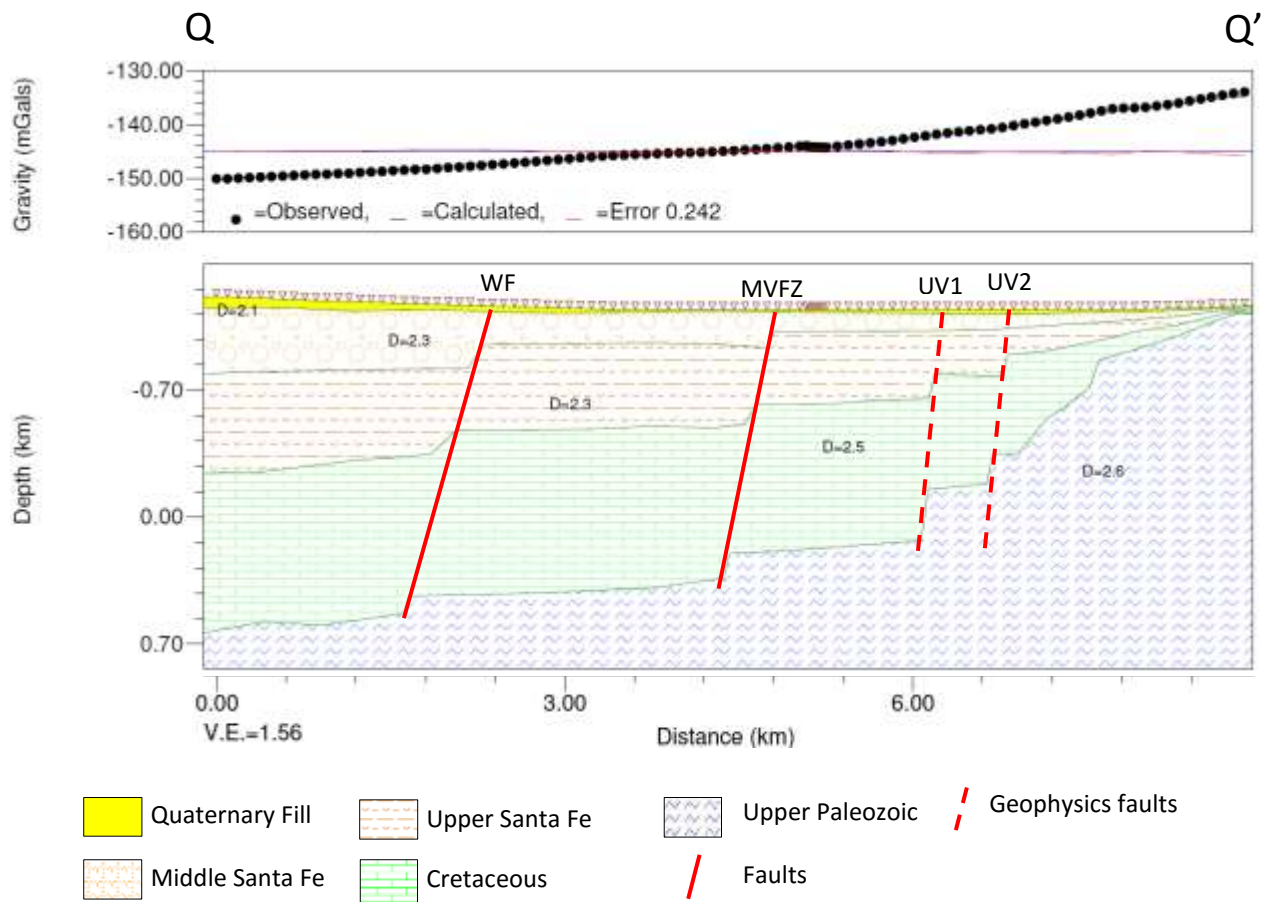


Figure 7.8 Two-dimensional gravity profile for section Q-Q' from Figure 7.4, densities constrained with profile K-K'. WF= Witcher Fault. MVFZ= Mesilla Valley Fault Zone. UV1= Upper Valley Fault 1. UV2= Upper Valley Fault 2

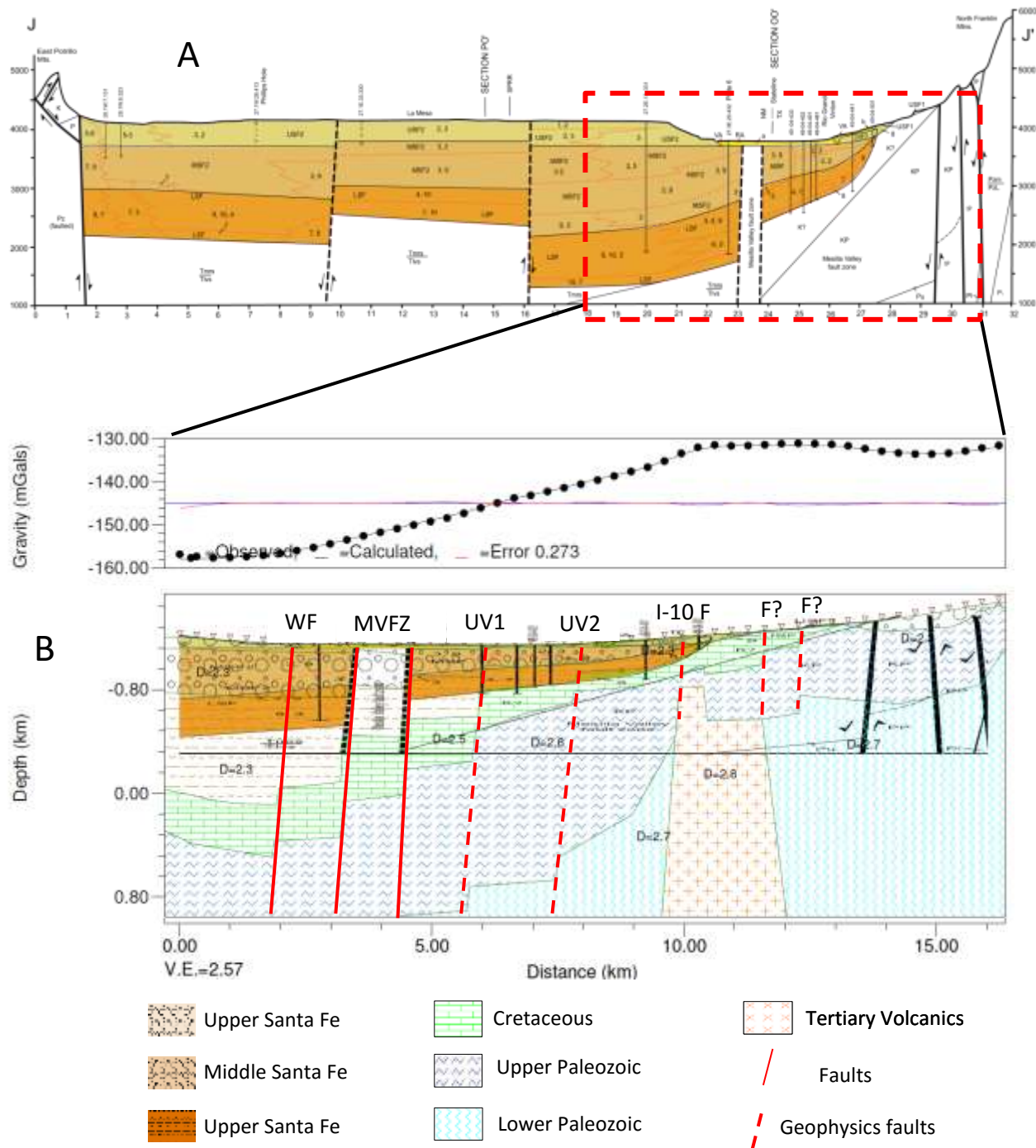


Figure 7.9. Figure A shows J-J' geologic cross-section from hydrostratigraphic framework of Hawley and Kennedy (2004). A portion of this cross section indicated by red dashed lines was used as a constraint for the two-dimensional density profile J-J' shown in part B. I-10 fault from Khatun (2004). F? indicates the location of possible faults based on gravity data.

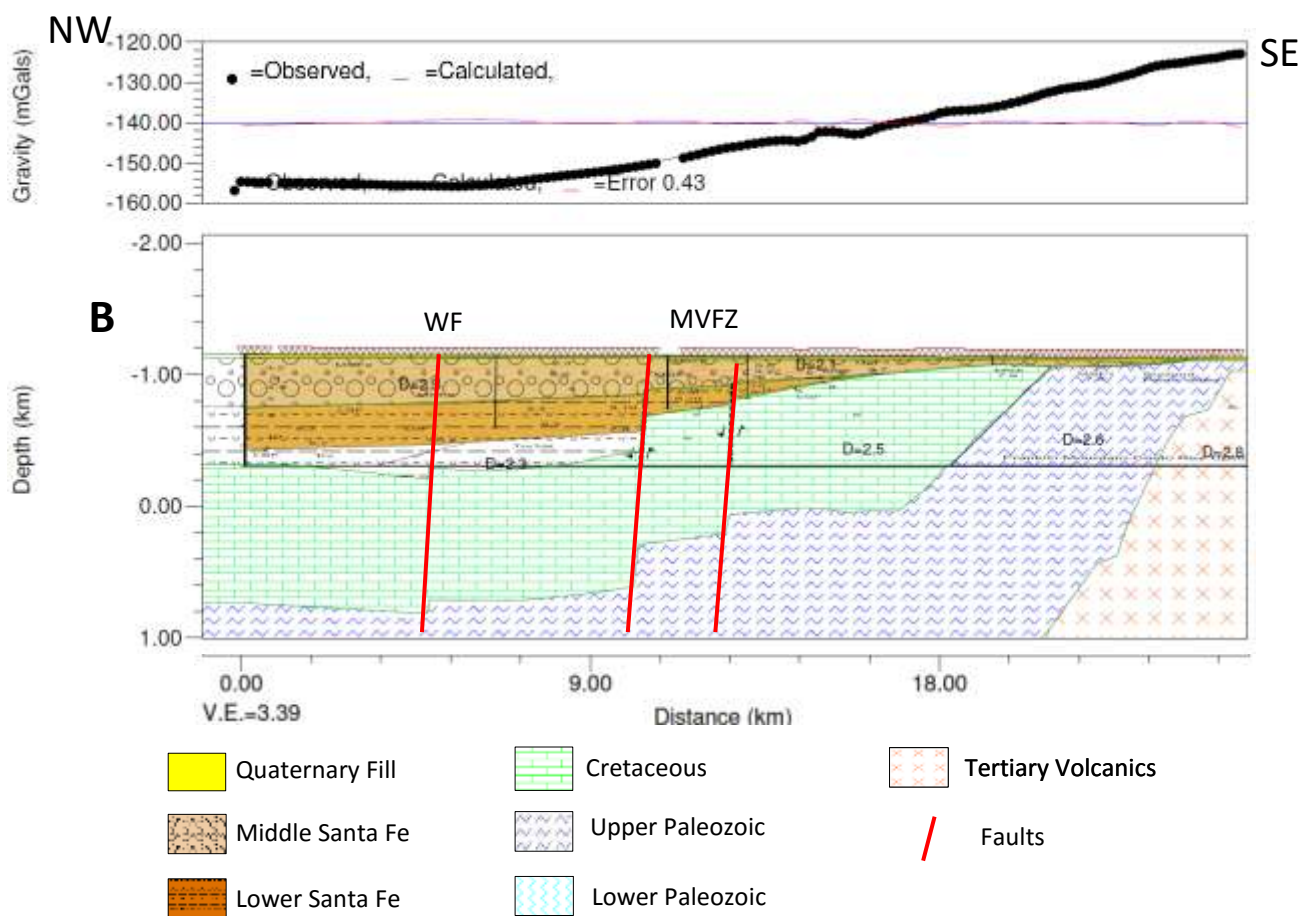
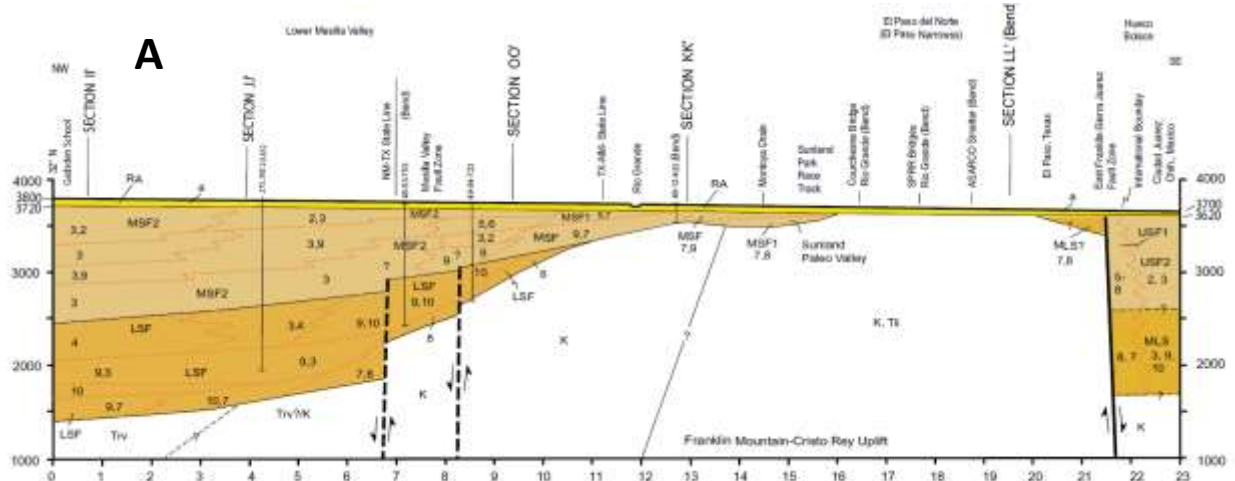


Figure 7.10 Figure A displays NW-SE geologic cross-section from hydrostratigraphic framework from Hawley 2004. Figure a two-dimensional gravity profile build from Complete Bouguer Anomaly data. Densities obtained from velocities model study from the Mesilla Bolson by Averill 2007.

## 7.5 References

- Averill, M. G., 2007, A lithospheric investigation of the southern Rio Grande Rift: 1 p.
- Averill, M. G., and K. C. Miller, 2013, Upper crustal structure of the southern Rio Grande rift: A composite record of rift and pre-rift tectonics: Geological Society of America Special Papers, v. 494, p. 463–474.
- Avila, V. M., D. I. Doser, O. S. Dena-Ornelas, M. M. Moncada, and S. S. Marrufo-Cannon, 2016, Using geophysical techniques to trace active faults in the urbanized northern Hueco Bolson, West Texas, USA, and northern Chihuahua, Mexico: *Geosphere*, v. 12, no. 1, p. 264–280, doi:10.1130/GES01228.1.
- Gardner, G, L Gardner & A Gregory, 1974. Formation velocity and density—the diagnostic basis for stratigraphic traps. *Geophysics* 39, 770–780
- Garcia, R. A., 1970, Geology and petrography of andesitic intrusions in and near El Paso, Texas, M.S.: United States -- Texas, The University of Texas at El Paso, 139 p.
- Hawley, J. W., J. F. Kennedy, A. Granados-Olivas, and M. A. Ortiz, 2009, Hydrogeologic Framework of the Binational Western Hueco Bolson-Paso Del Norte Area, Texas, New Mexico and Chihuahua: Overview and Progress Report on Digital-model Development: New Mexico Water Resources Research Institute.
- Hiebing, M.S., 2016. Using geochemistry and gravity data to pinpoint sources of salinity in the Rio Grande and fault networks of the Mesilla Basin
- Imana, E.M.C., 2002. The Mesilla Bolson: an integrated geophysical, hydrological, and structural analysis utilizing free air anomalies. PhD thesis / University of Texas at El Paso.
- Khatun, S., 2003. A precision gravity study of the Southern Mesilla bolson, West Texas (M.S.). The University of Texas at El Paso, United States -- Texas.
- Seager, W.R., 2004, Laramide (Late Cretaceous–Eocene) tectonics of southwestern New Mexico, in Mack, G.H., and Giles, K.A., eds., *The Geology of New Mexico, A Geologic History*: New Mexico Geological Society Special Publication 11, p. 183–202.
- Witcher, J. C., 1988, Geothermal Resources of southwestern Rio Grande Rift, New Mexico Geological Society 49<sup>th</sup> Annual Field Conference Guidebook. 93-100

## **CHAPTER 8**

### **Shear Wave Velocity of Soils and NEHRP Site Classification Map in El Paso West Texas**

#### **8.1 Abstract**

The Hueco and Mesilla basins are generally referred to as “alluvial basins”, and they are considered to have poorly consolidated basin fill deposits reaching thicknesses of 100’s meters. The fill deposits basin are not entirely of alluvial origin but also contain significant amounts of lacustrine, eolian and colluvial sediments. These deposits have the potential to amplify ground shaking during large earthquakes, similar to ones observed in the Quaternary record along the East Franklin Mountains Boundary fault (e.g. McCalpin, 2006) and other nearby faults. Studies in other basins have shown that the shear wave velocities in the upper 30 m of the basins Vs30 have the most influence on ground shaking. We have used the multi-channel analysis of surface wave (MASW) methodology at 70 selected sites in El Paso area to generate a NEHRP (National Earthquake hazards Reduction Program) classification soil map of the area. Not surprisingly, we find the soils with highest potential for amplification of ground motion due to earthquakes located in central El Paso where thick, water saturated fluvial deposits are found. Our results are also consistent with similar data collected in Ciudad Juarez.

#### **8.2 Introduction**

Site effects play an important role in earthquake strong motion, especially in basins. The Hueco and Mesilla basins are located within the boundaries of the active Rio Grande rift, (Keller 1990), and their basin fill is composed of different materials such as alluvial fans of Franklin Mountains and Rio Grande fluvial deposits, but also significant amounts of lacustrine and eolian sediments. Recent seismicity in the El Paso-Ciudad Juarez area has prompted evaluation and classification of these soils using measurements of shear wave velocity in the upper 30 meters

(Vs30) to assess potential hazards due to earthquake ground motion in this urbanized area where Quaternary faulting is present (Collins and Raney, 1990; McCalpin, 1996)

The most recent earthquake located within the city limits of El Paso was a M2.5 earthquake on March 6, 2012 (U.S. Geological Survey, 2016). Figure 8.1 shows the recent seismicity in El Paso-Juarez area from 2009 to 2015. The two most significant earthquakes that have occurred outside the El Paso-Juarez region, but were felt moderately to strongly in the region are the May 3, 1887 M7.4 Sonora earthquake over 300 km from El Paso where earthquake produced surface rupture of ~100 km along the Pitáycachi fault 100 km (Sutter 2002), and the August 16, 1931 M6.4 Valentine earthquake that occurred near the transition Southern Basin and Range-Rio Grande rift physiographic province (Doser 1987), about 160 km southeast of El Paso. The Valentine earthquake is the largest earthquake recorded in Texas.

### 8.3 Previous Studies

The Multi-channel Analysis of Surface Waves (MASW) technique has been used successfully used in research conducted by Universidad Autonoma of Ciudad Juarez to obtain Vs30 at over 370 seismic sites in Ciudad Juarez (Figure 8.2.) These data were then used to produce a map of average Vs30 in the urban area. (Figure 8.3). The National Earthquake Hazard Reduction Program (NEHRP) site classification based on shear wave velocity (Table 8.1) was used to produce a site classification map (Figure 8.4), and a frequency amplification site resonance map (Figure 8.5)

### 8.4 Methodology

NEHRP has developed a site classification system for near-surface geology that is based on Vs30. Classes (Table 8.1) range from hard rock (Class A), where little amplification is

expected, to very soft soils (class F) which have the potential to fail catastrophically in an earthquake.

Most studies of the variation in Vs30 rely on data collected through surface wave dispersion analysis. The advantage of using surface waves is that Rayleigh and Love waves dominate nearly every seismogram due to their 2-D geometrical spreading properties that causes less attenuation of signal with distance when compared to body waves. Surface wave dispersion can be readily compared to subsoil characteristics, as different frequencies of the waves sample different soil thicknesses and consequently travel at different velocities. This dispersion was measured by using the Multi-channel Analysis Surface Waves (MASW) survey method that can be directly related to shear wave velocity through analysis of the dispersion curve showing phase velocity versus frequency plot (Park et al., 1998). The MASW technique has been successfully used in many studies (e.g., Xia et al., 1999, 2000, 2002; Park et al., 1999; Tian et al., 2003; Kanli et al., 2006; Mahajan et al., 2007; Anbazhagan and Sitharam, 2008).

The Multi-Channel Analysis of Surface Waves (MASW) survey generates a surface wave dispersion curve for each site location. This is done for each shot gather (Figure 8.6A) by transforming to the frequency-phase velocity (F-V) domain in order to estimate a specific dispersion curve (Figure 8.6B) (Park et al., 1998). From the dispersion curve, the frequency-velocity spectrum can be obtained using a tau-p transform (Figure 8.6C). Estimation of the 1-D shear wave velocity at each location is obtained by using an iterative inversion algorithm which uses a least-squares approach that allows for automation of the inversion process. (Figure 8.6D)

#### 8.4.1. Survey

The MASW survey consisted in measuring surface waves at 70 sites distributed within the urbanized area of the El Paso (Figure 8.5). The spacing between stations varied from 1.5 km

to 1 km based on the availability of open lots or parks, where most of the surveys were done. The acquisition of the data consisted in deploying a 24 channel Geometrics seismograph with 4.5 Hz geophones with a 3 m spacing interval at each site (Figure 8.7). The geophones were deployed in a linear spread configuration and were interconnected by a cable. To create the surface waves we used a 20 and 12 pound sledge hammer that gave us flexibility at each site location to shoot at different offsets, and for a few select sites we used a hydraulic weight drop. A trigger switch is attached to the hammer to record the origin time of the source. Table 8.2 summarizes the parameters used in the field for the MASW survey. The resultant Vs curve is an average over the spread.

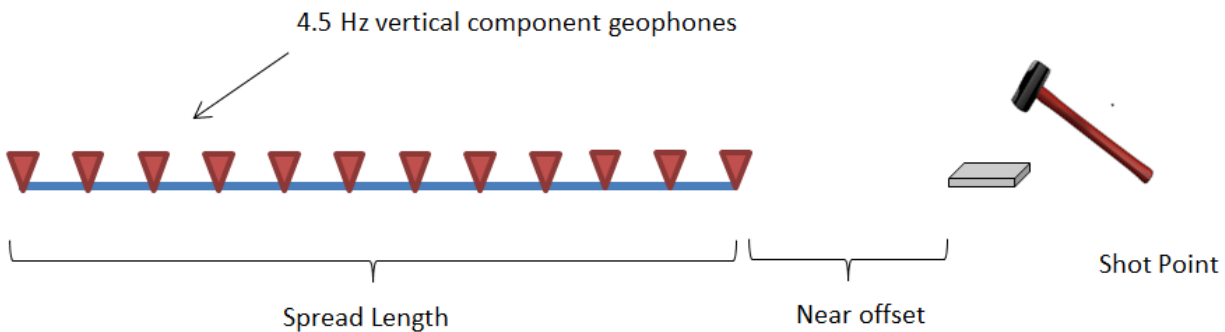


Figure 8.7. Shows the linear spread geometry for the 1D MASW Survey

## 8.5 Processing

For processing the 1D MASW, the SeisImager/SWTM software was utilized; this software provides several modules that are very useful for surface wave data analysis including Pickwin and WaveEq. Figure 8.8 shows the processing flow taken to obtain the Vs<sub>30</sub> for each site.

### 8.5.1 Pickwin Module.

The first step of the analysis consists of displaying the waveforms obtained at each location, and proceeding to check geometry and units. Then the user can optimize the travel time curve by increasing the amplitudes and the vertical and horizontal scale. The display of the waveforms also provides the ability to discriminate high and low quality data, as not all sites were exempt from noise; some stations near high traffic areas were contaminated with low frequency signals. This challenge was addressed by stacking more shots, using different distances for shot locations or waiting for quieter recording periods when doing the survey.

Figure 8.9 shows the contrast between high quality data and low quality data. High quality data will have a high signal to noise ratio and coherence from trace to trace. Low quality contains contamination by lower frequencies and a lack of coherency in surface wave signal. Once the highest quality data were selected, phase velocity-frequency transformation was made for each of the shot gathers to obtain the dispersion curve (figure 8.6b). The dispersion curve was produced by picking the maximum amplitudes within the dispersion envelope.

### 8.5.2 Wave Equation

After obtaining the dispersion curve the wave equation module is applied so the dispersion curve can be adjusted for low and high frequency picks at the ends of the curve. The 1D MASW analysis starts with an initial model of Vs with depth (Figure 8.10a) and the wave equation module continues to display the initial model, and set-up for the model inversion, where the number of iterations (between 5 and 10) can be specified depending on is more suitable for each site. The final model is obtained by using an iterative, non-linear, least squares inverse method where inversion is terminated when the percentage of the least square error <5. The

inversion produces a Vs curve and other optional model parameters such as P velocities and apparent velocity curves. (Figure 8.10b)

## 8.6 Results

The average Vs30 results for each site are shown in Figure 8.11, where low velocities are found close to the river within fluvial deposits and the high velocities close to the Franklin Mountains where bedrock is close to the surface. High velocities were also found near the Tertiary andesite outcrops around UTEP. These type of outcrops are scatter around the west side of the urbanized area of El Paso within the Mesilla Valley. The downtown area of El Paso where most of the tall buildings are located has an average Vs30= of 305 m/sec and is classified as type D soils. Soil maps for the he east side of El Paso show deep sands and sandy loam over caliche (U.S. Department of Agriculture, 2016). This is corroborated by the Vs30 measurements that higher velocity class D soils indicating that the caliche cementation found in these sands makes them fairly stable. Figure 8.12 shows site classifications within El Paso according to NEHRP site classification scheme.

Combined Vs30 results for El Paso and Ciudad Juarez (Figure 8.13) show consistency in values across the border. Note that there is a large portion of both cities that contain soils on the low end of class D. Regions closer to bedrock are class B to C soils, with higher velocity class D soils found on the mesa surfaces lying about the river valley.

## 8.7 Discussion

The Vs30 soil classification is a starting point for future studies of expected strong ground motion in the region from earthquakes. The maps clearly show that the highest shaking will occur within the river valley. It is important to point out that most Vs30 measurements were

taking during dry conditions. In the summer when the water table in the river valley is higher due to irrigation activities and monsoonal rainfall Vs30 could be even lower, with potential for strong shaking to be even higher during an earthquake. It will be important to re-occupy some observational points in the river valley during wet conditions to better estimate the total seasonal variations in Vs30 that may be expected. I will also be important to determine what critical facilities, such as schools, hospitals, police and fire stations, may lie within the region of poorest quality soils.

Another step will be to use the Vs30 measurements to predict resonant frequency amplification for El Paso and compare these frequencies to building stock within the city. Buildings with more stories tend to resonate at lower frequencies than 1 to 2 story buildings.

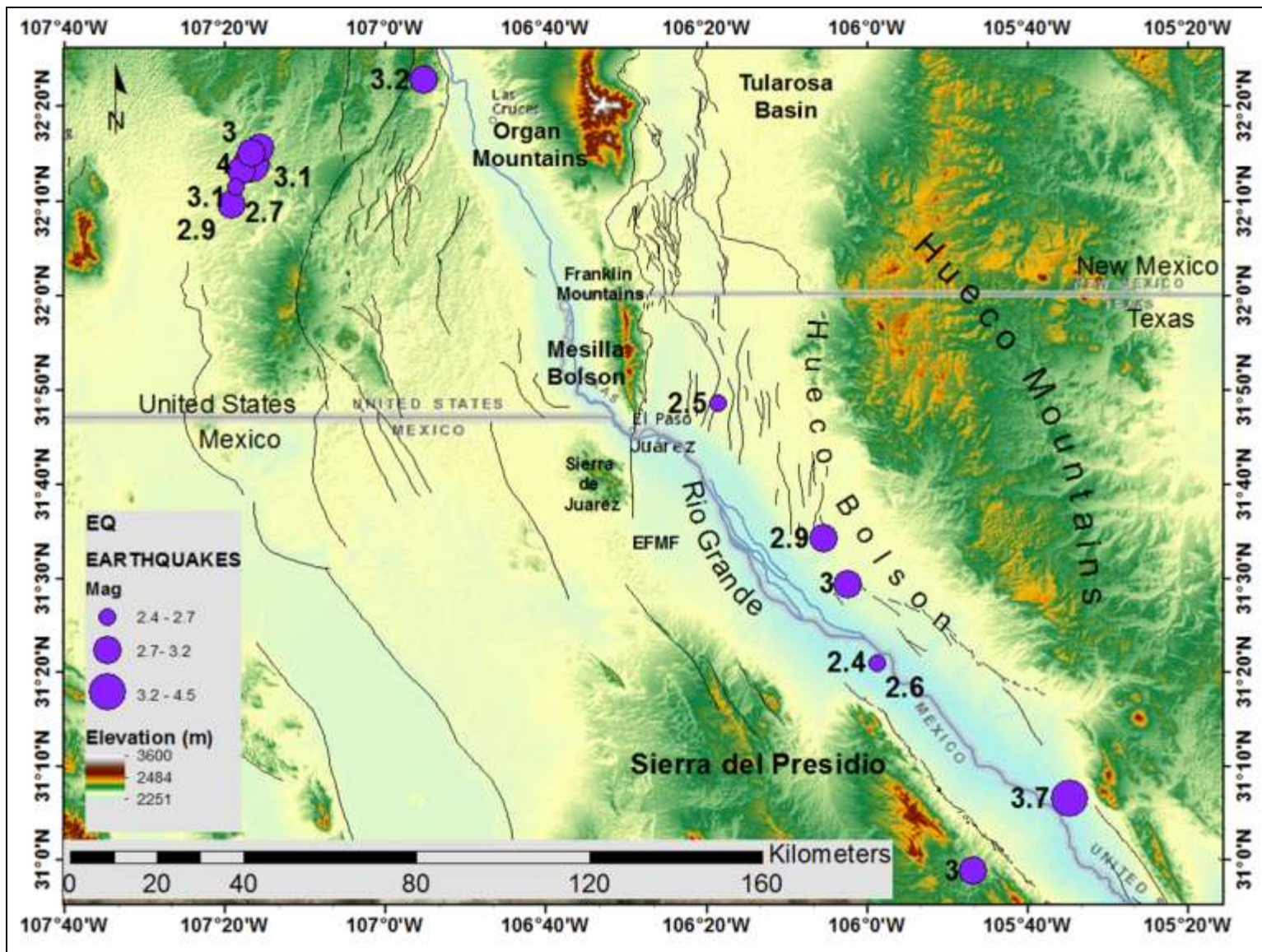


Figure 8.1. Seismicity in West Texas- Southern New Mexico, Northern Chihuahua from 2009-2016 from U.S. Geological Survey (2016)

Site Class	Velocity Range	Blow count range
A. Hard Rock	$5000 \text{ ft s}^{-1} \leq V_{100}$ $1500 \text{ m s}^{-1} \leq V_{S30}$	Not applicable
B. Rock	$2500 \leq V_{100} < 5000 \text{ ft s}^{-1}$ $760 \leq V_{S30} < 1500 \text{ m s}^{-1}$	$N_{100} \geq 100$
C. Very dense soil and soft rock	$1200 \leq V_{100} < 2500 \text{ ft s}^{-1}$ $360 \leq V_{S30} < 760 \text{ m s}^{-1}$	$50 \leq N_{100} < 100$
D. Stiff soil	$600 \leq V_{100} < 1200 \text{ ft s}^{-1}$ $180 \leq V_{S30} < 360 \text{ m s}^{-1}$	$15 \leq N_{100} < 50$
E. Soil	$V_{100} < 600 \text{ ft s}^{-1}$ $V_{S30} < 180 \text{ m s}^{-1}$	$N_{100} < 15$
f. Soils requiring site specific studies	Include liquefiable soils, peat or clay with high organic content. High plasticity clays. Very thick soft/medium stiff clay	

Table 3 Table 8.1 Definition of NEHRP site classes by velocity V100 (average shear velocity in the top 100 feet) VS30 and blow count N100. Modify from Building Seismic Safety Council (1997)

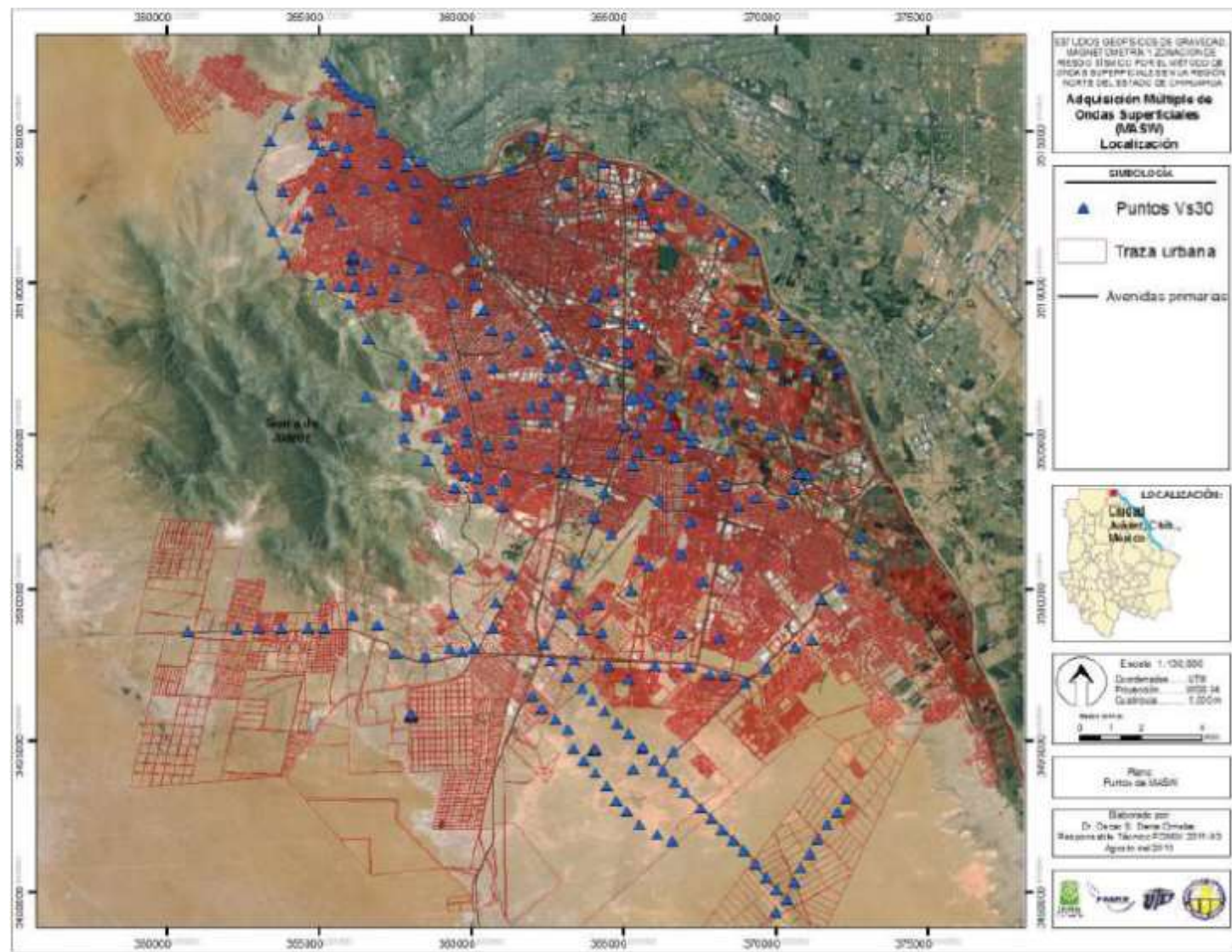


Figure 8.2 Location of 370 Seismic stations in Ciudad Juarez where Vs30 was determined using the MASW technique. Modified from Dena (2011)

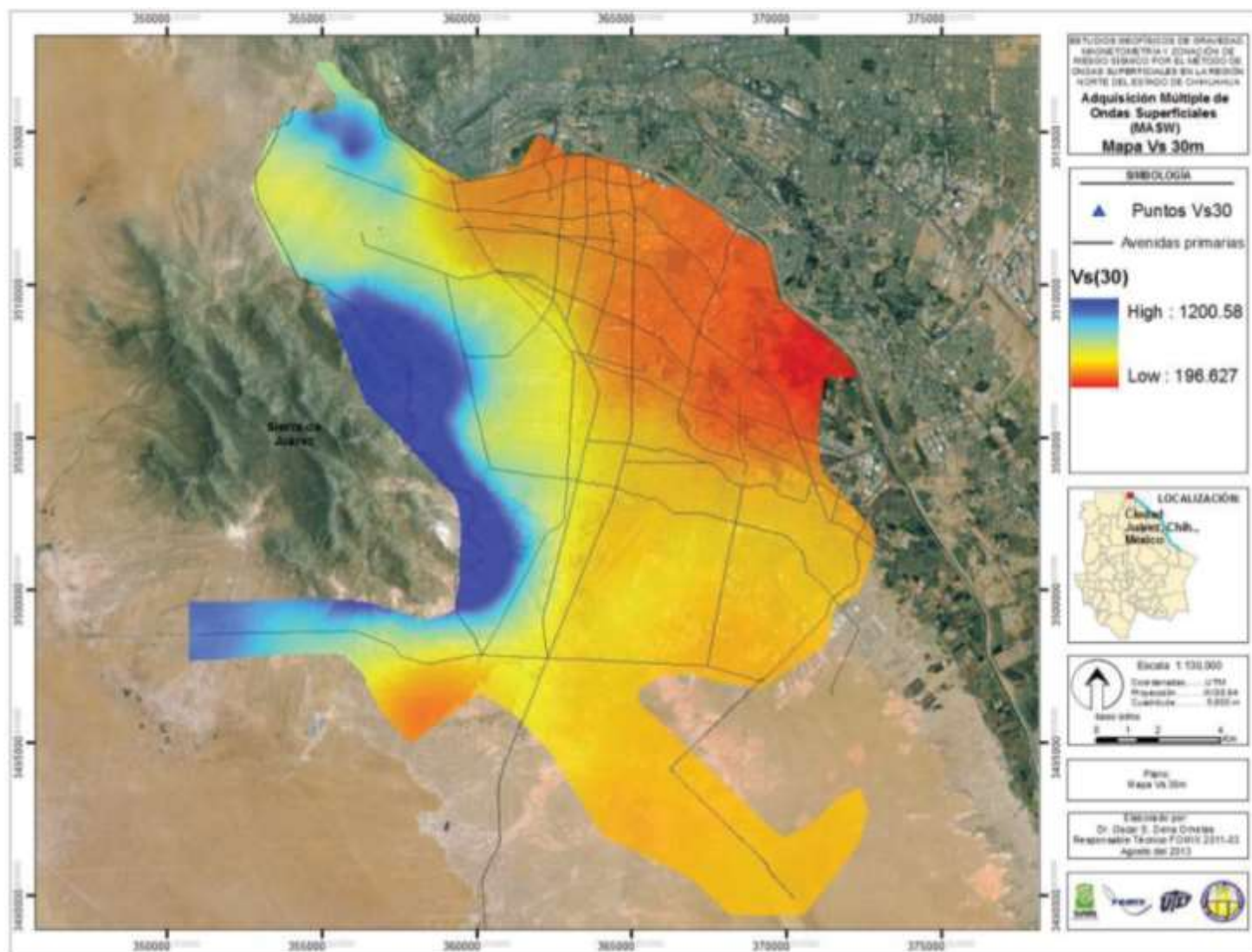


Figure 8.3 Average Vs30 determined for the Hueco Bolson in Ciudad Juarez using the MASW technique.  
Modified from Dena (2011)

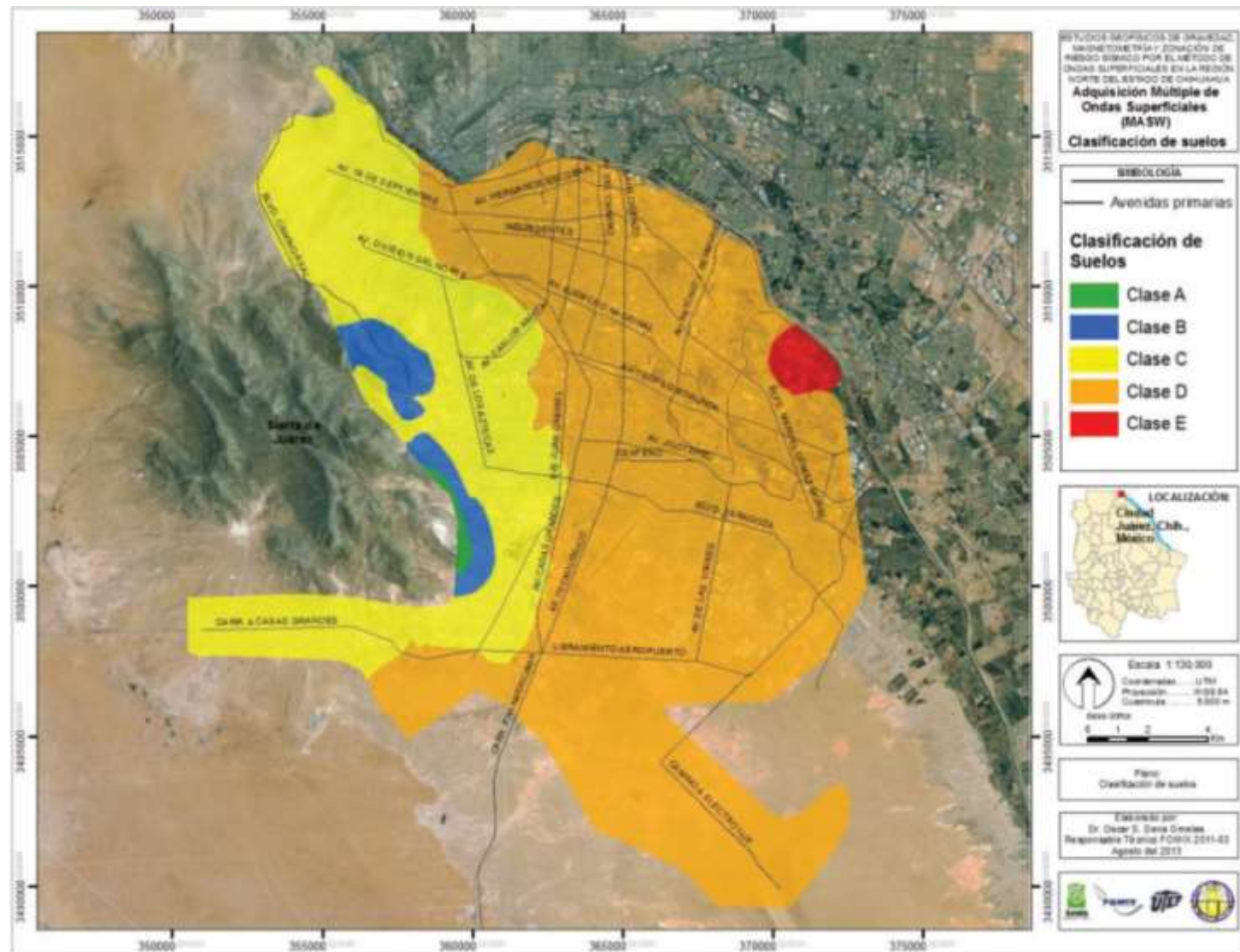


Figure 8.4 Site classification determined by relating Vs30 to soil type in Ciudad Juarez. Modified from Dena (2011).

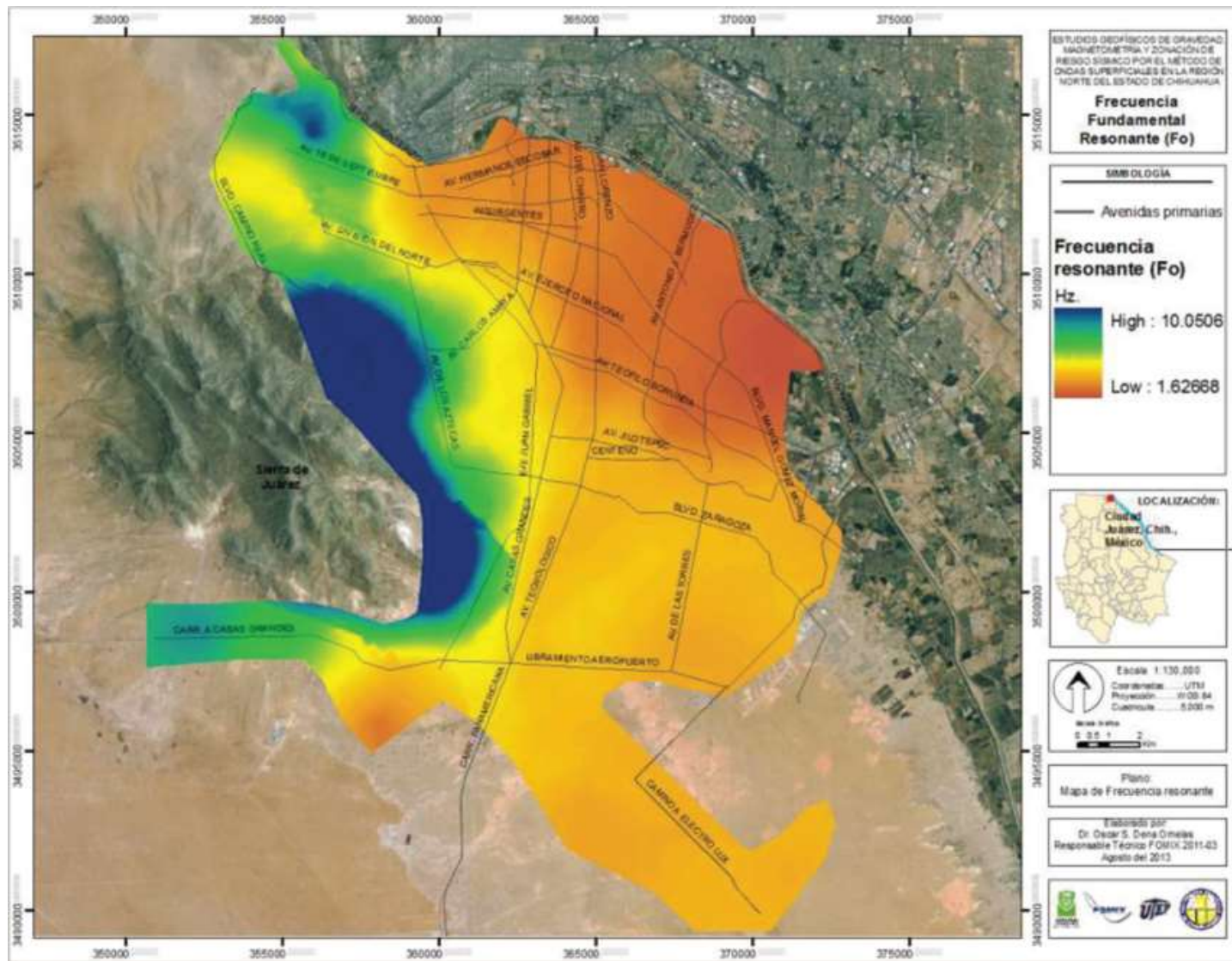


Figure 8.5 Expected resonant frequency amplification in Hz for Ciudad Juarez estimated from MASW and site classification. Modified from Dena (2011).

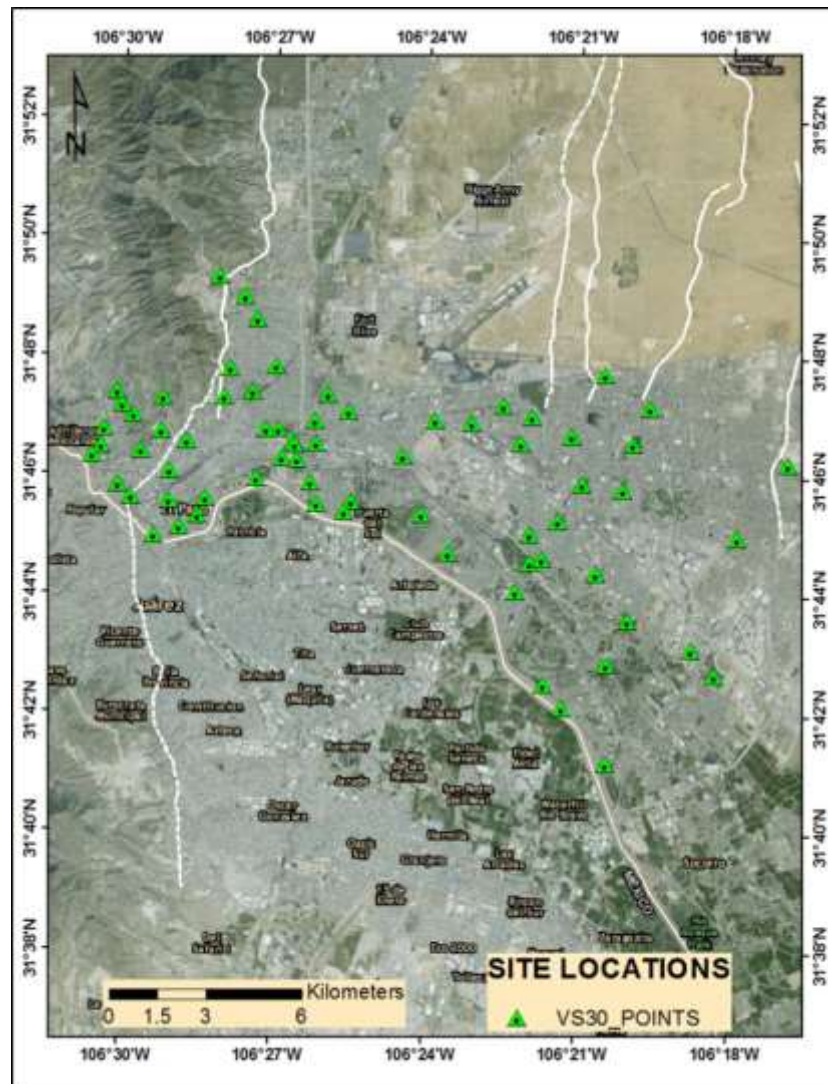


Figure 8.6. Vs30 locations (triangles) in the urban area of El Paso TX.

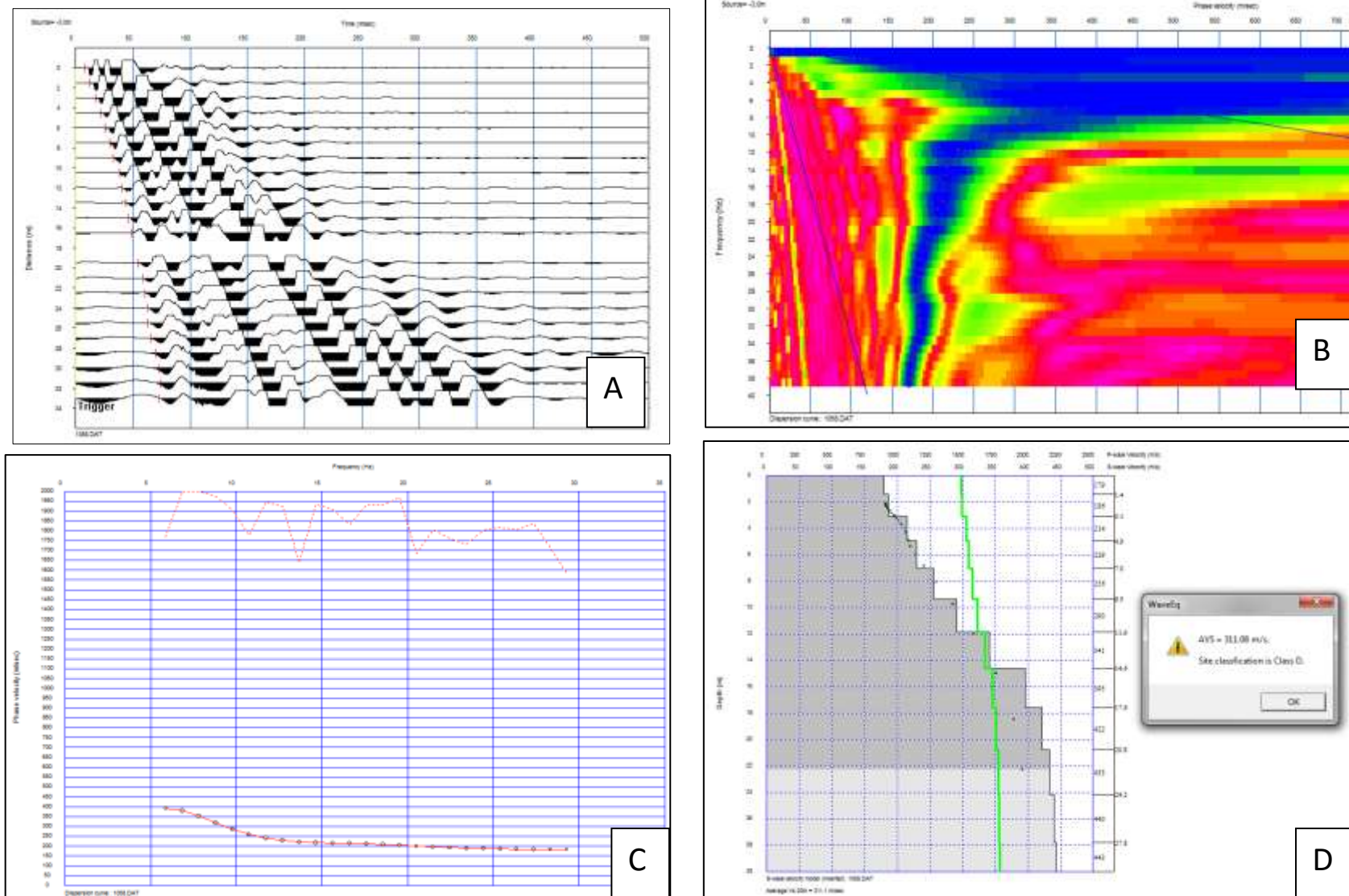


Figure 8.6 A) Example of shot gathers from site location. B) Dispersion curve (Pink dots) for the phase velocity (horizontal axis)-frequency (vertical axis) transformation. C) Dispersion curve but with phase velocity on vertical axis D) Vs30curve (black line?) is obtained by inverting the initial model. Table 8.2 Acquisition parameters for the MASW

---

<b>Parameter</b>	<b>Setting</b>
Spread configuration	Linear
Spread length	69 meters ( 3m spacing) , 34.5 meters (1.5m spacing)
Geophone interval	3 m (stations 18-70), 1.5 m (stations 1-18)
Total number of geophones	24
Geophone type	4.5 Hz vertical geophones.
Shot locations	From -3 m to -36 m off from the beginning of the line
Shot near offset	-3m, -6m, -12,m -18m, -24m, -30m, -36m
Source equipment	12& 20 pounds sledgehammer, and stations 64 to 70 hydraulic weight drop.
Trigger	Hammer switch tapped to sledgehammer
Sample interval	0.5 ms
Record length	2 seconds
Stacking	From 10 stacks to 40 stacks at each shot point to define the surface wave train

---

Table 4 Table 8.2 Acquisition parameters for the MASW Surveys

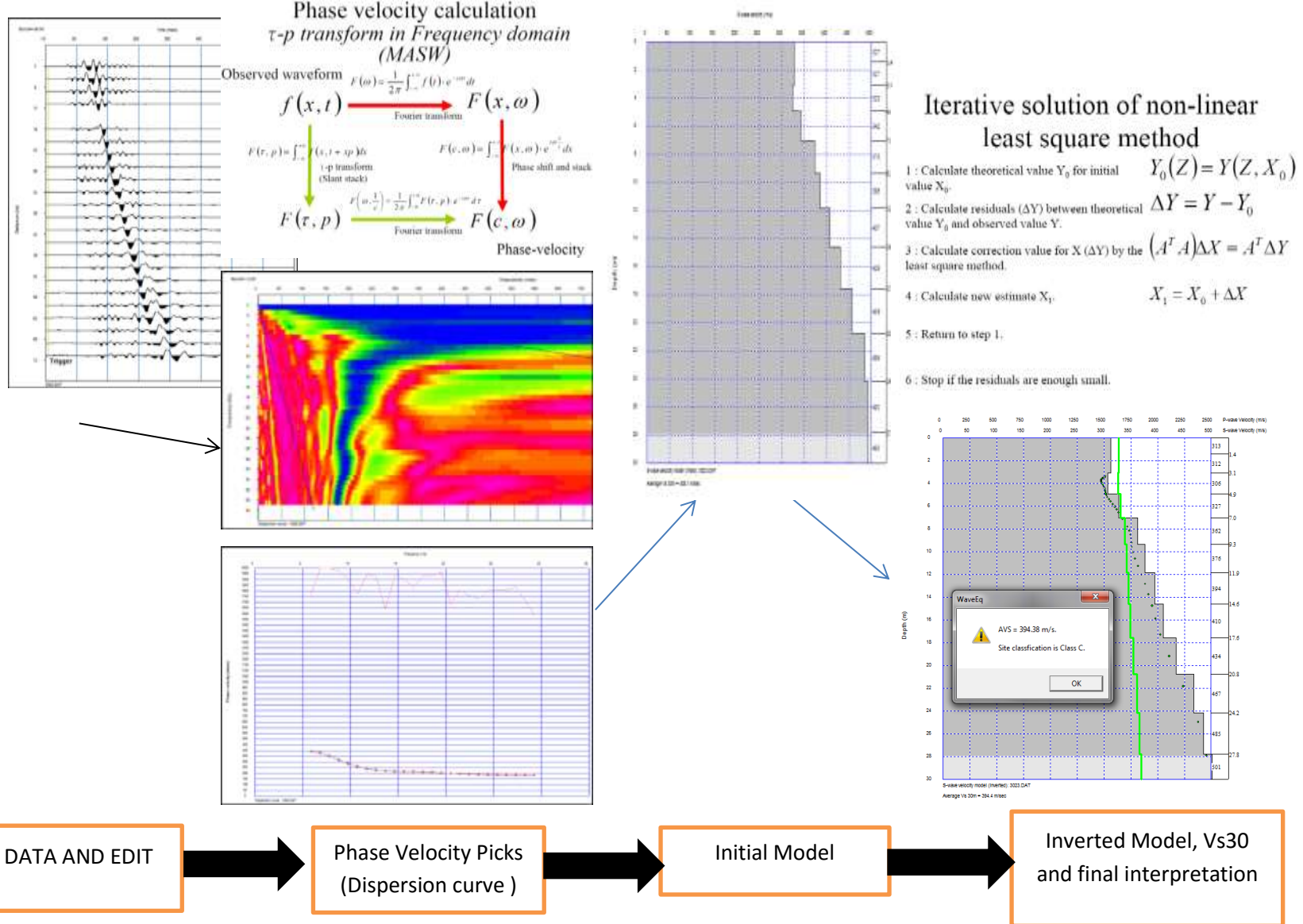


Figure 8.8 Process flow for processing 1D MSAW

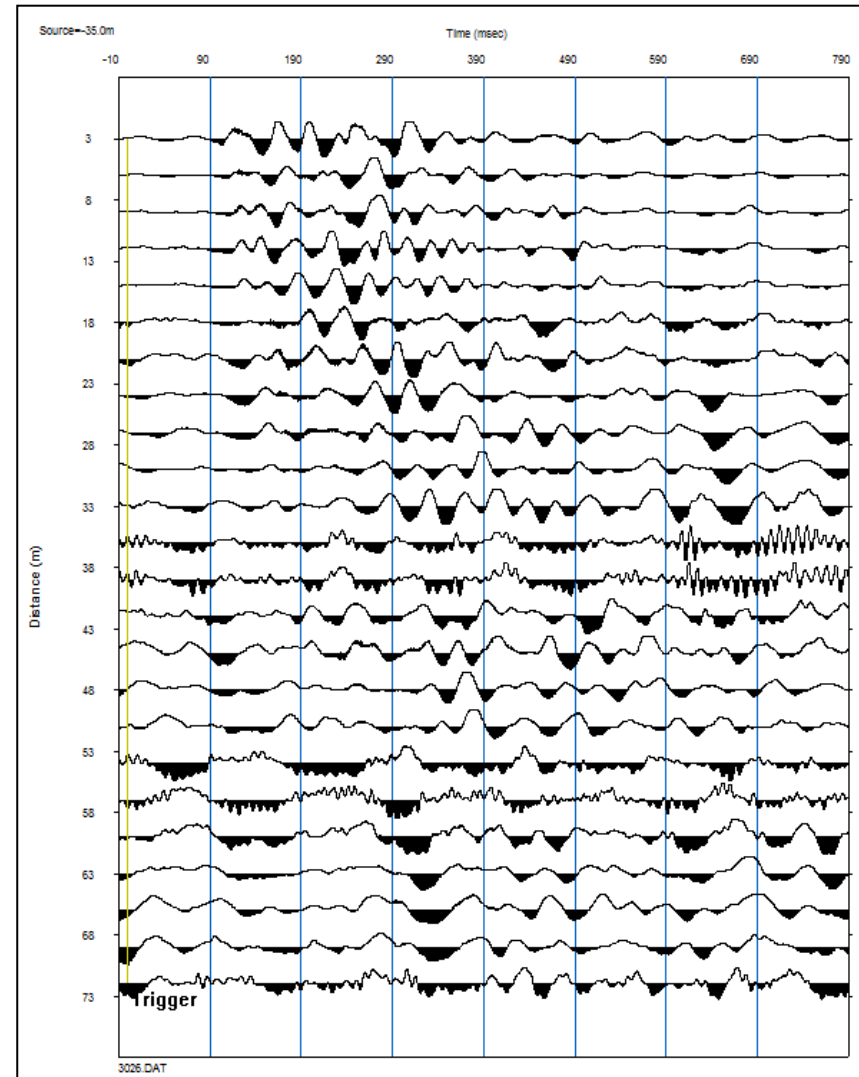
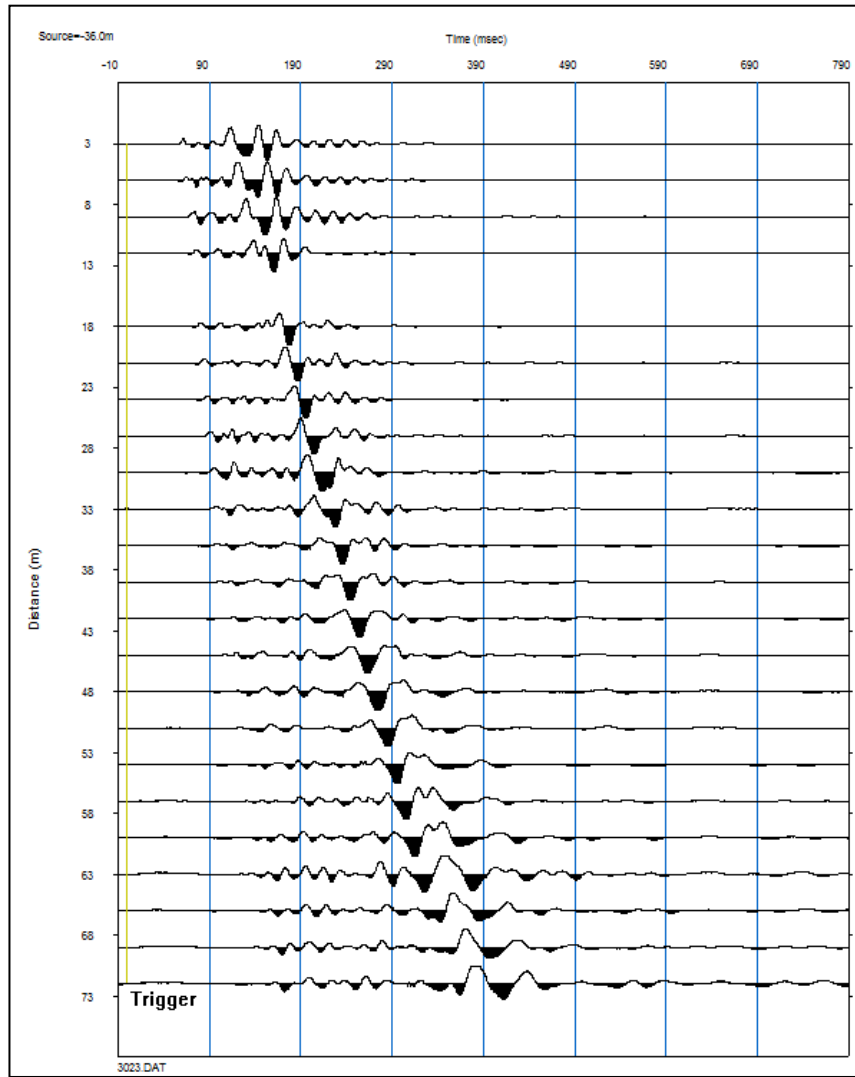


Figure 8.9 Left figure shows high quality data with high signal to noise ratio. Right figure shows low quality data with a lot of contamination with lower frequency signals.

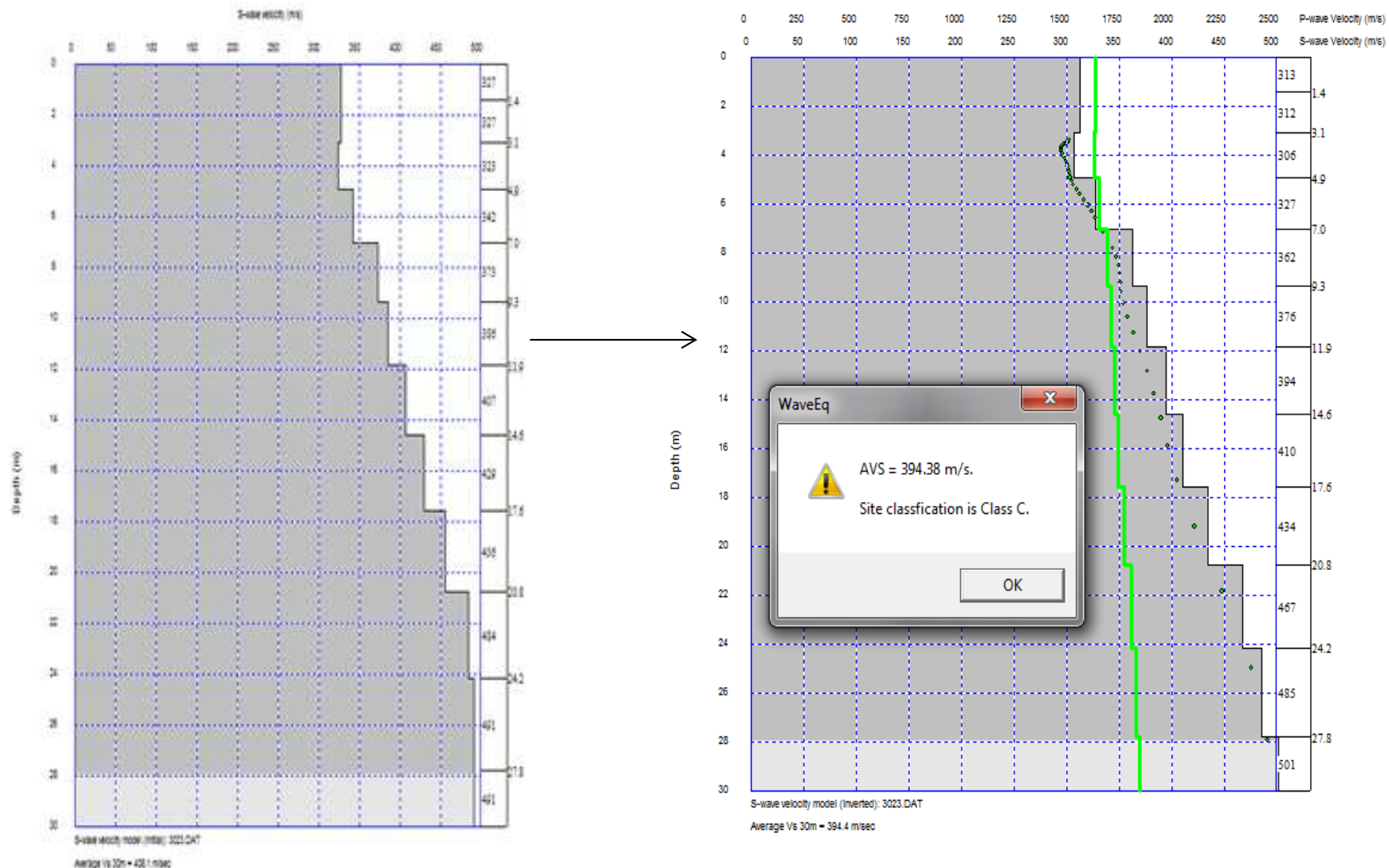


Figure 8.10 Initial shear velocity model from dispersion curve (left). Vs30model with optional parameters (right)

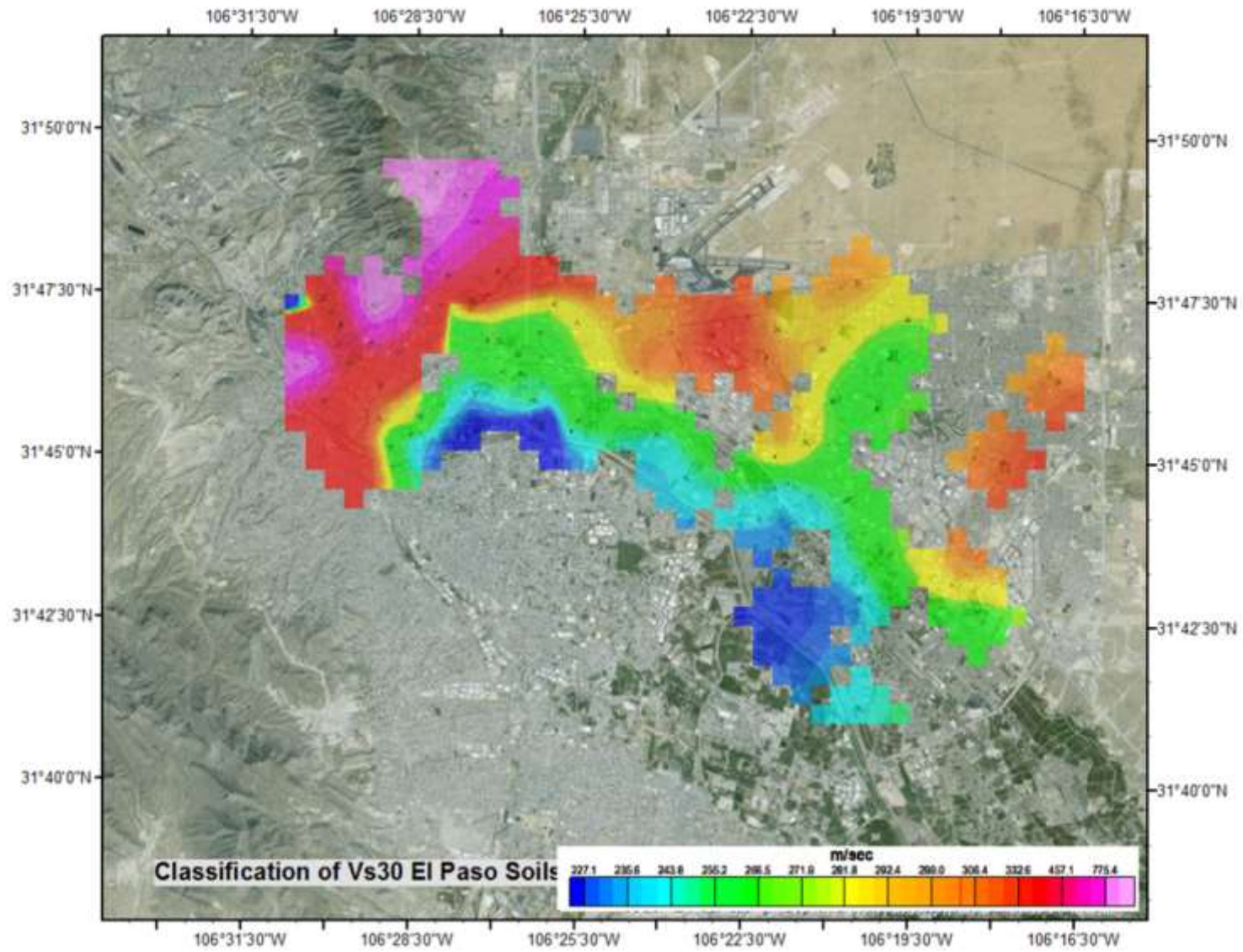


Figure 8.11 Vs30 map of the urbanized part of El Paso

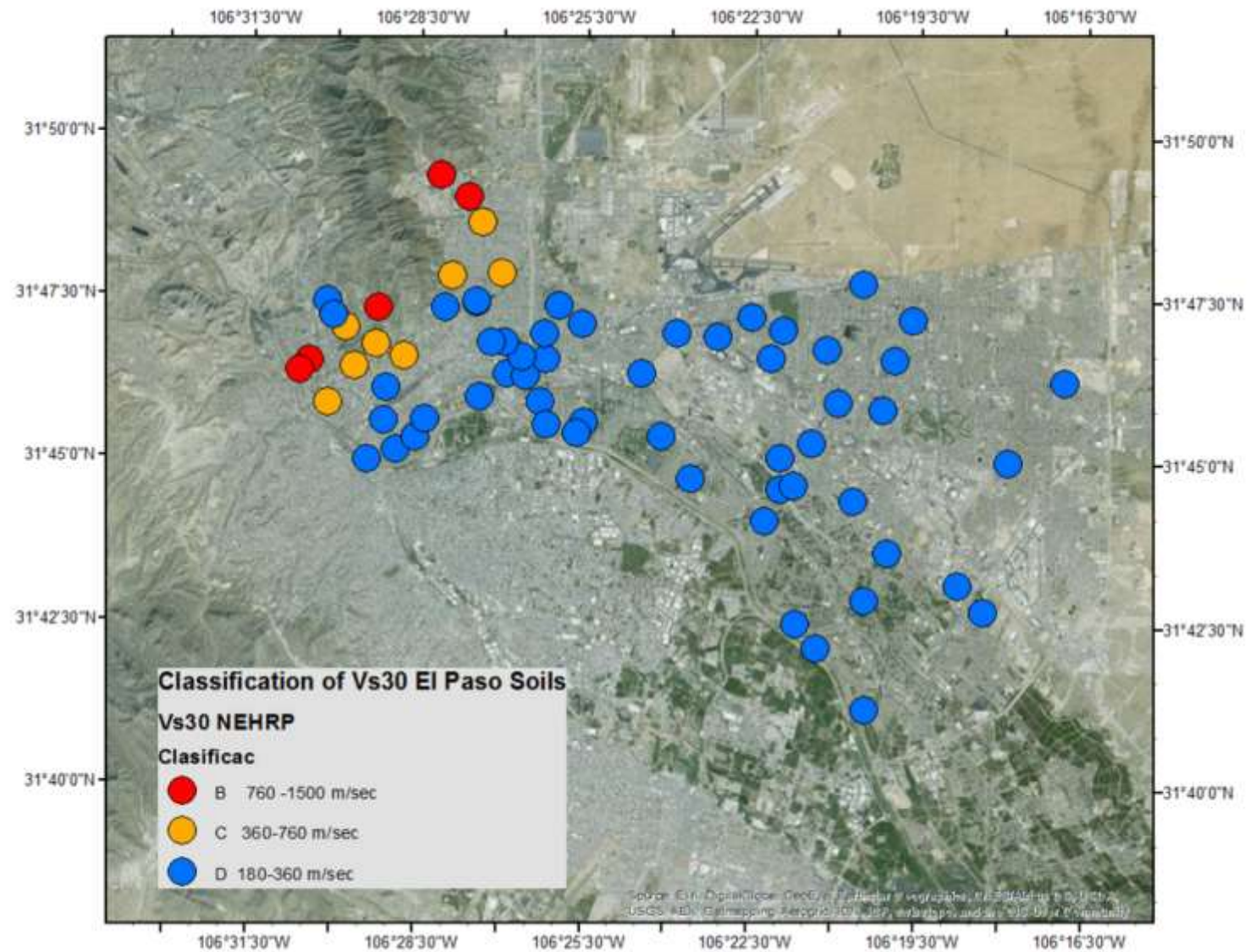


Figure 8.12 NEHRP site Classification for the Vs30 in the urbanized part of El Paso.

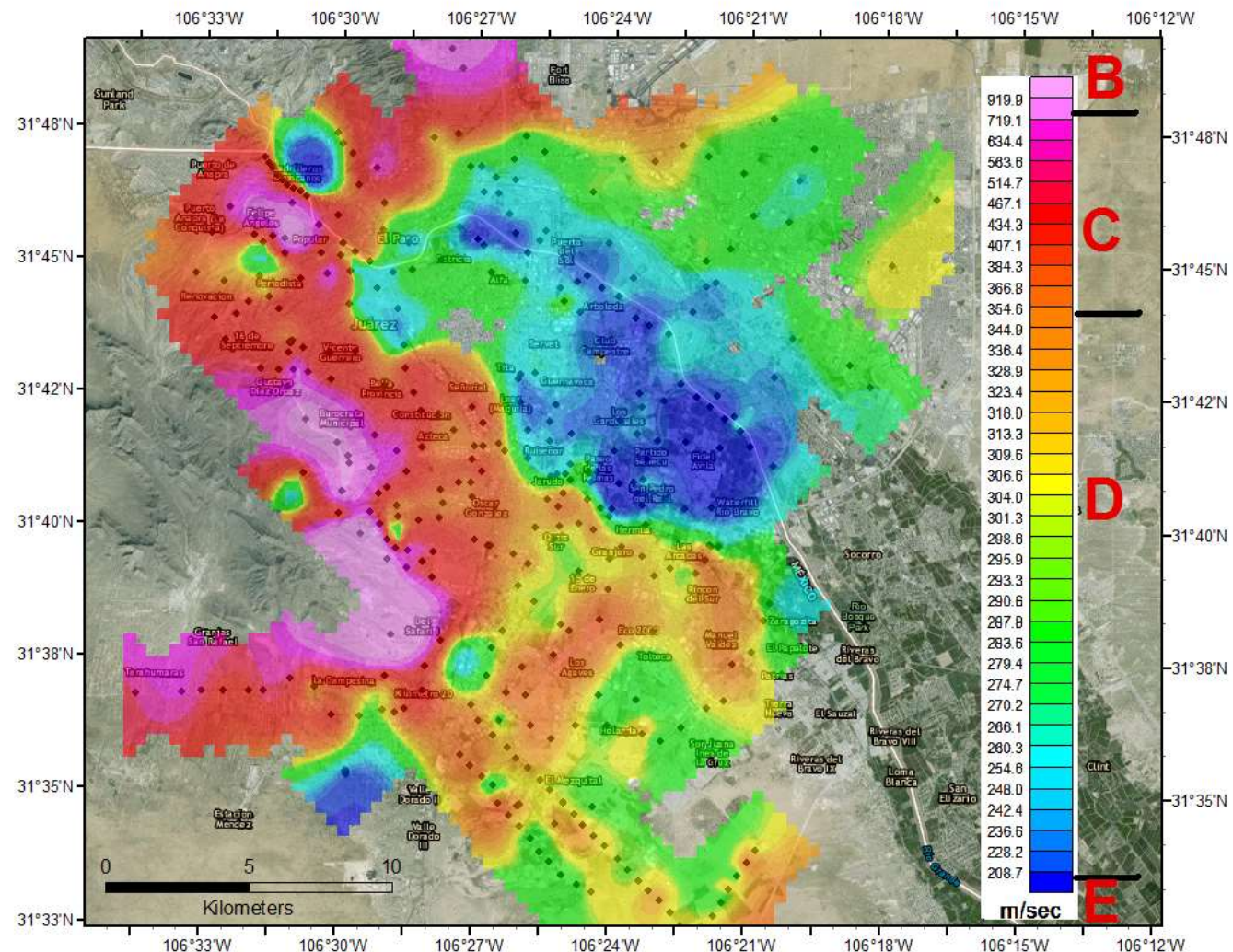


Figure 8.13 Combined Vs30 results for El Paso and Ciudad Juarez

## 8.8 References

- Anbazhagan, P., Sitharam, T.G., 2008. Site characterization and site response studies using shear wave velocity. *Journal of Seismology and Earthquake Engineering* 10, 53–67.
- Collins, E.W., Raney, J.A., 1994. Tertiary and Quaternary tectonics of the Hueco bolson, Trans-Pecos Texas and Chihuahua, Mexico, in: Geological Society of America Special Papers. Geological Society of America, pp. 265–282.
- Doser, D. I., 1987, The 16 August 1931 Valentine, Texas, earthquake: Evidence for normal faulting in west Texas: *Bulletin of the Seismological Society of America*, v. 77, no. 6, p. 2005–2017.
- Kanlı, A.I., Tildy, P., Prónay, Z., Pınar, A., Hermann, L., 2006. VS30 mapping and soil classification for seismic site effect evaluation in Dinar region, SW Turkey. *Geophysical Journal International* 165, 223–235. doi:10.1111/j.1365-246X.2006.02882.x
- Keller, G.R., Morgan, P., Seager, W.R., 1990. Crustal structure, gravity anomalies and heat flow in the southern Rio Grande rift and their relationship to extensional tectonics. *Tectonophysics, Heat and Detachment in Continental Extension* 174, 21–37. doi:10.1016/0040-1951(90)90382-I
- Mahajan, A.K., Slob, S., Ranjan, R., Sporry, R., Ray, P.K.C., Westen, C.J. van, 2007. Seismic microzonation of Dehradun City using geophysical and geotechnical characteristics in the upper 30 m of soil column. *J Seismol* 11, 355–370. doi:10.1007/s10950-007-9055-1
- N.E.H.R.P., Provisions, B.P. on I.S.S., 1998. NEHRP Recommended Provisions (National Earthquake Hazards Reduction Program) for Seismic Regulations for New Buildings and Other Structures: Provisions. Building Seismic Safety Council.
- Suter, M., and J. Contreras, 2002, Active Tectonics of Northeastern Sonora, Mexico (Southern Basin and Range Province) and the 3 May 1887 Mw 7.4 Earthquake: *Bulletin of the Seismological Society of America*, v. 92, no. 2, p. 581–589, doi:10.1785/0120000220.
- Park, C.B., Miller, R.D., Xia, J., 1999. Multichannel analysis of surface waves. *Geophysics* 64, 800–808. doi:10.1190/1.1444590
- Tian, G., Steeples, D.W., Xia, J., Miller, R.D., Spikes, K.T., Ralston, M.D., 2003. Multichannel analysis of surface wave method with the autojuggie. *Soil Dynamics and Earthquake Engineering* 23, 61–65. doi:10.1016/S0267-7261(02)00214-2

Xia, J., Cakir, R., Miller, R.D., Zeng, C., Luo, Y., 2009. Estimation of near-surface shear-wave velocity by inversion of Love waves. *Geophysics*. Society of Exploration Geophysicists, pp. 1390–1395. doi:10.1190/1.3255109

Xia, J., Miller, R.D., Park, C.B., Hunter, J.A., Harris, J.B., 2000. Comparing Shear-Wave Velocity Profiles from MASW with Borehole Measurements in Unconsolidated Sediments, Fraser River Delta, B.C., Canada. *Journal of Environmental and Engineering Geophysics* 5, 1. doi:10.4133/JEEG5.3.1

Xia, J., Miller, R.D., Park, C.B., Hunter, J.A., Harris, J.B., Ivanov, J., 2002. Comparing shear-wave velocity profiles inverted from multichannel surface wave with borehole measurements. *Soil Dynamics and Earthquake Engineering* 22, 181–190. doi:10.1016/S0267-7261(02)00008-8

## CHAPTER 9

### 9.1 Future Directions

One of the major goals of this dissertation was to use geophysical and geological information to locate faults within the Mesilla and Hueco Bolsons that may be capable of generating earthquakes. In addition, these studies have provided important information on the thicknesses of basin sediments and changes in basin shape.  $V_s^{30}$  studies have been used to characterize the expected more localized response due to variations in soil conditions throughout the urbanized region.

Although much has been learned in these studies, many gaps in knowledge still exist. I propose the following steps should be taken to collect additional data and further analyze the data collected for this dissertation.

### 9.2 Data Collection

- More gravity data are needed to trace the continuation of mapped intrabasin faults in the easternmost portion of the Hueco Bolson (Figure 9.1).
- Additional gravity data need to be collected in the westernmost Mesilla Bolson study area to better characterize the Mesilla Valley fault zone and image the projected edge of Laramide deformation. Data should be collected east of I-10 to better trace two inferred faults that pass beneath this region (Figure 9.2)
- $V_s^{30}$  data should be collected in the El Paso Lower Valley region (e.g., Socorro, San Elizario, Clint) and in the Mesilla Valley. Repeat  $V_s^{30}$  surveys should be conducted with the river valley to determine how much seasonal variation in  $V_s^{30}$  exists.

### 9.3 Data Compilation and Modeling

- Two dimensional gravity profiles should be combined to build 3-D models of the Mesilla and Hueco Bolson. These basin geometries are important starting points for modeling strong ground motion effects of the basins such as focusing points caused by basement topography and resonant frequencies of the basins.
- $V_s^{30}$  results should be combined with 3-D structural models to more completely capture expected site effects during a large earthquake.

### 9.4 Communication of Results

- Geo-referenced soil classification maps, maps of inferred faults, sites of possible ground failure (due to faulting or liquefaction) and landslides, and expected resonant frequencies should be constructed and shared with city planners, engineers, emergency managers and resiliency offices on both sides of the border.
- Knowledgeable geoscientists should provide understandable, public friendly reports, hold information sessions and disseminate other information to city officials and the general public to insure the public becomes aware of earthquake risk within the region, and steps that can be taken to reduce earthquake losses.

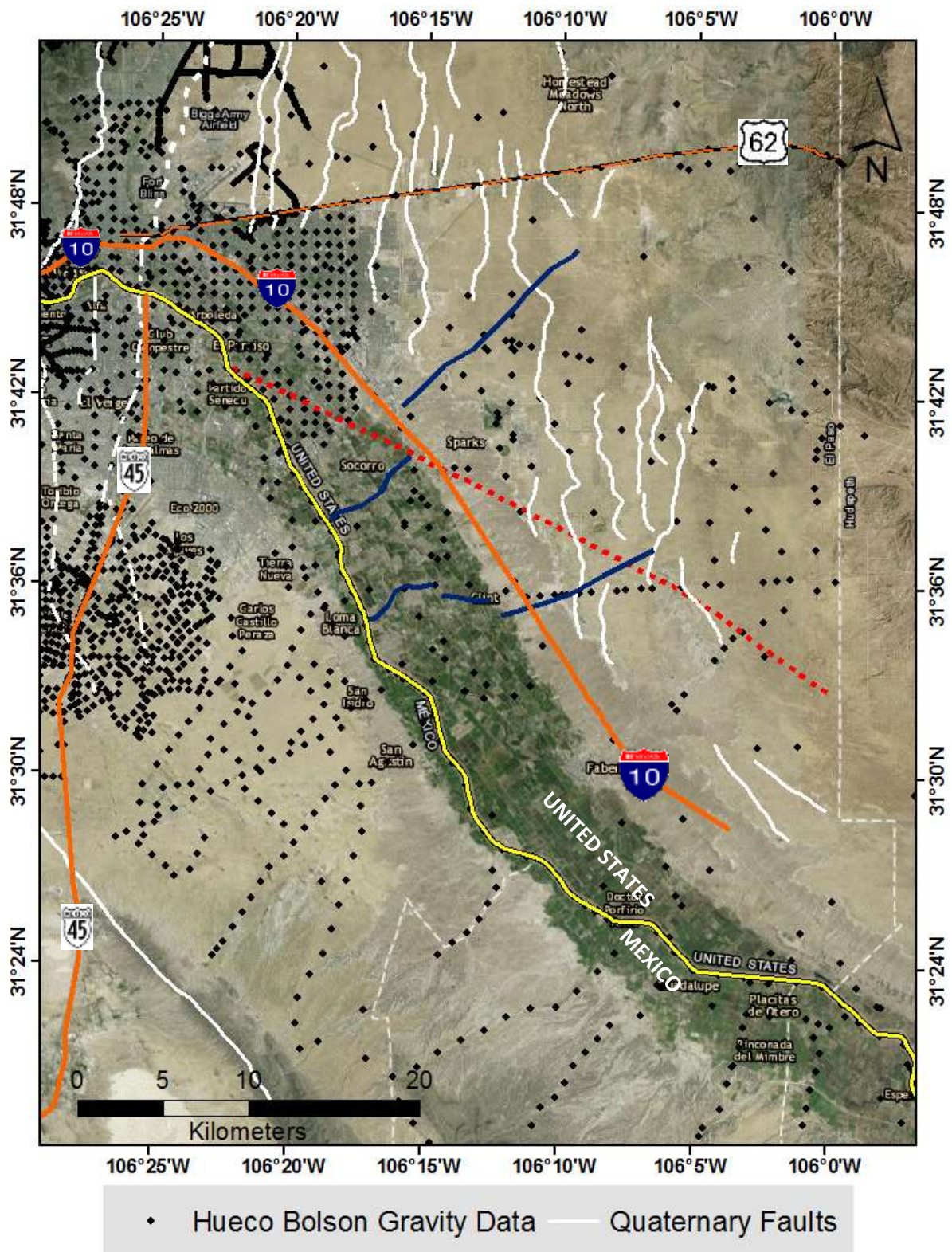


Figure 9.1 Hueco Bolson gravity data needs to be collected to continue studding the faults

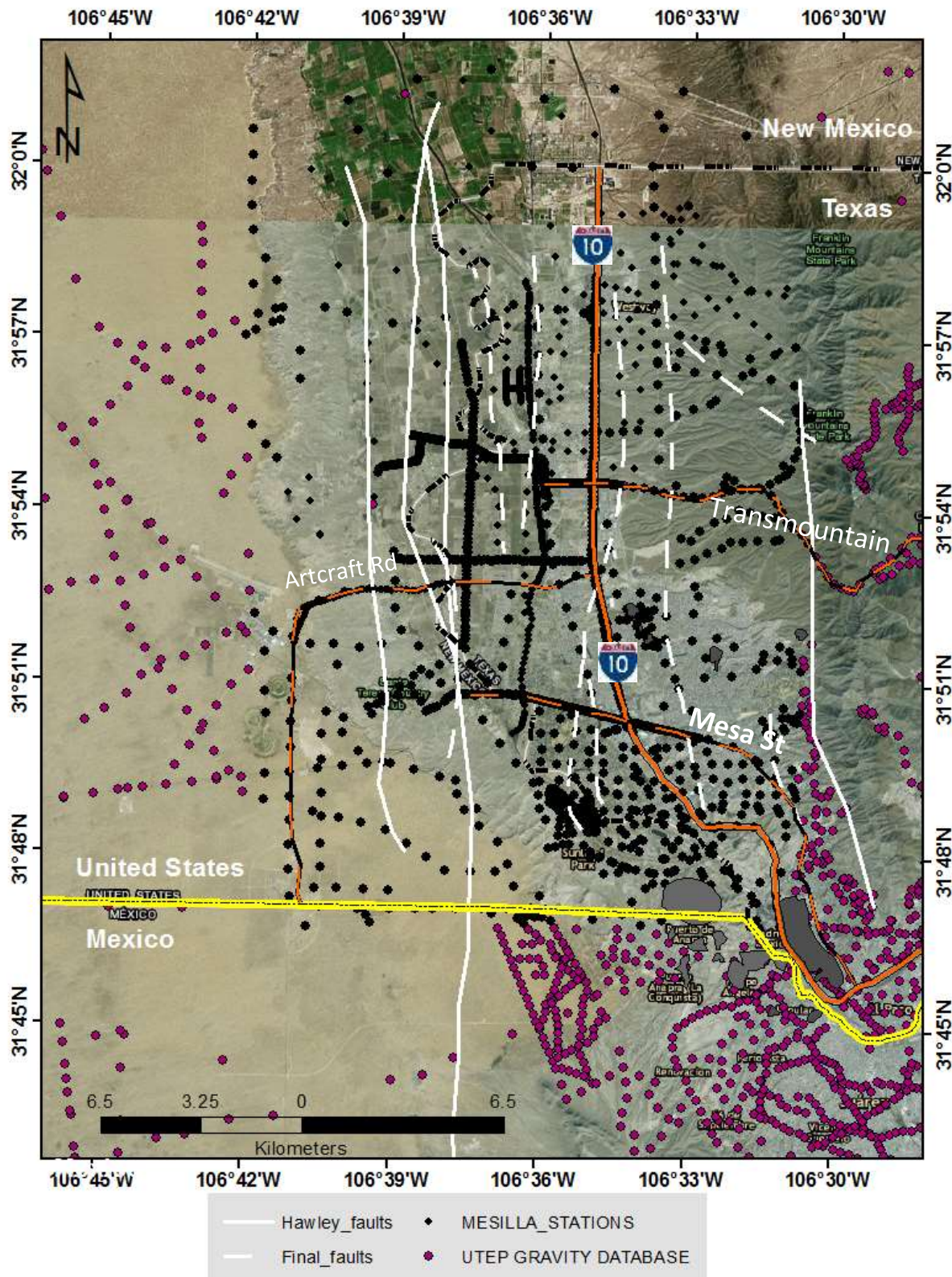


Figure 9.2 Gravity database for Mesilla Bolson

## CURRICULUM VITA

Victor Avila son of Manuel Avila Jaime e Irma Rosa Amaya Nuñez born in Ciudad Juárez. First in His family to obtain a Ph.D. degree. Victor earned his Bachelors of Electro-Mechanical Engineering from Instituto Tecnológico of Ciudad Juarez (ITCJ) in 1998. In 2011, he received his Master in Science degree in Geophysics and continued with the Doctoral program in Geological Sciences at the University of Texas at El Paso.

Victor Avila was the recipient of the CONACYT scholarship to pursue his Ph.D., and also received other scholarships while in the program, such as Vernon G. & Joy Hunt Geology, and other awards from the Geology Department.

While pursuing his Degree, he participated in numerous research projects, such as seismic experiments for deep crustal studies, with the UTEP geology department. Victor lectured Physical and Historical Geology at El Paso community College. He also participated. He also participated in seismic risk assessment for the state of Chihuahua, representing UTEP in 2012.

Victor has presented his research; at Geological Society of America conference celebrated in 2012 in Denver Colorado, in collaboration with Dr. Diane Doser published an article, in online Journal Geosphere (The Geological Society of America journals): Using geophysical techniques to trace active faults in the urbanized northern Hueco Bolson, West Texas, USA, and northern Chihuahua, Mexico

Victor's dissertation entitled, "Geophysical Constraints on The Hueco and Mesilla Bolsons: Structure and Geometry" was supervised by Dr. Diane I. Doser.

Permanent address: Solar de Claveles 2350-27

Ciudad Juárez

This dissertation was typed by Victor Avila.